Ministery of Higher Education and Scientific Research

وزارة التعليم العالي والبحث العلمي

Badji Mokhtar Annaba University
Université Badji Mokhtar – Annaba
Faculty of Technology

Metallurgy Department

جامعة باجي مختار – عنابـــة

كـليـة التكنـولـوجيـا

قسـم التعدين

Thesis

Presented to obtain the degree of

Doctorate Third Cycle (LMD)

Field: metallurgy

Specialty: foundry

By:

CHARMATI Djihad

Theme:

Effect of Microstructure on the Mechanical, Tribological and Electrochemical Behavior of Boride-Hardened Spheroidal Graphite Cast Iron (SG)

PhD thesis defended on 20/02/2025 in front of the jury composed of:

N°	Full name	Grade	Establishment	Quality
01	MECHACHTI S	Prof.	University of Badji Mokhtar Annaba	President
02	TOUHAMI M.Z	Prof.	University of Badji Mokhtar Annaba	Reporter
03	TLILI S	SR.	Research Center in Industrial Technologies CRTI	Co-Reporter
04	Khettach A	Prof.	University of Badji Mokhtar Annaba	Examiner
05	BELAID M	Assoc. Prof.	University of Sciences and Technology Houari Boumediene	Examiner
06	GUEDRI A	Prof.	University of Mohamed-Cherif Messaadia Souk Ahras	Examiner

DEDICATION

To my beloved parents,

Mohammed** & **D.Zouaoui

I cannot express my gratitude enough for your unwavering support and countless sacrifices that have been the foundation of my success. This thesis is a tribute to your love and guidance that have helped me reach this milestone in my life.

To my dear sisters and brother,

Salwa, Sara, Dalel; Hanan, Manel and Oussama

Your encouragement and understanding have been a constant source of strength for me. I am truly grateful for your presence in my life and for always being there for me, no matter what.

To my nephews,

Loudjain, Chiraz, Abed Elmonaim, Assia , Mouad, Razan** , **Abed Elrahman** and **Ritel

You are the next generation of our family, and I dedicate this thesis to you with the hope that it inspires you to pursue your dreams with determination and passion.

To my colleagues and friends,

I feel blessed to have had your collaboration and camaraderie throughout this journey. Your support, advice, and shared passion for knowledge and growth have enriched my experience beyond measure. This thesis is dedicated to all of us and our collective pursuit of excellence.

And lastly, to myself,

I want to celebrate the perseverance and dedication that have brought me to this moment. This thesis is a testament to our resilience and determination, and a reminder that we can achieve anything we set our minds to.

To all those who have supported and encouraged me, thank you.

With deepest gratitude and love,

Djihad Charmat

ACKNOWLEDGEMENTS

In the journey of completing this thesis, I have been surrounded by a constellation of support, guidance, and inspiration that has illuminated my path. To all those stars, I extend my deepest gratitude.

To my thesis advisor, Prof. Touhami M.Z, your guidance has been the North Star of this endeavor, always pointing me in the right direction with your wisdom and expertise. I also want to extend my gratitude to my thesis co-advisor Mrs. Tlili.S for her guidance

I would like to express my gratitude to the members of my dissertation defense committee Prof. Mechachti.S; Prof. Khettach.A; Assoc. Prof. Belaid .M and Prof.Guedr.A for their invaluable assistance in reviewing this dissertation and helping me to bring it to fruition.

To all those who encouraged and propelled me to embark on this PhD journey, especially Pr.Hacini.M and Boudebanne.S, I am profoundly grateful. Their unwavering support has been the cornerstone of my academic pursuit.
To my friends, Dr. (Taleb Ahlem, Maroua.L, Karima.B, Rania.B , Rym Chaima.T , Hanane.A, Khaia.G, and Samira.B) who have stood by me through thick and thin, thank you for your laughter, your understanding, and for reminding me to take breaks and enjoy the journey.

To my colleagues, who have shared their knowledge and expertise, thank you for your collaboration and camaraderie. Special thanks to Dr. Bahi.Raid, Dr.Chehaidia.SE for their valuable insights and feedback.

To the participants of my study: from the SNVI Ruiba foundry to Zouaid, Ksantini.R, Ourti.N; to Pr. Omar Alaoui from the unisiversity of l'agouat, Taleb Ahlem, soumaya meddah, bourbiaa mounira, Houda Grisa, Kamilia, Houass Ghous, Noura Remdan, Lemboub Samia , Hakima.S, Hichem.B, Linda, and Wafa.B, Linda and L.sihem, without whom this research would not have been possible, thank you for your time and willingness to share your experiences.

To my family, who have been my constant cheerleaders, thank you for your unconditional love and support. To my parents, for instilling in me a love for learning and the importance of perseverance. To my siblings, for always being there with a listening ear and words of encouragement.

And finally, to myself, for the determination, resilience, and courage to embark on this challenging yet rewarding journey of academic pursuit.

With heartfelt thanks,

"Failure is simply the opportunity to begin again, this time more intelligently." — Henry Ford

« تأثير البنية المجهرية على السلوك الميكانيكي والقبلي والكهروكيميائي للجرافيت الكروي (SG) المصلَّب بالبور »

خلاصة:

تبحث هذه الدراسة في تأثير تفاوت سمك الطبقة Fe_2B على البنية المجهرية والخصائص الميكانيكية والسلوك الكهروكيميائي والقبلي للحديد الزهر القابل للطي والرمادي من خلال البور. تم إجراء البورون عند 950 درجة مئوية لمدة ساعة وأربع ساعات باستخدام طريقة حمل عبوات B_4C-Na_2CO_3. تم استخدام التقنيات التحليلية المتقدمة، بما في ذلك الفحص المجهري الضوئي، والمسح المجهري الإلكتروني(SEM) ، والتحليل الطيفي للأشعة السينية المشتتة للطاقة (EDS)، وحيود الأشعة السينية(XRD) ، واختبار فيكرز للميكروهاردس، لتحليل التغييرات الهيكلية المجهرية والخصائص الميكانيكية. لتقييم فعالية ومتانة العلاج، تم إجراء اختبارات الالتصاق واختبارات الخدش واختبارات الالتصاق Daimler-Benz Rockwell-C.بالإضافة إلى ذلك، تم إجراء الاختبارات القبلية في ظل ظروف خاضعة للرقابة والتجارب الكهروكيميائية لتقييم الاحتكاك وخصائص التآكل ومقاومة التآكل. يهدف هذا البحث إلى تقديم رؤى حول عمليات التحمل لتحسين أداء مكونات الحديد الزهر عبر القطاعات الصناعية، بما في ذلك السيارات وبناء السفن والزراعة. علاوة على ذلك، يساهم البحث في فهم أوسع للسلوك المادي في علم المواد.

الكلمات الرئيسية: الحديد الزهر ؛ Fe_2B ؛ السلوك الميكانيكي ؛ الالتصاق ؛علم القبائل ؛ مواد التشحيم ؛ السلوك الكهروكيميائي.

« Effet de la microstructure sur le comportement mécanique, tribologique et électrochimique des fontes grises à graphite sphéroïdale (GS) durcies par boruration »

Résumé :

Cette étude examine l'influence de la variation de l'épaisseur de la couche de Fe_2B sur la microstructure, les propriétés mécaniques, le comportement électrochimique et tribologique de la fonte ductile et grise par boruration. La boruration a été effectuée à 950°C pendant une et quatre heures en utilisant une méthode de boruration par paquets de B_4C-Na_2CO_3. Des techniques analytiques avancées, notamment la microscopie optique, la microscopie électronique à balayage (MEB), la spectroscopie à rayons X à dispersion d'énergie (EDS), la diffraction des rayons X (XRD) et les essais de microdureté Vickers, ont été utilisées pour analyser les changements microstructuraux et les propriétés mécaniques. Pour évaluer l'efficacité et la durabilité du traitement, des essais d'adhésion, des essais de rayure et des essais d'adhésion Daimler-Benz Rockwell-C ont été réalisés. En outre, des essais tribologiques dans des conditions contrôlées et des expériences électrochimiques ont été menés pour évaluer le frottement, les caractéristiques d'usure et la résistance à la corrosion. Cette recherche vise à mieux comprendre les processus de boronisation afin d'optimiser les performances des composants en fonte dans tous les secteurs industriels, y compris l'automobile, la construction navale et l'agriculture. En outre, la recherche contribue à une compréhension plus large du comportement des matériaux dans la science des matériaux.

Mots-clés : Fonte ; Fe_2B ; comportement mécanique ; adhésion ; tribologie ; lubrifiant ; comportement électrochimique.

« Effect of Microstructure on the Mechanical, Tribological and Electrochemical Behavior of Boride-Hardened Spheroidal Graphite Cast Iron (SG) »

Abstract:

This study examines the influence of varying Fe_2B layer thickness on the microstructure, mechanical properties, electrochemical, and tribological behavior of ductile and gray cast iron through boriding. Boronizing was conducted at 950°C for one and four hours using a B_4C-Na_2CO_3 pack-boriding method. Advanced analytical techniques, including optical microscopy, scanning electron microscopy (SEM), energy-dispersive X-ray spectroscopy (EDS), X-ray diffraction (XRD), and Vickers microhardness testing, were employed to analyze microstructural changes and mechanical properties. To assess the effectiveness and durability of the treatment, adhesion tests, scratch tests, and Daimler-Benz Rockwell-C adhesion tests were conducted. Additionally, tribological testing under controlled conditions and electrochemical experiments were conducted to assess friction, wear characteristics, and corrosion resistance. This research aims to provide insights into boronizing processes to optimise the performance of cast iron components across industrial sectors, including automotive, shipbuilding, and agriculture. Furthermore, the research contributes to the broader understanding of material behavior in materials science.

Keywords: Cast iron; Fe_2B; mechanical behavior; adhesion; tribology; lubricant; electrochemical behavior.

TABLE OF CONTENTS

LIST OF FIGURES

LIST OF TABLES

GENERAL INTRODUCTION

The field of research surrounding the boriding has experienced a surge in recent years, as evidenced by a 7.3% annual increase in publications (García-León, 2021)[1], This growth is driven by the necessity for the development of advanced surface engineering techniques with the aim of enhancing the mechanical and tribological properties of metallic components. Boriding is a thermochemical surface treatment process that involves the diffusion of boron atoms into the surface layer of a material, resulting in the formation of hard boride compounds that enhance wear resistance, hardness, and corrosion resistance [2-7].

Gray and ductile cast iron has gained significant popularity in the manufacturing sector due to its favorable characteristics, including ease of casting, machinability, and affordability. Gray and ductile cast iron is a material utilized as a staple in a multitude of industries, including automotive, oil, shipbuilding, and agriculture [8-10]. Despite its extensive use, there is a notable absence of research on the boronizing of both ductile and gray cast iron. This is evidenced by the paucity of studies conducted in this area, as documented in existing literature [10-12].

This study represents a significant advancement in the optimization of boriding processes tailored for cast iron. The study offers insights into the factors influencing boride layer formation, the effects of process parameters on microstructure and properties, and the challenges encountered in boriding cast iron. The findings will facilitate the design and optimization of boriding treatments, thereby enhancing the performance and durability of cast iron components across various industrial sectors, including automotive, aerospace, and machinery. Moreover, this work identifies research gaps, thereby guiding future investigations towards the development of novel materials or techniques. This will facilitate the advancement of boriding technology and the development of tailored solutions for specific cast iron applications. In conclusion, this comprehensive examination of cast iron boriding aims to foster improved mechanical, electrochemical, and tribological properties in cast iron components, thereby contributing to the broader field of surface engineering and inspiring further advancements in boriding technology.

The objective of this thesis is to investigate the boronizing process applied to ductile and gray cast iron through a systematic program of experimentation and analysis. By examining the experimental results, this study seeks to understand the effects of boron diffusion and reaction on the microstructure, mechanical properties, tribological, and electrochemical performance of these materials. The objective is to provide insights that can inform the

optimization of boronizing processes for improved performance and durability of cast iron components across various industrial sectors, including automotive, shipbuilding, and agriculture.

In order to achieve the aforementioned objectives, the work is divided into three chapters:

- Background and Literature Review, offers a comprehensive examination of the characteristics and potential enhancement of cast irons through boriding treatments. The review examines the chemical composition, microstructures, and properties of cast irons, with a particular focus on their modification for enhanced mechanical properties. The study examines boriding techniques, analysing the phases and parameters that affect the kinetics of boride formation. The review also demonstrates how borided layers enhance surface properties, such as hardness and wear resistance, which are beneficial for a range of engineering applications. In conclusion, the research contributes to the body of knowledge on the enhancement of cast iron performance through tailored treatments and surface engineering strategies.

- Materials and Experimental Techniques, This chapter delves into the meticulous world of experimental materials science, with the aim of unravelling the mysteries surrounding material behaviour and properties. In particular, it focuses on the boriding treatment process, which has the potential to enhance material surface properties in the face of environmental and mechanical challenges. A variety of advanced techniques are employed, including optical microscopy, scanning electron microscopy (SEM), energy-dispersive X-ray spectroscopy (EDS), X-ray diffraction (XRD), and a Vickers microhardness test, in order to establish microhardness profiles as a function of boriding time. This allows for the scrutiny of the structural, chemical, and mechanical attributes of materials. Adhesion tests, including scratch tests and Daimler-Benz Rockwell-C adhesion tests, are essential for evaluating the effectiveness and durability of the treatment. Tribological testing under controlled conditions helps us understand the friction and wear characteristics of the material post-treatment. Additionally, electrochemical experiments shed light on the corrosion resistance and electrochemical behavior of the material. The aforementioned methodologies are employed with the dual objective of elucidating the intricacies of boriding treatment and contributing to the broader understanding of material behavior, thereby advancing the field of materials science.

- Results and Discussions, presents a comprehensive analysis of the experimental endeavors undertaken, with a particular focus on the materials subjected to boriding treatment. The examination commences with an investigation of the structural and compositional alterations induced by boriding, employing techniques such as optical microscopy, scanning electron microscopy (SEM), energy-dispersive X-ray spectroscopy (EDS), and X-ray diffraction (XRD). This is followed by a discussion of the underlying mechanisms and material performance implications. Adhesion tests, including scratch tests and Daimler-Benz Rockwell-C adhesion tests, in conjunction with tribological testing under a range of conditions, provide insight into the adhesion properties, friction, wear characteristics, and lubrication requirements of borided materials. Electrochemical analyses employing techniques such as EIS and potentiodynamic polarization elucidate corrosion resistance and surface reactivity. Discussions delve into electrochemical mechanisms affecting borided material performance. Chapter 3 exemplifies our commitment to elucidating the complexities of materials behavior, advancing knowledge in surface engineering, tribology, and electrochemistry.

The present study is concluded with a general conclusion and prospects for further studies.

The following organizational chart illustrates the structure of work presented in this thesis manuscript.

Probing Boronizing Techniques: Experimental Insights into Cast Iron Enhancement

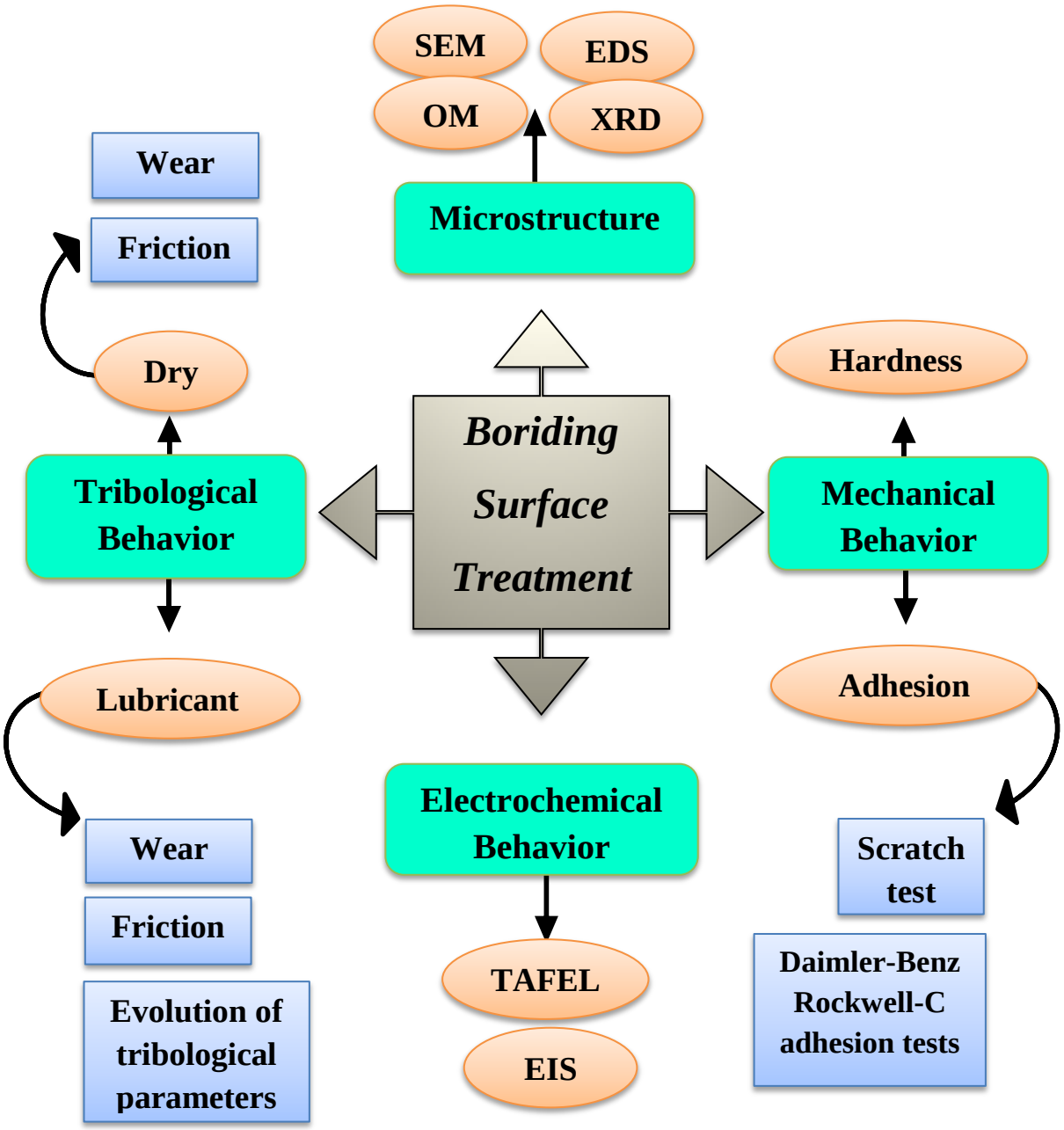

References

[1] R. A. García-León, J. F. Martínez-Trinidad, and I. J. T. o. t. I. I. o. M. Campos-Silva, "Historical Review on the Boriding Process using Bibliometric Analysis," vol. 74, pp. 541 - 557, 2021.

[2] K. Li *et al.*, "The tribological properties of bulk Fe2B with pre-oxidation treatment at 750° C in air," 2019.

[3] M. Kulka, M. Kulka, and Castro, *Current trends in boriding*. Springer, 2019.

[4] I. E. Campos-Silva and G. A. Rodriguez-Castro, "Boriding to improve the mechanical properties and corrosion resistance of steels," in *Thermochemical surface engineering of steels*: Elsevier, 2015, pp. 651-702.

[5] M. J. C. T. i. B. Kulka, "Trends in Thermochemical Techniques of Boriding," 2018.

[6] S. A. da Costa Aichholz, M. S. Meruvia, P. C. S. Júnior, R. D. J. S. Torres, and C. Technology, "Tribocorrosion behavior of boronized AISI 4140 steel," vol. 352, pp. 265-272, 2018.

[7] T. Murakami, K. Matsuzaki, Y. Gomi, S. Sasaki, and H. J. M. O. P. L. Inui, "Microstructure and tribological properties of gray cast iron specimens coated by aluminizing, boronizing, chromizing and siliconizing," vol. 1516, no. 1, pp. 115-120, 2013.

[8] I. L. Velázquez, N. Lopez-Perrusquia, M. Doñu-Ruiz, E. G. J. M. Bustos, and Microanalysis, "Analysis Microstructural on Gray Cast Iron Boriding and Hydrogen of Permeation," vol. 25, no. S2, pp. 1602-1603, 2019.

[9] M. Paczkowska, W. Ratuszek, W. J. S. Waligóra, and C. Technology, "Microstructure of laser boronized nodular iron," vol. 205, no. 7, pp. 2542-2545, 2010.

[10] O. Azouani, M. Keddam, O. Allaoui, A. J. P. o. M. Sehisseh, and P. C. o. Surfaces, "Characterization of boride coatings on a ductile cast iron," vol. 53, no. 2, pp. 306-311, 2017.

[11] U. Sen, S. Sen, F. J. I. L. Yilmaz, and Tribology, "Effect of process time on the tribological properties of boronized GGG-80 ductile cast iron," 2005.

[12] R. Ipek, B. Selçuk, M. Karamiş, V. Kuzucu, and A. J. J. o. M. P. T. Yücel, "An evaluation of the possibilities of using borided GG25 cast iron instead of chilled GG25 cast iron (surface properties)," vol. 105, no. 1-2, pp. 73-79, 2000.

CHAPTER 1

BACKGROUND

AND LITERATURE REVIEW

Introduction:

This chapter provides an overview of the fundamental background and a literature review. It is divided into three sections. Section 1.1 Exploring the Historical Evolution of Cast Iron: A Comprehensive Review. Section 1.2 presents the background on boriding thermochemical surface treatment. Section 1.3 provides fundamental background information on mechanical properties, tribology, and electrochemistry, with a specific focus on borided materials. The section also discusses the effects of microstructure on the mechanical, tribological, and electrochemical behavior of borided alloys.

1.1 Exploring the Historical Evolution of Cast Iron: A Comprehensive Review

In the realm of modern engineering and manufacturing, cast iron remains a prominent material cherished for its exceptional mechanical properties, thermal conductivity, and cost-effectiveness. As industries strive for enhanced performance and durability, the engineering community consistently seeks novel methods to improve the surface properties of cast iron components. One such technique gaining considerable attention is boriding – a surface modification process that imparts unique wear, corrosion, and hardness characteristics to cast iron materials.

1.1.1 Historical Overview of Cast Iron

Cast iron has a long history dating back thousands of years. It was first produced in China around the 5th century BC using a primitive blast furnace. The knowledge of cast iron was making spread to the Middle East and Europe, where it became a valuable material for various applications, including tools, weapons, and architectural elements.

In the 17th century, advancements in iron smelting techniques, such as the use of coke as a fuel, led to the widespread production of cast iron in Europe. The industrial Revolution began with the widespread use of cast iron in machinery, infrastructure, and transportation.

Throughout the 19th and 20th centuries, cast iron remained a popular material in construction, engineering, and manufacturing due to its strength, versatility, and affordability. It was commonly used in a variety of applications, including bridges, buildings, machinery, and cookware.

Cast iron remains an important material in various industries today, although its use has declined in some areas due to the development of new materials and manufacturing processes. Its unique properties, such as excellent castability, good machinability, and high wear resistance, ensure that cast iron will continue to have a place in modern engineering and design.

1.1.2 Varieties of Cast Iron: Microstructural Insights and Chemical Composition.

Cast iron is a highly versatile material that has various types, each with unique properties and applications. Elliott (1988) has classified cast irons into flake, malleable, spheroidal, and compacted/vermicular types based on graphite morphology [1] (Fig 1.1.1). Ngqase (2020) has focused on white cast irons and high chromium white cast irons, which are used in high wear resistance applications[2]. Chakrabarty (2017) has discussed the role of heat treatment in enhancing the properties of different cast iron types such as gray iron, malleable iron, ductile iron, and high-alloy irons [3]. Radzikowska (2004) has provided a comprehensive overview of the composition and microstructures of cast irons, including non-alloyed and alloyed types[4].

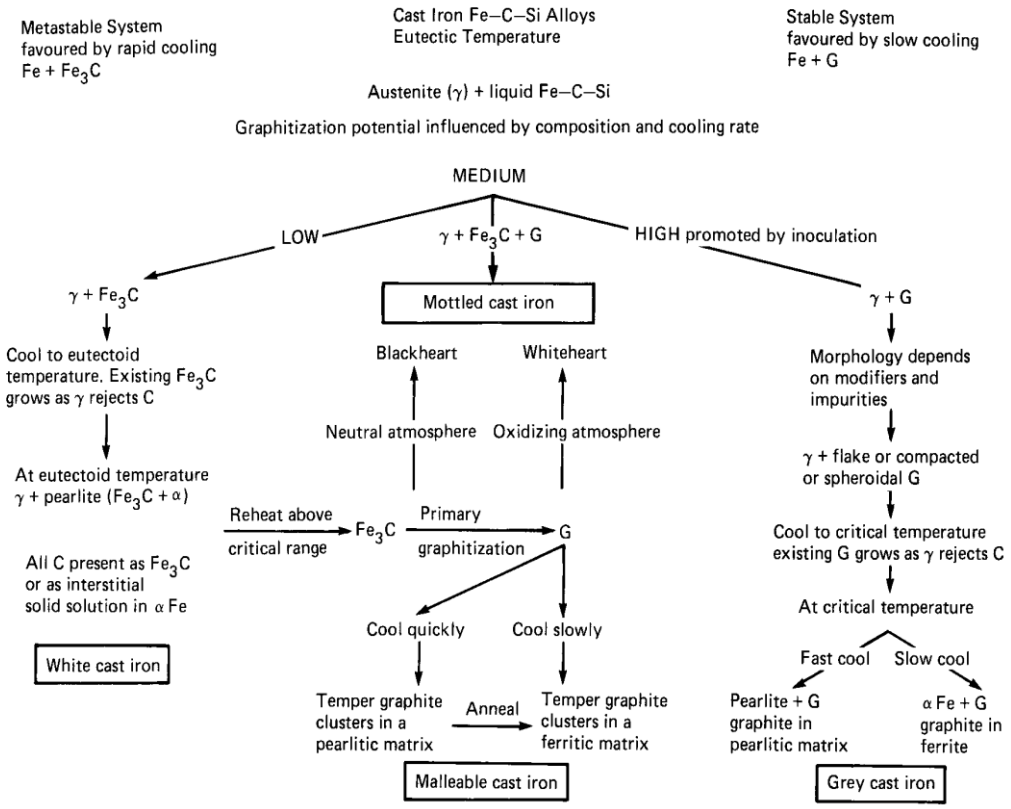

Figure 1.1.1 Schematic representation of the cast iron family [1]

The chemical composition of cast iron greatly influences its mechanical strength and microstructure (Vdovin, 2013; Tokova, 2019)[5, 6]. Non-alloyed cast irons typically contain 2.03% carbon, while alloyed irons have a wider range of compositions, often including higher amounts of silicon and manganese, as well as special additions such as nickel, chromium, and molybdenum (Radzikowska, 2004)[4]. In addition, the form of carbon precipitation and the matrix structure are important factors in determining the properties of cast irons. For example, carbides contribute to hardness and wear resistance, while graphite contributes to machinability and wear resistance (Elliott, 1988)[1].

Property	*S.I.*	*M.I.*	*F.I.*	*C.S.*	*W.I.*
Castability	1	2	1	4	3
machinability	2	2	1	3	-
Reliability	1	3	5	2	4
Vibration damping	2	2	1	4	4
Surface hardenability	1	1	1	3	-
Elastic modulus	1	2	3	1	-
Impact resistance	2	3	5	1	-
Wear resistance	2	4	3	5	1
Corrosion resistance	1	2	1	4	2
Strength/Weight ratio	1	4	5	3	-
Cost of manufacture	2	3	1	4	3

S.I. Spheroidal iron
M.I. Malleable iron
F.I. Flake iron
C.S. 0.3% C steel
W.I. White iron
1 = Best; 5 = Worst

Table.1.1.1 Comparing the Characteristics of Different Types of Cast Iron with 0.3% Cast Steel[1]

Mikhailovich (2013) and Silman (2014) both provide detailed classifications of cast iron types based on their structure and properties [7, 8]. Mikhailovich focuses on high-alloy white cast irons, while Silman's review covers common gray cast irons with different forms of graphite. Radzikowska (2003)[9] expands on this by discussing the solidification of graphite in cast irons and the different types of cast irons based on carbon content. Elliott (1988) provides a comprehensive overview of the nature of cast irons, including their properties and the importance of inoculation in their production. Taken together, these studies contribute to a

deeper understanding of the different types of cast irons based on their structure and properties **[**1**]**.

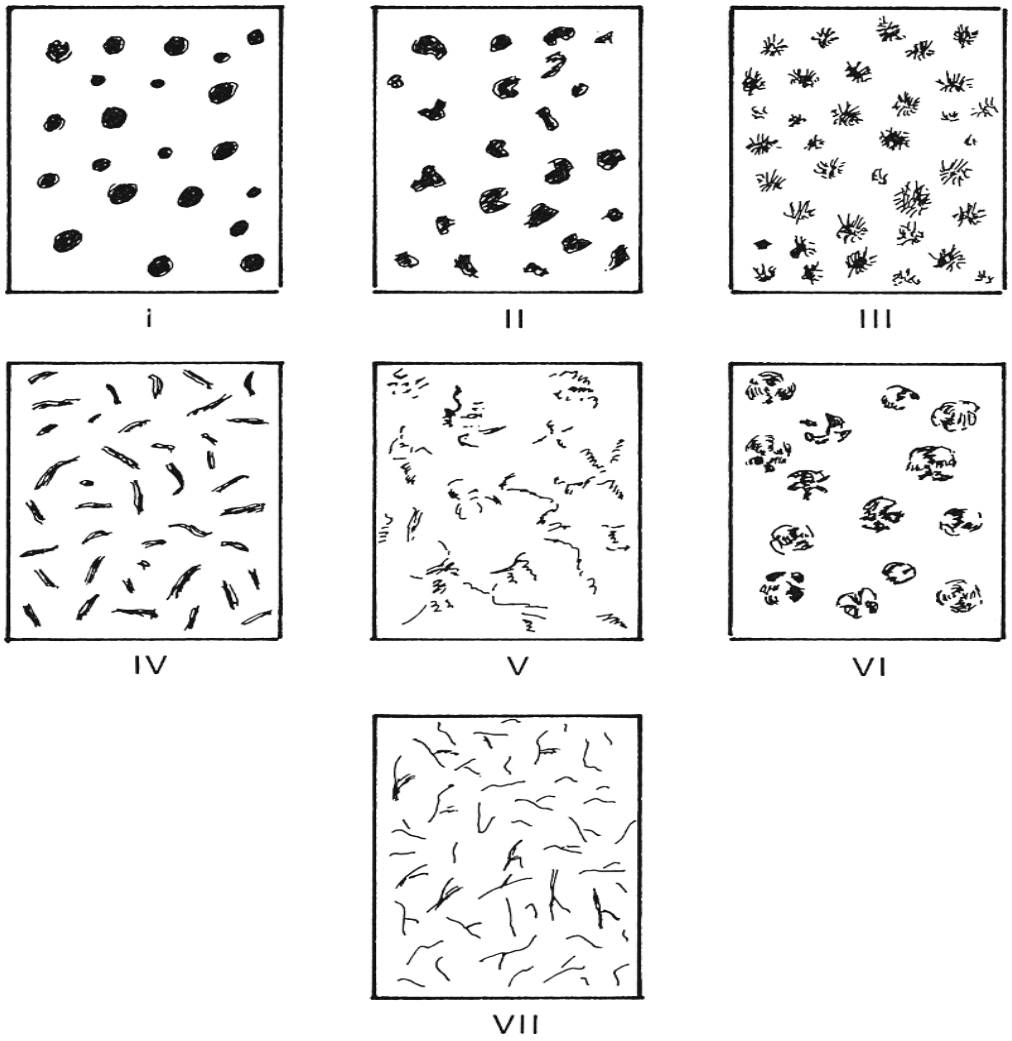

Figure 1.1.2 Seven Graphite Morphologies Defined in ASTM A247 [1]

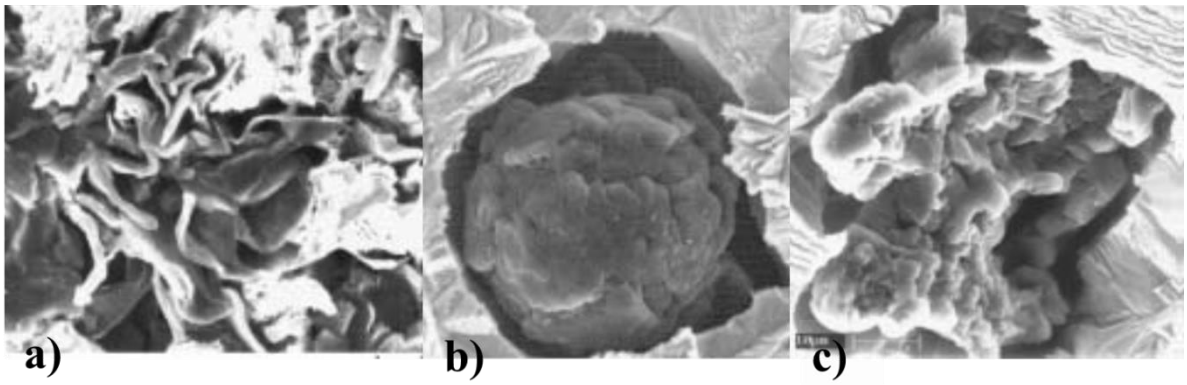

Figure 1.1.3 SEM examination of Flake graphite in as-cast gray iron (a) ;Nodular graphite in as-cast ductile iron(b); Compacted graphite(c). Samples was deeply etched with 50% HCl. [4]

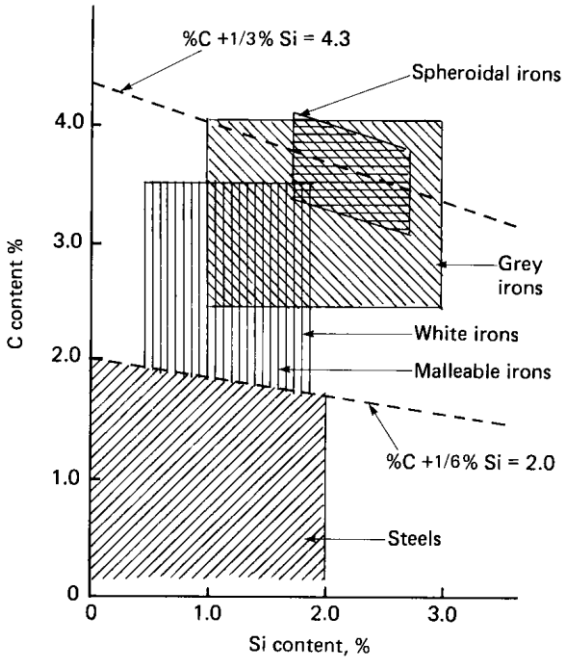

Figure 1.1.4 Range of different cast irons and steels in terms of C and Si composition [1].

1.1.3 The Significance of Cast Iron in Industrial Applications

The importance of cast iron in industry is underscored by its use in mining and metallurgy, where it enhances the durability of equipment (Lubyanoi, 2020)[10] . Quality management is crucial in this context, and innovative production facilities have been developed to improve resource conservation and environmental indicators (Farisov, 2022) [11] . The machinability of cast iron is also an important factor, and its use in various applications depends on this property (Sousa, 2018)[12].

1.1.4 Enhancing the Surface of Cast Irons: Rationale and Importance

Improving the surface of cast irons is essential for enhancing their mechanical properties and corrosion resistance (Rasulov, 2020)[13]. This can be achieved through methods such as surface impregnation and alloying, which can significantly increase wear resistance (Vodolazskaya, 2020) [14]. Furthermore, surfacing with globular graphite can improve the properties of high-strength cast irons (Govorun, 2018)[15]. Furthermore, studies have shown that modifying the surface of Ni-hard 4 cast iron with titanium can increase its hardness and wear resistance (Anandh, 2019) [16]. These findings emphasize the significance of surface improvement in enhancing the performance and longevity of cast iron products.

Thermochemical treatments, such as carbonitration, boronizing, and boro-austempering, have been shown to significantly improve the surface properties of cast irons. These treatments can increase surface hardness, wear resistance, and mechanical properties, making the cast irons more suitable for a wider range of applications (Vodolazskaya, 2020; Şen, 2004; Mariani, 2017)[14, 17, 18]. Furthermore, laser surface engineering (LSE) has been suggested as a highly localized treatment that minimizes workpiece distortion, thus improving the surface of cast irons (Boccardo, 2021)[19].

Boriding thermochemical treatments have been shown to significantly improve the surface properties, including the mechanical, tribological, and electrochemical behavior of cast irons. Şen (2004) demonstrated that boronizing at higher temperatures and for longer durations increased hardness and reduced fracture toughness, indicating that boriding can enhance the surface properties of ductile cast irons[17]. Mariani (2017) improved the mechanical properties of gray cast iron through boro-austempering treatments, which increased surface hardness [18]. Additionally, boriding treatments were found to be effective in enhancing the mechanical properties of gray cast irons. Medvedovski (2016) demonstrated that boride-based coatings significantly reduce wear losses and improve thermal and chemical stability in cast iron. Additionally, boride-based coatings have the potential to protect cast iron from wear, as these coatings show significantly lower wear losses compared to bare cast iron[20]. Meriç (2006) also reported improved abrasive wear behavior in boronized cast iron[21]. These studies collectively demonstrate the potential of boriding treatments to improve the surface properties of cast iron, making it more durable and wear-resistant. Krelling (2015) further supported these findings by showing that borided H13 steel exhibited a significant improvement in wear resistance[22].

1.1.5 Selection Rationale for Boriding Treatment

Boriding treatment is an affordable way to enhance the properties of cast iron. This treatment method significantly boosts surface hardness and wear resistance, making it ideal for severe service conditions (Medvedovski, 2016)[20, 23]. In addition to that, boriding treatment can be combined with other heat treatments such as austempering to further improve the mechanical properties of cast iron (Mariani, 2017)[18]. The addition of boron during heat treatment can lead to the formation of globular secondary carbides which can further improve wear resistance and hardness (Zeytin, 2011)[24]. Moreover, boronizing creates a boride layer that enhances the abrasive wear behavior of cast iron (Meriç, 2006)[21].

1.1.6 Impact of Boriding on the Microstructure of Cast Iron

The addition of boron to cast iron, known as boriding, significantly impacts the material's microstructure. Studies by Zhang (2010) and Bedolla-Jacuinde (2021) have shown that boron can increase the hardness of cast iron[25] [26]. Bedolla-Jacuinde (2021) specifically noted that this is due to a higher carbide volume fraction and the strengthening of the iron matrix[26]. Zhang (2010) and Mindivan (2016) both observed that the treatment can lead to the spheroidization of borides, resulting in increased toughness and wear resistance[25] [27]. This is further supported by Zhang (2011) and Kayali (2011), who found that the treatment can break up the boride network and distribute the particles uniformly in the matrix, improving toughness and microstructural properties. These changes in microstructure can increase toughness and wear resistance and lead to the formation of different matrix structures [28, 29].

1.2 Boriding Surface Treatment: An Introduction and Overview

The field of boriding cast iron has emerged as a significant area of research in recent years, driven by the necessity for the development of advanced surface engineering techniques with the objective of enhancing the mechanical and tribological properties of cast iron components. Boriding is a thermochemical surface treatment process that involves the diffusion of boron atoms into the surface layer of a material, forming hard boride compounds that improve wear resistance, hardness, and corrosion resistance. In order to effectively exploit the potential of boriding for cast iron, it is essential to have a comprehensive understanding of the existing literature.

1.2.1 Overview of the boriding treatment story:

The early discovery and development of the boriding process, also known as boronizing or boron diffusion, is not clearly associated with any one individual and was recognized as an effective surface treatment for metals in the early 20th century. As early as the 1930s, boriding was being used to improve the wear resistance of cutting tools, resulting in longer tool life and improved performance in metalworking operations. During World War II, the demand for improved surface properties on steel components led to further development and optimization of the boriding process. Boriding was applied to military equipment such as tank components and artillery, improving their durability and performance. Over the years, researchers refined the boriding process and developed various methods for introducing boron into the surface of metals. These methods included pack boriding, gas boriding and plasma boriding, each offering different advantages depending on the application requirements. As the understanding of boriding grew, its applications expanded beyond cutting tools and military equipment. The automotive, aerospace, and petrochemical industries began using boriding to improve the wear resistance and corrosion protection of various components such as engine parts, gears, and valves. Throughout the 20th century and into the 21st century, boriding received considerable attention from researchers and academia. Numerous studies focused on characterizing the boride layers, understanding the boriding mechanisms, and exploring the potential of boriding for new materials and applications.

The boriding process, a type of hardened material treatment, has seen a significant increase in scientific publications over the past few decades (García-León, 2021)[30]. This process

involves the diffusion of boron into the surface of metals, resulting in increased surface hardness and wear resistance (Cataldo, 2000)[31]. It is particularly beneficial for ferrous materials, improving their mechanical properties and corrosion resistance (Campos-Silva, 2015)[32]. The use of boriding in the industrial treatment of details and tools is also discussed, focusing on the factors that influence the choice of boriding technology (Krukovich, 2016)[33].

Boriding has become an integral part of the field of surface engineering and tribology, the study of friction, wear and lubrication. The development of advanced boriding techniques, such as duplex treatments that combine boriding with other surface modification processes, further expanded its capabilities fig1.2.1. Today, boriding remains an important surface treatment for improving the wear resistance, hardness, and corrosion resistance of various metals and alloys. Its applications span a wide range of industries and contribute to the improved performance and longevity of critical components. Ongoing research and technological advances promise even more exciting developments in the history of boriding in the years to come.[30]

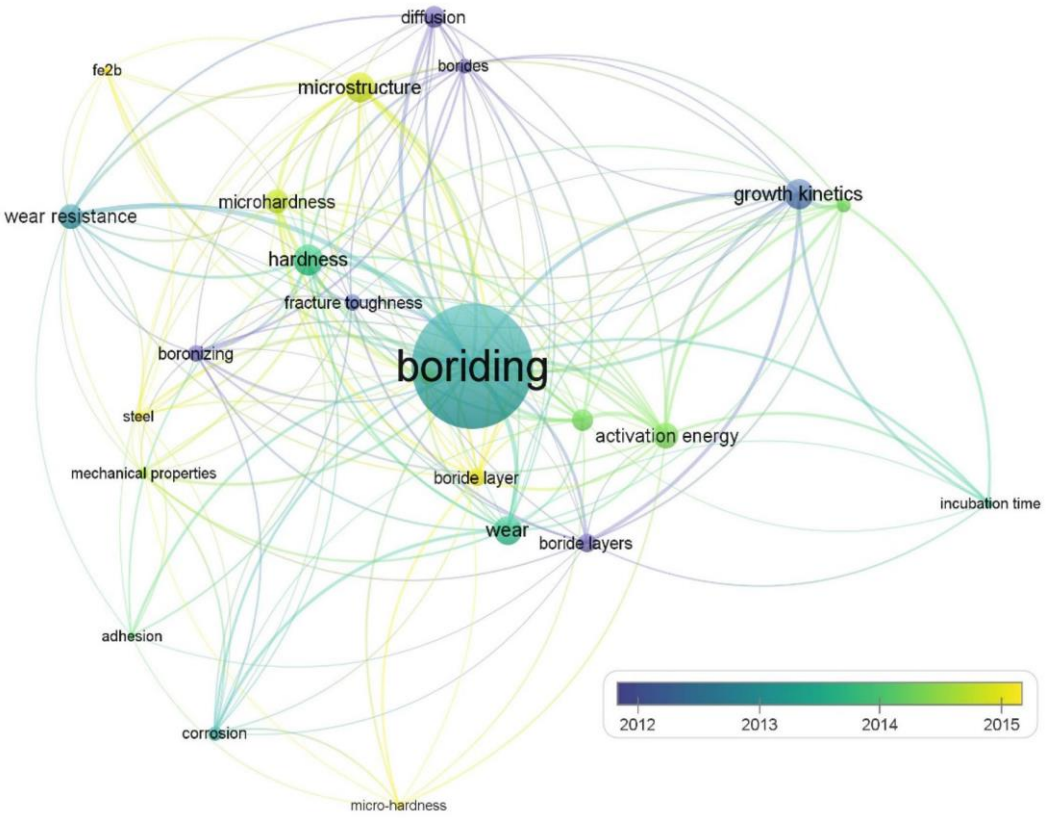

Figure 1.2.1 Keywords co-occurrence in boriding studies.[30]

1.2.2 Surface Thermochemical Treatments: A Focus on Boriding

Thermochemical treatments, also known as thermo-chemical treatments, are surface treatment processes applied to metallic materials to modify their physical, mechanical and chemical properties. These treatments involve the controlled exposure of metal parts to elevated temperatures and specific chemical environments to achieve desired surface characteristics.

There are several types of thermo-chemical treatments, the most common of which are:

- **Cementation:** This treatment consists of adding carbon to the surface of a material by heating it in the presence of a carbon source, such as carbon powder or carbon dioxide. Case hardening improves the hardness of the surface, creating a hardened outer layer while keeping the core of the material relatively soft.

- **Nitriding:** In this process, nitrogen is diffused into the surface of the material by heating it in the presence of nitrogen gas or nitrocarburising salts. Nitriding improves the wear, corrosion and oxidation resistance of the treated surface.

- **Nitriding-cementation:** This treatment is a combination of the two techniques mentioned above. It consists of enriching the surface of the steel with carbon and nitrogen simultaneously, creating a highly resistant outer layer.

- **Carbonitriding:** This treatment combines carburising and nitriding, resulting in a hardened, nitrogen-rich surface layer that offers improved wear and corrosion resistance.

- **Boriding:** In this process, boron is added to the surface of the metal material by heating it in the presence of boron powder or boron gas. Boriding improves hardness, wear resistance and corrosion resistance.

Thermochemical treatments are widely used in industry to improve the properties of metal parts, such as hardness, wear resistance, corrosion resistance and hardenability. These treatments are frequently applied to parts used in demanding applications such as automotive, aerospace, oil and gas, machine tools and many others.

1.2.3 Classification of Boriding Techniques: A Comprehensive Review

Boriding is a process that improves the properties of metal surfaces by coating them with boron. This can be achieved through three methods: solid media, liquid media, and gaseous boriding. Solid media boriding involves packing boron-rich powders around the metal and heating it in a furnace. Liquid media boriding involves immersing the metal in a bath of molten boron and other chemicals. Gaseous boriding exposes the metal to boron gas in a high-temperature environment.

1.2.3.1 Boriding in Solid Media

Solid boriding is a thermochemical process in which boron diffuses into a solid substrate by exposure to a boron-containing medium at high temperatures. The medium used in solid boriding can be a powder mixture, a salt bath, or a paste. Kulka on "Trends in Thermochemical Techniques of Boriding"[34] emphasizes that the powder-pack method is the most commonly used method for solid boriding.

The two main techniques of boriding in solid media have been classified: powder pack boriding and paste boriding.

a- Powder-Pack Technology

In this technique, the parts to be treated are placed in steel boxes filled with powder mixtures and then heated in muffle furnaces for a sufficient period of time. The time spent in the furnace must ensure that the temperature is homogenized throughout the volume of the parts to be treated. Kunst and Schaaber [35] were the first researchers to study solid boriding in powders in detail. This boriding technique uses a powder mixture consisting of a boron source, an activator and a diluent:

- Boron source: can be boron carbide B4C, ferroboron or amorphous boron.
- Activator: can be either $NaBF_4$, KBF4, $(NH_4)3BF_4$, NH4C1, Na_2CO_3 or BaF_2, which is a halogenated compound that transports the diffusing element (boron) in volatile halide form and releases it to diffuse into the substrate.
- Diluent: This is silicon carbide SiC or aluminum oxide Al_2O_3. The diluent is an inert substance added to the powder mixture to prevent sintering and reduce the boron potential.

The powder blends below are the most widely available on the market and are in use on an industrial scale.

- 5% B_4C, 90 % SiC, 5% $NaBF_4$
- 5% B_4C, 90 % SiC, 5% KBF_4
- 50% B_4C, 45 % SiC, 5% KBF_4
- 85% B_4C, 15 % $Na2CO_3$
- 95% B_4C, 5% Na2 CO_3
- 84% B_4C, 16% $Na_2B_4O_7$

Recent research in solid boriding has focused on optimizing the boriding parameters to improve the boride layer's microstructure and properties (Pandeeswari et al., 2023). Additionally, the use of alternative boron sources, such as boron carbide, has been investigated to enhance the boride layer's wear and corrosion resistance (Li et al., 2023). Furthermore, studies have been conducted on the growth kinetics of boride coatings during the boriding process and their effects on the fracture toughness and tool life of borided steels (Campos-Silva et al., 2008, 2013) as well as the characterization of rough interfaces obtained by boriding (Campos-Silva et al., 2008). These recent research efforts aim to improve the efficiency and effectiveness of solid boriding in enhancing the performance of metal substrates.

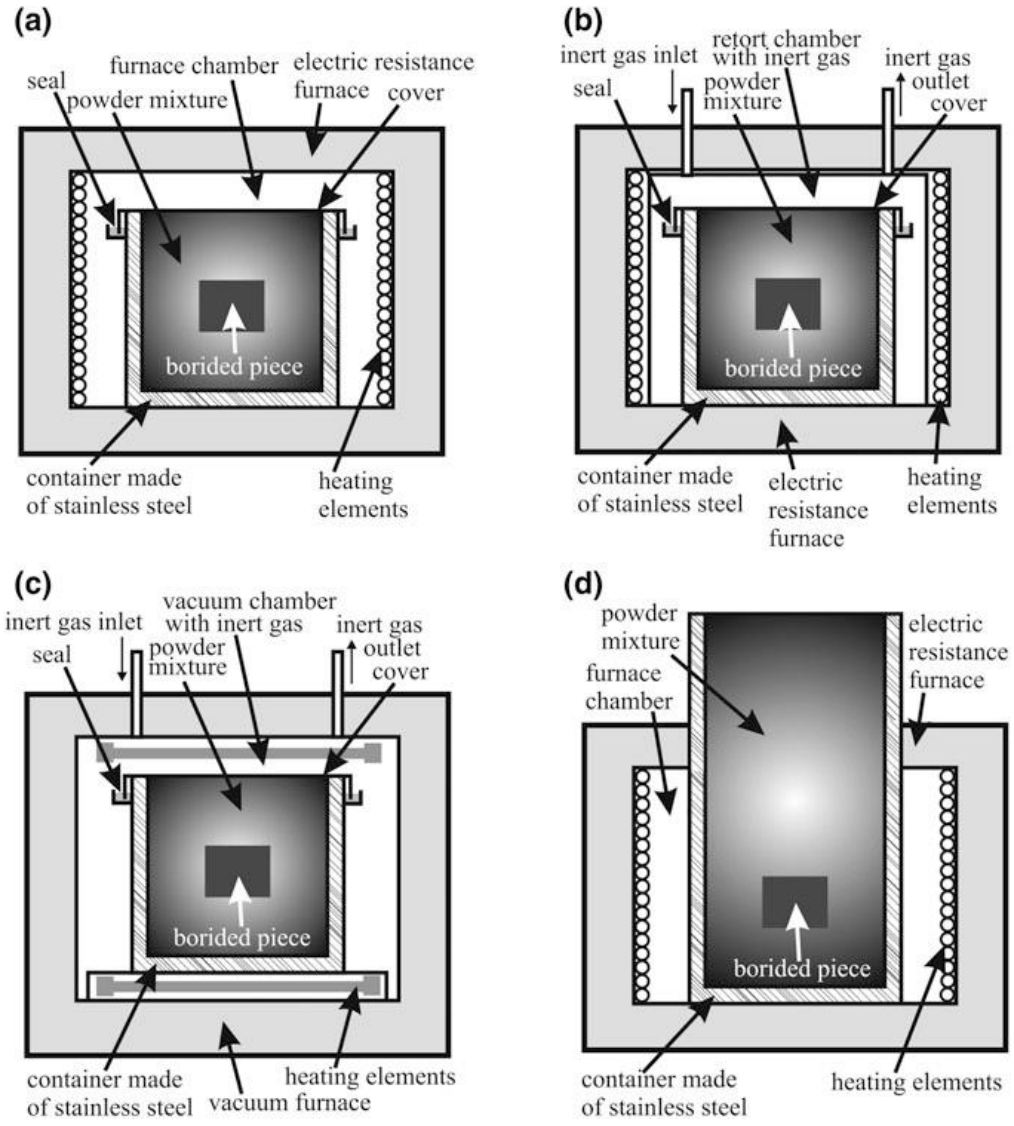

Figure 1.2.2 schematic illustrates the most efficient and simplified methods for powder pack boriding.[34]

b- Paste Technology

The paste-boriding method has been extensively studied for its safety, cost-effectiveness, and efficiency (Lee, 1999)[36]. (Kouba, 2015) (Kouba, 2015) has proposed a new model to simulate the paste boriding process, which predicts the kinetics of boride layer growth and the profiles of boron concentration [37].(Gunes, 2011) found that plasma paste boronizing produces thicker boride layers at lower temperatures than conventional methods [38]. While Campos (2007) conducted an evaluation of boron mobility during the paste boriding process, providing insights into the diffusion coefficients of boron in borided steels [39].

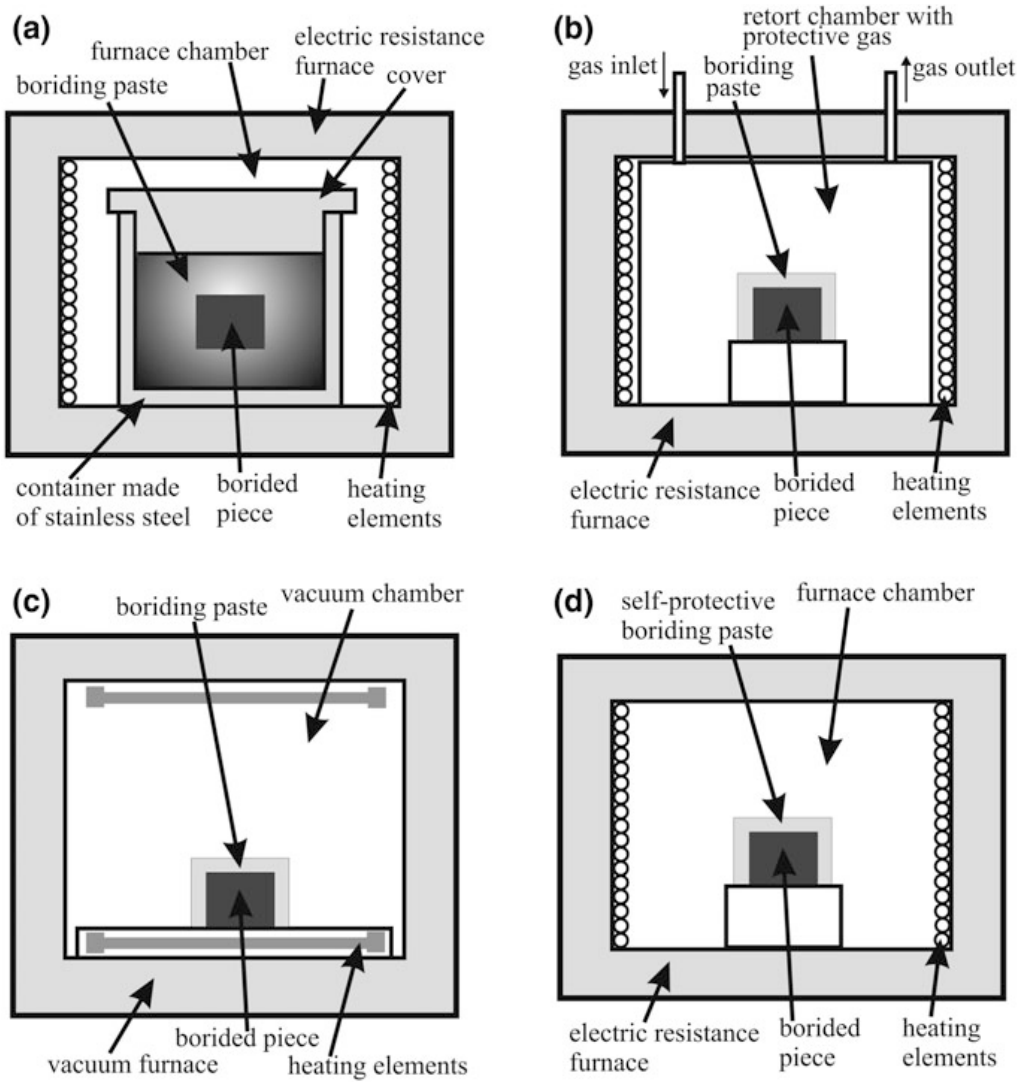

Figure. 1.2.3 2D schematic illustrations of the most effective and simplest paste boriding techniques. [34]

1.2.3.2 Liquid Boriding

Liquid boriding is a surface treatment process that enhances the hardness, wear resistance, and corrosion resistance of metals. This process involves immersing the material in a molten salt bath that contains boron-containing compounds, such as borax (sodium borate) or borax mixed with ferro-boron. The bath is heated to temperatures ranging from 800°C to 1050°C, depending on the material and desired properties. The material is immersed in a bath for a specific duration to enable boron diffusion into the surface, resulting in the formation of hard boride layers. The thickness and properties of the boride layers are determined by the duration of the treatment and the composition of the bath. Following the boriding process, the material is taken out of the bath, cooled, and cleaned to eliminate any remaining salts. Liquid boriding is recognized for its capability to generate consistent and regulated boride layers, rendering it appropriate for a broad spectrum of uses, such as automotive, aerospace, and tooling.

The liquid-boriding method is a thermochemical technique that has been the subject of investigation for boriding materials. As outlined by Anthymidis (2002) and Anthymidis (2003), the utilization of this method in a fluidized bed reactor results in the formation of boride coatings with high adherence and uniformity, as well as the generation of specific boride phases on diverse substrates[40] [41]. Kulka (2018) additionally compared this method with other boriding techniques, emphasizing its advantages and disadvantages.[34]. Nevertheless, Smol'nikov (1982) warned that the liquid-boriding method may not be suitable for high-speed steels with specific technical specifications[42].

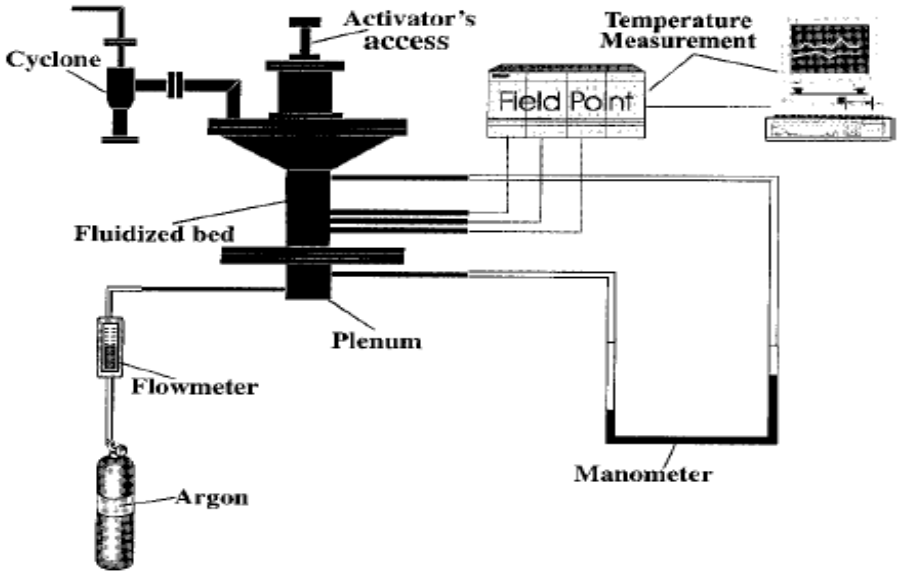

Figure 1.2.4 Schematic diagram of the fluidized bed reactor system utilized for boriding treatment[40]

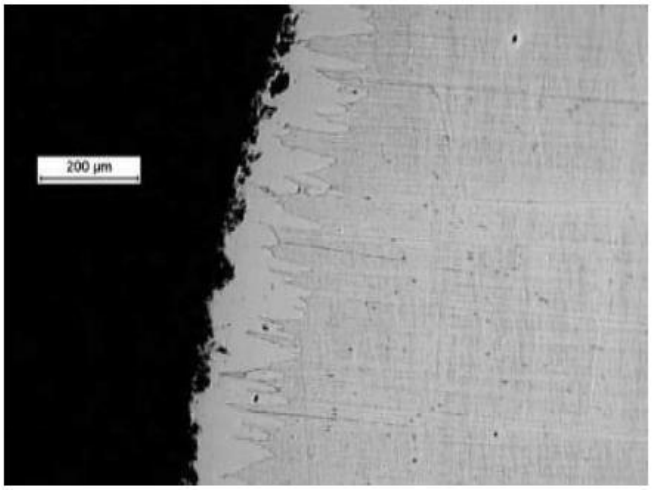

Figure 1.2.5 Typical micromorphology of boride coating on Co obtained in a fluidized bed reactor at 950°C after 3h [40]

1.2.3.3 Gas-boriding

Gas-boriding is a thermochemical surface treatment method that introduces boron into a material's surface to form hard boride layers. The process involves several key steps. First, the material is cleaned and prepared to remove any surface contaminants or oxides. Then, it is placed in a sealed chamber or retort with a boron-containing solid, such as boron carbide (B_4C) or boron nitride (BN), and a source of activator, such as aluminum or silicon. The chamber is purged with an inert gas, such as argon, to create a controlled atmosphere before being heated to the boriding temperature. This temperature typically ranges from 800°C to 1100°C, depending on the material and desired properties. The heating process is usually carried out in stages to ensure uniform formation of the boride layer. At the boriding temperature, boron from the solid source reacts with the activator to form reactive boron species, such as boron halides or boron oxides. These species diffuse into the material surface and react with the base metal to form hard boride layers. Once the boriding process is complete, the material is slowly cooled to room temperature to relieve internal stresses. Depending on the material and desired properties, the material may be quenched in oil or water to further enhance the hardness and structure of the boride layers. Some boriding processes may include post-treatments, such as tempering or stress relieving, to optimize the mechanical properties of the treated material. Gas-boriding is a complex process that requires precise control of temperature, atmosphere, and processing parameters to achieve the desired thickness and properties of the boride layer.

Various studies have explored the gas boriding method for boriding materials. Lee (1999) investigated the use of micro-pulsed PECVD to enhance boriding efficiency, while Skugorova (1973) identified optimal parameters for gas boriding using boron chloride and hydrogen[36] [43]. Kulka (2012) proposed a two-stage gas boronizing process in an N(sub 2)-H(sub 2)-BCl(sub 3) atmosphere to accelerate boron diffusion and limit the formation of brittle FeB phase[44]. Qin (2012) improved the process by simultaneously boriding and molybdenum alloying using the double glow plasma surface alloying technique. This resulted in an increased deposition rate and improved layer adherence [45].

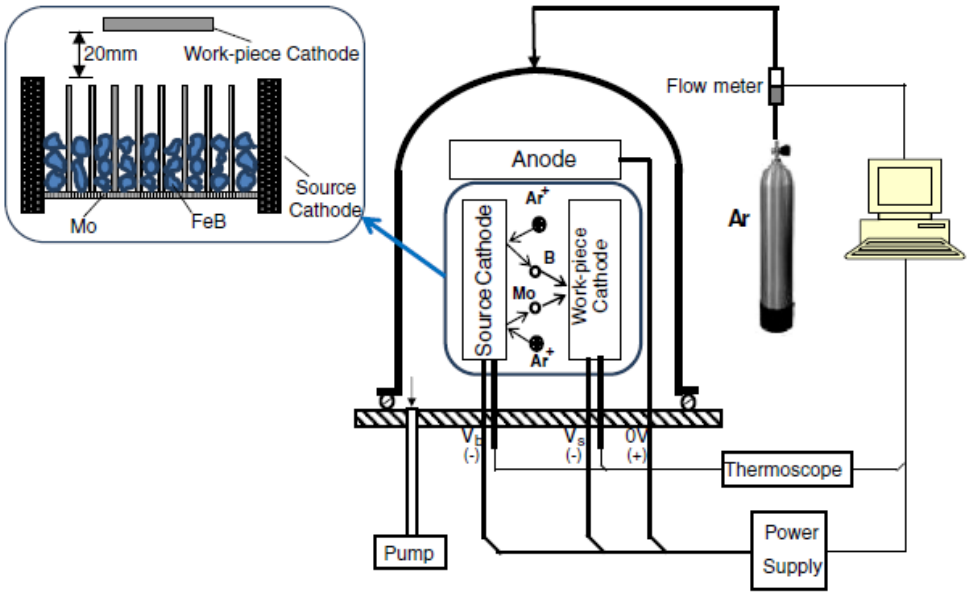

Figure. 1.2.6 2D schematic diagram of the double glow plasma surface Mo–B alloying process. [45]

1.2.3.4 The Plasma Boriding Technique

Plasma-boriding is a surface treatment process that enhances the hardness, wear resistance, and corrosion resistance of metals. The process involves cleaning the material surface to remove contaminants and subjecting it to a low-pressure plasma environment created using gases such as hydrogen and argon. Boron-containing gases, such as boron trichloride (BCl_3) or diborane (B_2H_6), are introduced into the plasma. They ionize and react with the material surface to form hard boride layers. The plasma's high energy ensures uniform and deep penetration of boron into the material. Following the boriding process, the material is cooled and may be quenched to further enhance the hardness of the boride layers. Plasma-boriding offers several advantages, including shorter processing times, lower treatment temperatures, and the ability to treat complex shapes. It finds applications in industries that require high wear resistance and durability, such as automotive, aerospace, and tooling.

The plazma-boriding method, a type of boriding, has been explored in various studies for its potential to enhance the mechanical properties and oxidation resistance of materials. Yavas (2019) demonstrated the formation of a molybdenum boride layer on TZM using the spark plasma sintering method, which significantly reduced mass loss during oxidation [46]. He (2015) developed a low-temperature boriding method for high-carbon steel, resulting in a thick boronized coating with increased surface hardness and reduced friction [47]. Lee

(1999) investigated the use of boron paste boriding and micro-pulsed PECVD for steel, while Ueda (2000) studied the boriding of nickel using a powder-pack method, both of which showed improvements in high-temperature hardness and friction and wear characteristics[36] [48]. These studies collectively highlight the potential of plazma-boriding for enhancing the properties of various materials.

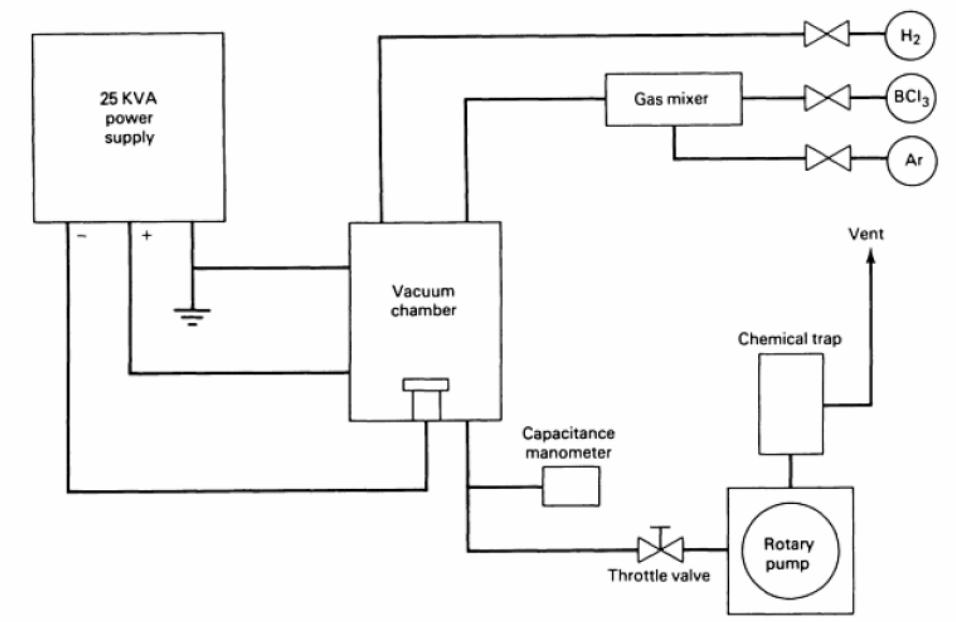

Fig. 1.2.7 Schematic diagram system utilized for Plasma boriding treatment

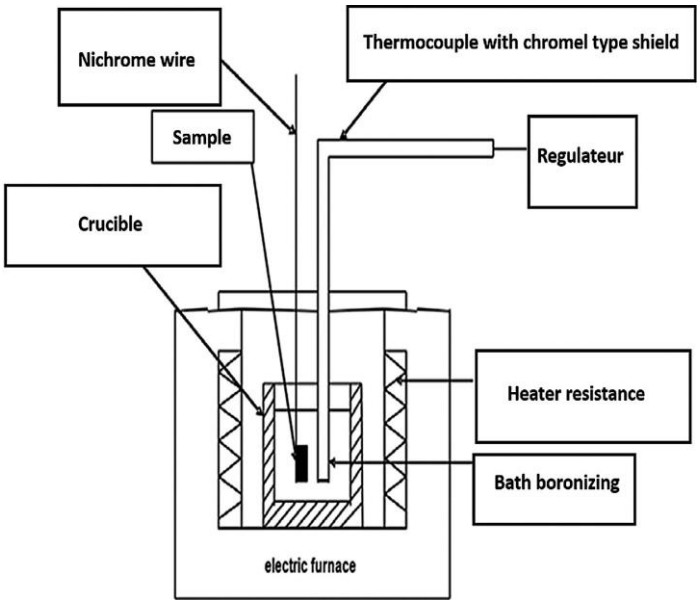

Fig. 1.2.8 Schematic illustration of the electrochemical cell process used to deposit boride. ***Kaouka*** **[49].**

1.2.4 Classification of Boriding Techniques: A Comprehensive Review of the Newly Proposed Classification.

Kulka, et al. (2019) proposes a simplified classification of boriding techniques into two main groups: chemical and physical, focusing on the technological aspects of the process. The classification is based on the production of active boron atoms or ions, which can be adsorbed onto metal alloy surfaces and diffuse into the substrate [50]. The most advanced techniques are presented in Figure below, which illustrates current trends in boronizing.

Krukovich, et al. (2016) proposed a comprehensive classification of boriding processes, which is partly similar to that of Minkevich (1965). The classification considers four aspects: the mechanism of generating saturating boron atoms, technological specifics, phase composition, structure and properties, as well as processing temperature and use [33] [51].

The process of generating saturating boron atoms is described, including the characteristics of the generation process and the methods used to generate saturating atoms or transport subions to the treated surface. Boriding methods are characterized by considering the flow and circulation of the gaseous atmosphere, contact processes in solid and liquid media, processes in liquid media with or without electrolysis, an electrostatic field, or ion implantation by immersion in plasma, as well as laser or electron beam treatment.

Kulka, et al. (2019) in his work suggests a classification of boriding methods, highlighting both physical and chemical techniques**[**50**]**. The means of saturating boron generation or subion transport are detailed, including boron halides, boranes, alkyd boron compounds, powder mixtures, aqueous salt solutions, and suspensions, as well as electromagnetic fields. The classification considers the phase composition, structure, and properties of boride layers, distinguishing between surface technological boride layers and coatings. Additionally, it categorizes iron alloy boriding processes based on temperature, with high-temperature boriding occurring above 900°C, medium-temperature boriding occurring between Ac1 and 900°C, and low-temperature boriding occurring between 550°C and Ac1. The simplified classification, based on Przybyłowicz's earlier work, highlights the main trends in boriding. It distinguishes between chemical (thermo-chemical) and physical techniques (glow discharge, ion implantation, high-energy methods).

Kulka, et al. (2019) work proposes modifications to the classification of boriding techniques, with a focus on physical techniques**[**50**]**. The methods are categorized into three groups: glow discharge boriding, boron ion implantation, and high-energy methods. Glow discharge boriding techniques are further divided into four methods based on the boron source (gas, paste, liquid, and powder). Ion implantation can be performed using beamline or plasma immersion processes. The phrase 'laser alloying with boron' has been replaced with 'surface alloying with boron' and is classified as one of the high-energy techniques. High-energy techniques are characterized by two groups: surface alloying with boron and the formation of boride coatings. Boride coatings can be produced through thermal spraying, detonation spraying, and coating. Powder boriding methods also include the use of electrically conductive powder. In addition to conventional gas boriding methods, the text specifies a further method: gas boriding using boron powder in a hydrogen atmosphere. The text highlights the most advanced methods and distinguishes between two main types of boron-coated surface layers: surface technology layers and coatings. Boron-containing surface technology layers are produced using non-decremental techniques. Coatings can be produced through various methods, including thermal spraying, hot-dip metallization, and CVD and PVD techniques. High-energy methods, such as thermal spraying, detonation spraying, and boron coating, are considered the most effective for producing boride coatings**[**50**]**.

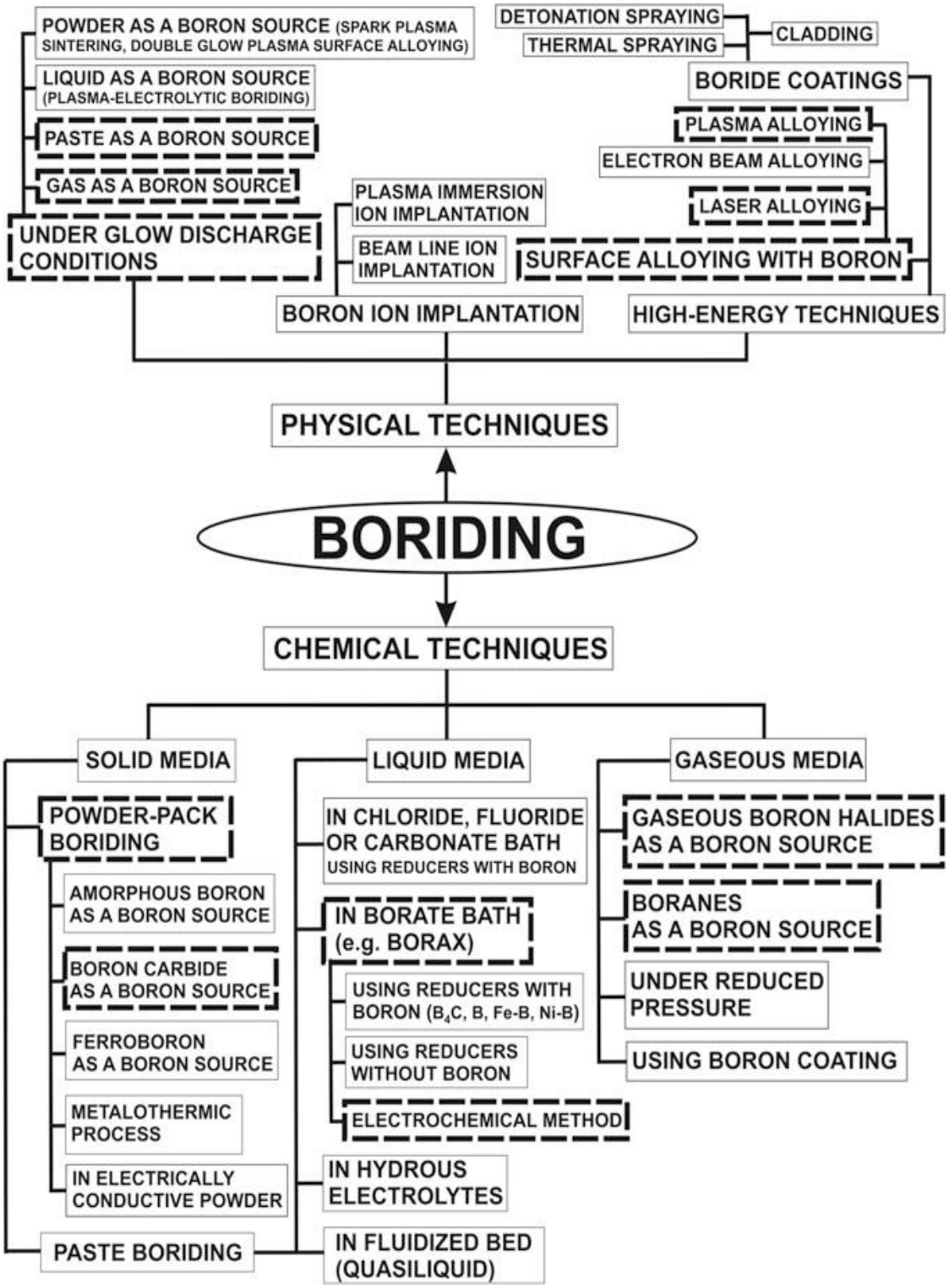

Figure 1.2.9 Boriding Techniques Classification [49]

1.2.5 Boron-Treated Substrates

Borided materials encompass a diverse array of substrates, including iron alloys, which span a wide spectrum of compositions and properties. These iron alloys, ranging from steels to cast iron and cast steels, are frequently subjected to boriding treatments, as they exhibit excellent responsiveness to the process, resulting in augmented mechanical properties and wear resistance. Furthermore, non-ferrous materials, including nickel-based, cobalt-based, and titanium alloys, are also frequently subjected to boriding treatments to enhance their surface characteristics Fig 1.2.10. This versatility extends boriding's applicability across a broad range of materials in various industries, underscoring its significance in surface engineering and materials science.

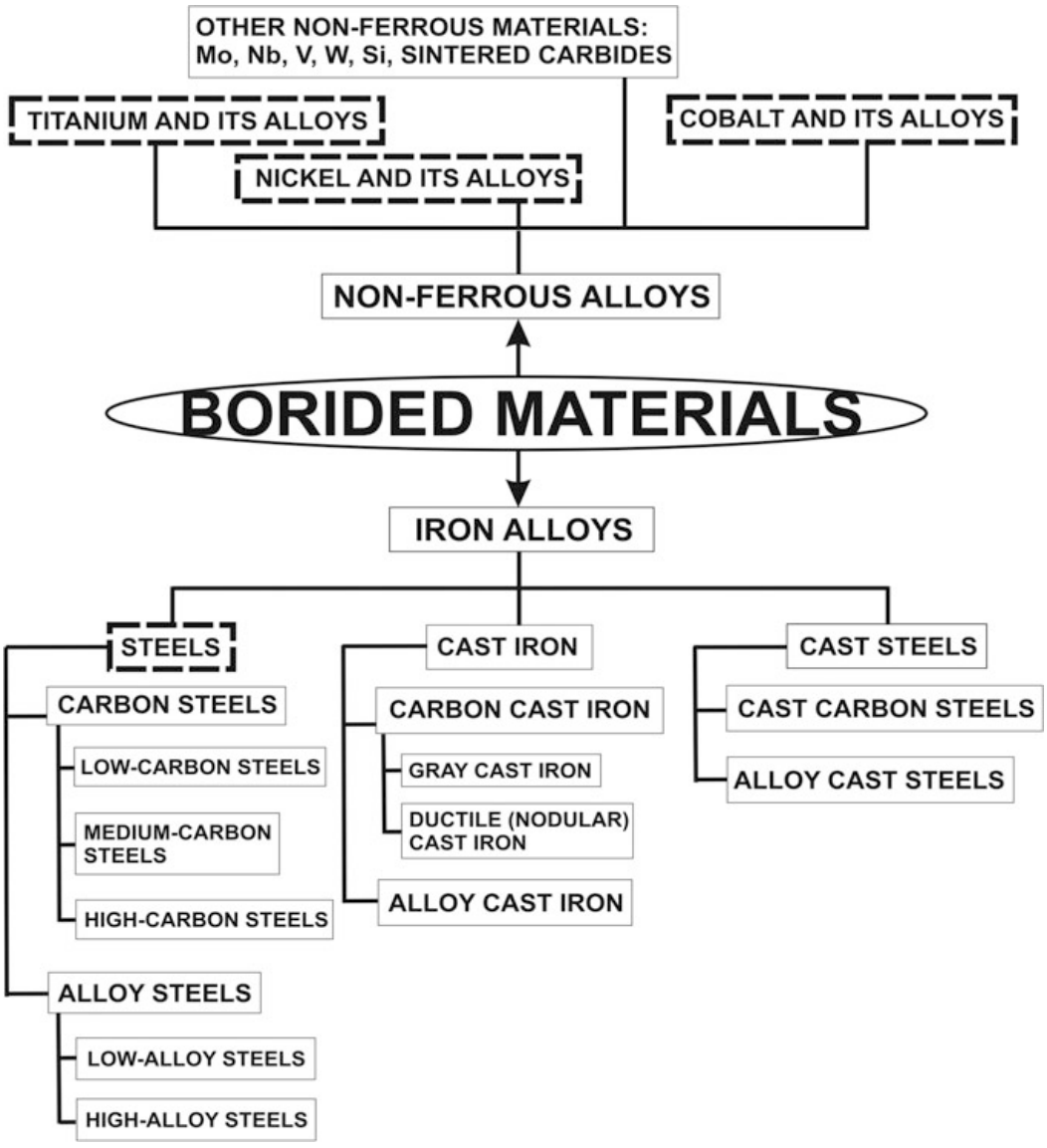

Figure 1.2.10 The principal substrates utilized in the production of boride coatings [50]

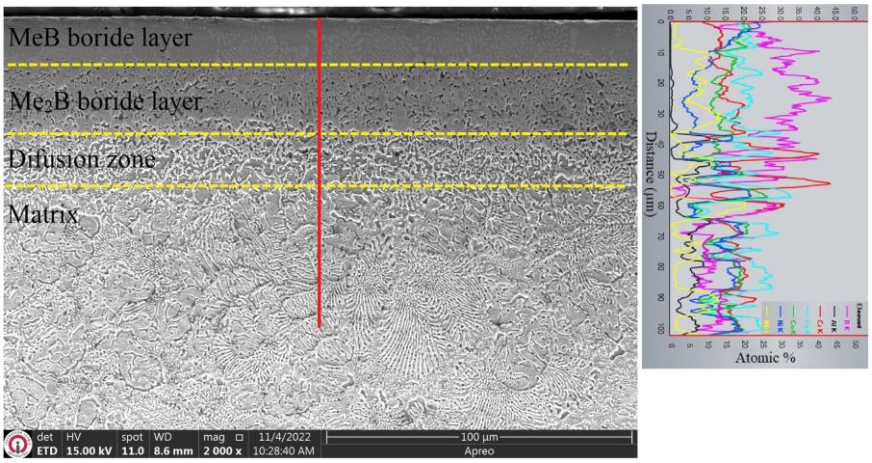

Fig 1.2.11. A sectional surface scan using SEM and EDS line analysis of the CoCrFeNiAl0.5Nb0.5 high-entropy alloy (HEA) after boriding at 1000°C for three hours is presented [52]

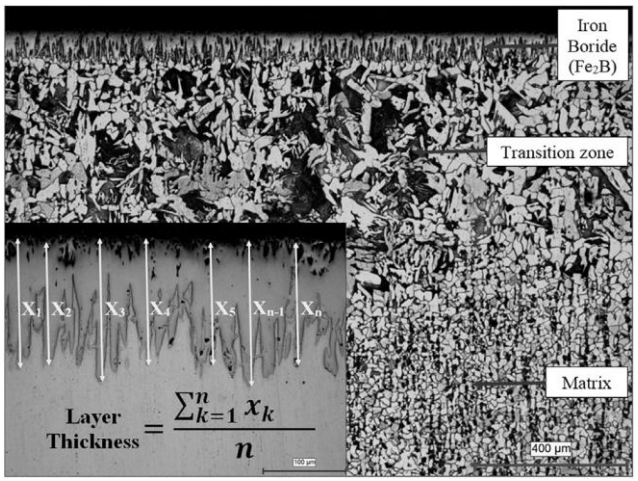

Fig 1.2.12. A schematic illustration of the procedure for measuring the thickness of the boride layer accompanies the cross-sectional view of borided SAE 1020 steel. [53]

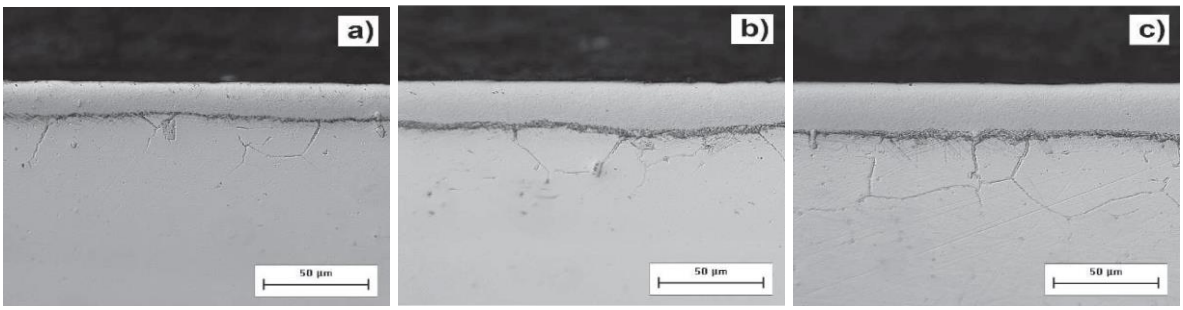

Fig 1.2.13. Cross-sectional examinations of borided Inconel 718 superalloy at 1223 K with exposure durations: (a) 2 hours, (b) 4 hours, and (c) 6 hours [54].

1.2.6 Different Phases of Boriding Iron Alloys

The boriding process can result in the formation of several distinct phases of borides on the surface of iron alloys. These phases include:

1.2.6.a Iron Borides (FeB and Fe_2B):

Iron borides, such as FeB and Fe2B, are the primary boride phases formed during boriding. These compounds exhibit high hardness and wear resistance, contributing to the improved surface properties of irons alloys.

1.2.6.b Intermetallic Borides:

Depending on the specific boriding conditions and alloying elements present in the irons alloys iron, other intermetallic borides may form. These borides can further enhance the material's surface properties, such as oxidation resistance and high-temperature stability.

1.2.6.c Influence of Boriding Parameters:

The parameters of the boriding process, including temperature, duration, boron source, and the composition of the irons alloys, significantly influence the resulting boride layers and their properties. These parameters control the diffusion kinetics and the formation of specific boride phases.

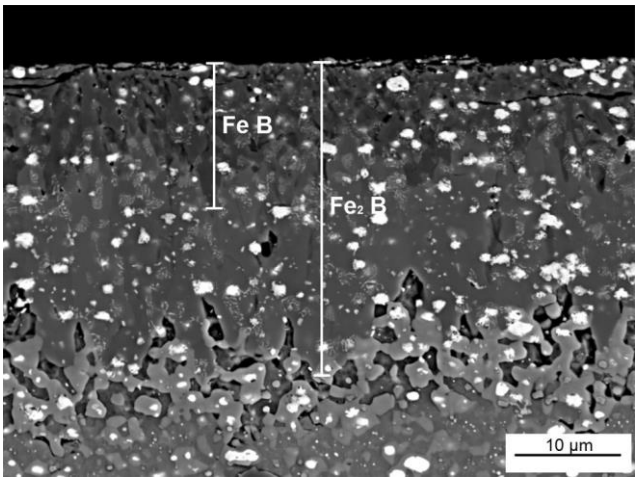

Fig 1.2.14. A representative cross-sectional view of the boride formed in AISI M2 steel when the boriding process was carried out at 1173 K and for duration of 6 hours. [55]

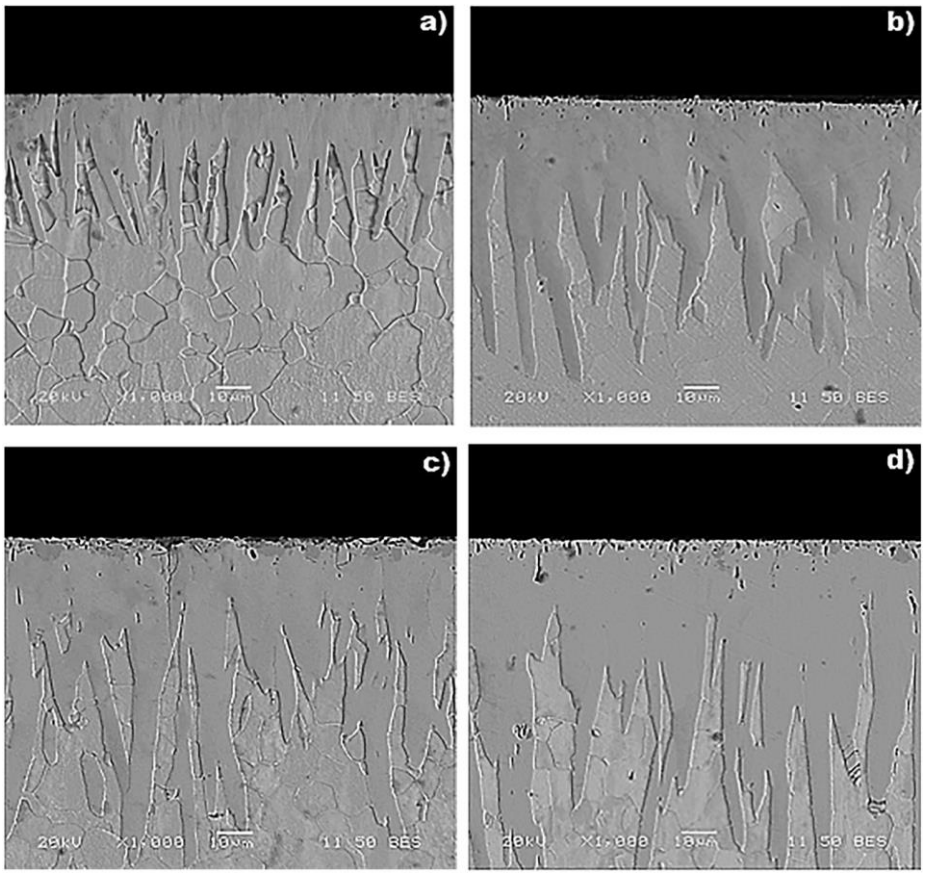

Fig 1.2.15. The preceding figures present cross-sectional views of boronized ASTM A1011 steel samples at 1123 K for increasing exposure times. The samples were observed at a) 2 h, b) 4 h, c) 6 h, and d) 8 h.[56]

1.2.7 Effects on Surface Properties:

Boriding leads to significant improvements in the mechanical and surface properties of iron alloys. The formation of hard boride layers enhances the material's hardness, wear resistance, and corrosion resistance. Borided iron alloys exhibit reduced friction, improved surface integrity, and extended service life in demanding applications.

In summary, thermochemical treatments, specifically boriding, offer a means to enhance the surface properties of irons alloys. The diffusion of boron into the material's surface forms hard boride layers, resulting in improved hardness, wear resistance, and corrosion resistance. The specific boriding method, boriding parameters, and resulting boride phases can be tailored to meet the requirements of different applications, providing irons alloys with enhanced surface performance in challenging environments.

1.3 Mechanical, Tribological, and Electrochemical Behavior of Borided Layers: A Comprehensive Review

The mechanical, tribological, and electrochemical behavior of borided layers on cast irons is a topic of significant interest as it provides insights into the enhanced surface properties and performance of the material. The borided layers, formed through the boriding process, exhibit distinct characteristics that impact their mechanical, tribological, and electrochemical behavior.

1.3.1 Mechanical Properties

The borided irons alloys exhibit improved mechanical properties compared to the unborided material. The formation of hard boride compounds, such as FeB and Fe_2B significantly enhances the surface hardness and wear resistance. The borided layers typically exhibit a higher surface hardness than the base material, providing enhanced resistance to abrasive wear and minimizing material loss. Furthermore, the borided layers can exhibit improved adhesion strength with the substrate, ensuring better mechanical integrity and durability.

Mechanical properties are essential characteristics of materials that define their behavior under applied forces or loads. These properties are crucial in engineering and materials science as they determine how a material will perform in various applications. Strength, one of the key mechanical properties, describes a material's ability to withstand applied forces without deformation or failure. It includes parameters such as yield strength, ultimate tensile strength, and compressive strength. Hardness is an important property that indicates a material's resistance to deformation, indentation, or scratching, and is an indicator of its wear resistance. Elasticity refers to a material's ability to deform reversibly under stress and return to its original shape when the stress is removed, as quantified by Young's modulus. Ductility measures a material's ability to deform plastically without fracturing and is often assessed through elongation or reduction in area tests. Toughness is the combination of strength and ductility, which represents a material's ability to absorb energy before fracturing. Other important properties to consider in material selection and design include fatigue resistance, creep resistance, and impact resistance. These properties are critical for ensuring the reliability and longevity of engineered components.

1.3.1.1 Hardness

Hardness is a fundamental mechanical property that describes a material's resistance to deformation, indentation, or scratching. It is a key indicator of a material's strength and durability in various applications. Hardness can be measured using different scales, such as the Mohs scale, which rates the hardness of minerals from 1 (softest) to 10 (hardest), or the Vickers scale, which measures hardness by indenting a diamond-shaped pyramid into the material surface. The composition, microstructure, and processing methods of a material influence its hardness. High hardness materials are more resistant to wear and abrasion, making them ideal for applications where durability and longevity are critical, such as cutting tools, bearings, and wear-resistant coatings.

1.3.1.2 Adherence

Adherence, also known as adhesion, is a material property that describes its ability to stick or bond to another surface. This property is crucial in various applications where two materials need to be joined or bonded together, such as in coatings, adhesives, and composites. Adherence is influenced by factors such as surface roughness, surface energy, and the presence of contaminants. Good adherence is characterized by strong bonding between materials, while poor adherence can result in delamination, peeling, or bond failure. Surface treatments, such as cleaning, roughening, or using adhesion-promoting agents, can enhance the bonding between materials and improve adherence. Adherence is crucial for ensuring the reliability and performance of bonded materials in various applications. To ensure the reliability and performance of bonded materials, it is crucial to understand and control adherence.

1.3.1.3 Rockwell-C indentation adhesion test

The Rockwell-C indentation cohesion test is a standard method used to evaluate the cohesion or internal strength of materials, particularly metallic materials. It involves using a Rockwell-C hardness testing machine to apply a specific force to a material through an indenter, which is usually a diamond cone or a hardened steel ball. The depth of penetration is then measured. This test is primarily used to assess the mechanical properties of materials, including their hardness and strength.

In this test, a standardized indenter is pressed into the surface of the material to create an indentation. The depth of the indentation is then measured and correlated with the material's mechanical properties. The Rockwell-C scale is commonly used for harder materials such as steel and alloys. The cohesion of the material can be inferred from the shape and size of the indentation, as well as any cracks or deformations around the indentation site.

This test provides valuable information about a material's ability to resist deformation and fracture under applied loads. It is a common practice in quality control and materials testing in various industries, including manufacturing, construction, and aerospace.

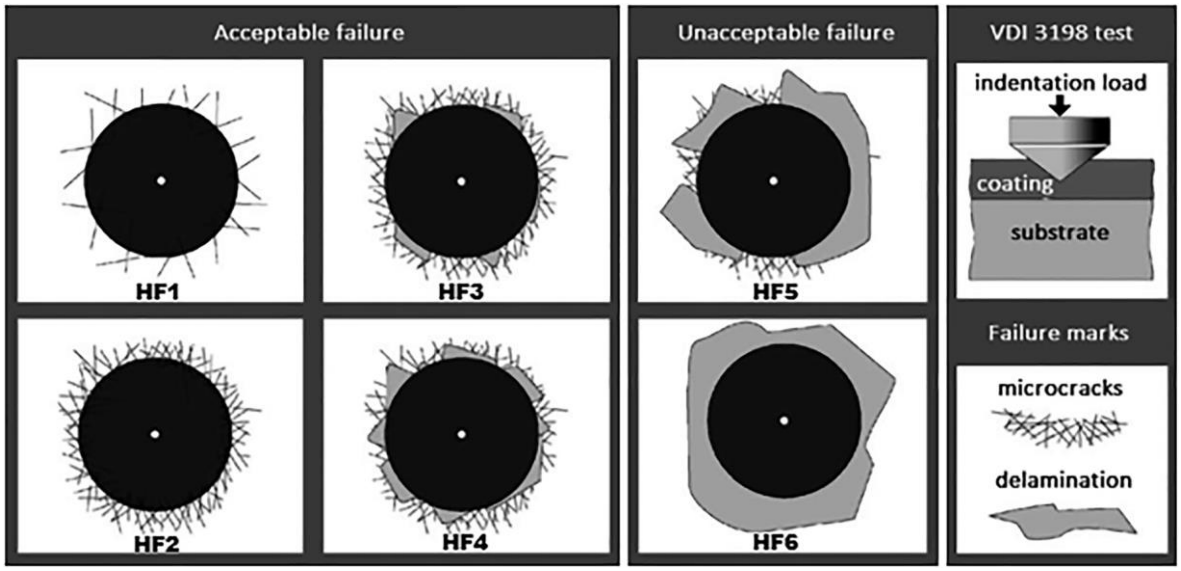

Figure 1.3.1 Rockwell-C Indentation Cohesion Test Comparative Maps[56] **[**[57]**]**

A recent study examined the cohesion behavior of various borided alloys:

- In his investigation, Irving Morgado-González, *et al. (2022)* employed the Rockwell-C indentation cohesion test, which is recommended by the VDI 3198 norm. This test was used to evaluate the cohesive nature of boride layers with respect to the ASTM A1011 steel substrate, which has been pack-boronized in the interval of 1123–1273 K for 2–8 hours [56].

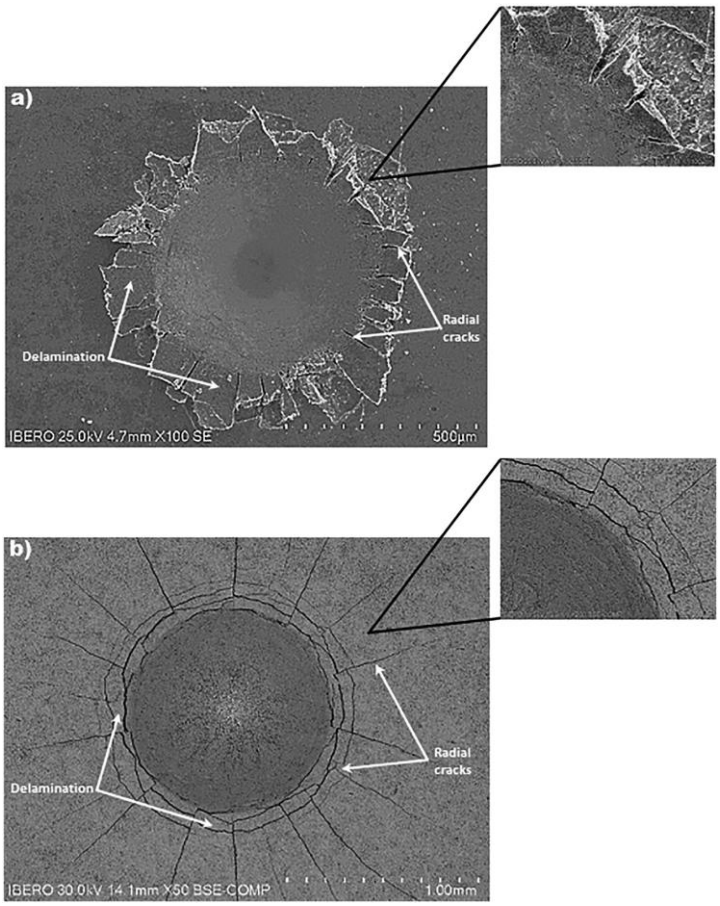

Figure 1.3.2 SEM micrographs of intended surfaces of boronized specimens by Rockwell C indentation tests for two boriding conditions [56].

Irving Morgado-González, et *al.* discovered that samples subjected to boronization at temperatures of 1123 K for 2 hours and 1273 K for 8 hours showed adequate cohesion, as confirmed by Rockwell-C indentation tests. Observations under a scanning electron microscope indicated the presence of indentation craters and cracks, but no delamination failure was observed in any of the tested samples. The cohesive strength of the boride layers

formed at different temperatures and durations corresponds to the HF4 and HF3 grades, respectively[56].

- The adherence of the boride layer to the AISI A572 steel was assessed by *Kheddam et al (2023)*[58]. using a Rockwell-C indentation cohesion test in accordance with the VDI 3198 Standard. After conducting this test, they compared the actual damage to the boride layer with the HF1 – HF6 cohesive strength quality maps.

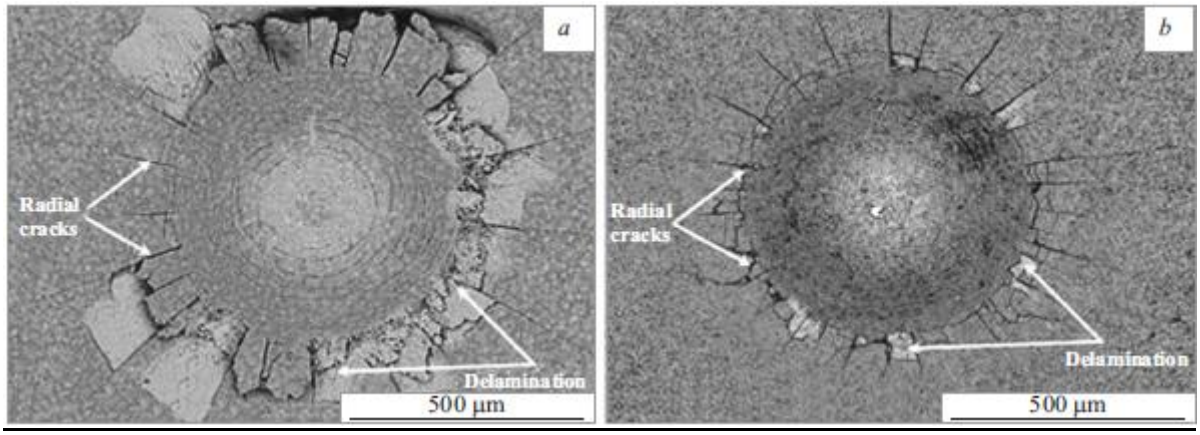

Figure 1.3.3 The microstructure of the friction surface of steel ASTM A572, observed via scanning electron microscopy (SEM), following 2-hour boriding at 1123 K (Figure a) and 8-hour boriding at 1273 K (figure b). [58]

Kheddam et al. observed that boriding steel AISI A572 resulted in the formation of craters on the surface, accompanied by radial cracks indicating delamination. This was evident after 2 hours of boriding at 1123 K and 8 hours of boriding at 1273 K. The cohesion of the borided steel matched the HF4 and HF3 categories, respectively, and remained acceptable for both treatments, in accordance with previous findings. The cohesion of Fe_2B iron diboride was found to be superior to that of double-phase boride layers. The adhesion of Fe_2B layers to steel Hardox-450 exhibited variability with the boriding conditions. Notably, 8-hour boriding at 1273 K provided an acceptable level of cohesion to the ASTM A572 substrate.

1.3.1.4 Scratch resistance

Scratch resistance is a mechanical property that refers to a material's ability to withstand surface damage caused by abrasion or scratching. This property is particularly important in applications where the material is exposed to abrasive forces, such as in automotive coatings, electronic displays, and protective coatings. The scratch resistance of a material depends on factors such as its hardness, elasticity, and surface roughness. Materials that exhibit high scratch resistance are less likely to display visible damage or wear when exposed to abrasive forces, resulting in increased durability and longevity in these applications.

Boriding treatment is a surface modification process that involves the diffusion of boron into a material substrate. This process has a significant impact on the mechanical properties of the material, particularly its hardness, scratch resistance, and adherence. Boriding forms hard boride layers on the material surface, which significantly increases its hardness. This enhanced hardness is crucial for applications that require resistance to deformation and scratching, as the hardened surface is better able to withstand abrasive forces. Furthermore, boride layers can improve the scratch resistance of materials, reducing the likelihood of surface damage and wear. Additionally, boriding treatment can enhance material adherence, improving its ability to bond with other surfaces. This is especially advantageous in applications where a strong bond between materials is crucial for optimal performance and reliability. Ongoing academic research in this field is exploring new boriding techniques and materials to further improve these properties for a variety of applications. Overall, boriding treatment is a promising approach for improving the mechanical properties of materials, making them more suitable for a wide range of applications where hardness, scratch resistance, and adherence are critical factors.

Various boriding techniques and materials have been studied to improve mechanical properties, hardness, scratch resistance, and adhesion. Campos-Silva (2016) demonstrated that diffusion annealing can enhance the adhesion resistance of boride coatings on steel substrates[59]. Eckardt (2000) found that introducing a hydrocarbon reactive gas during the sputtering process can decrease the coefficient of friction in boron carbide coatings[60]. Telle (1988) discussed the potential of grain size refinement and crack-propagation-influencing mechanisms in strengthening and toughening boride and carbide hard material composites[1].

Chiang (1996) demonstrated that ion implantation can modify the mechanical properties and adhesion of boron carbide films. Nitrogen ion implantation was found to reduce hardness and friction coefficient[61].

A recent study examined the scratching behavior of various borided alloys:

- A scratch test was conducted by Meneses-Amador (2017) on borided steel, AISI M2, at a temperature of 1173 K for a period of six hours. The objective was to assess the behavior of normal force and overall friction coefficient [55].

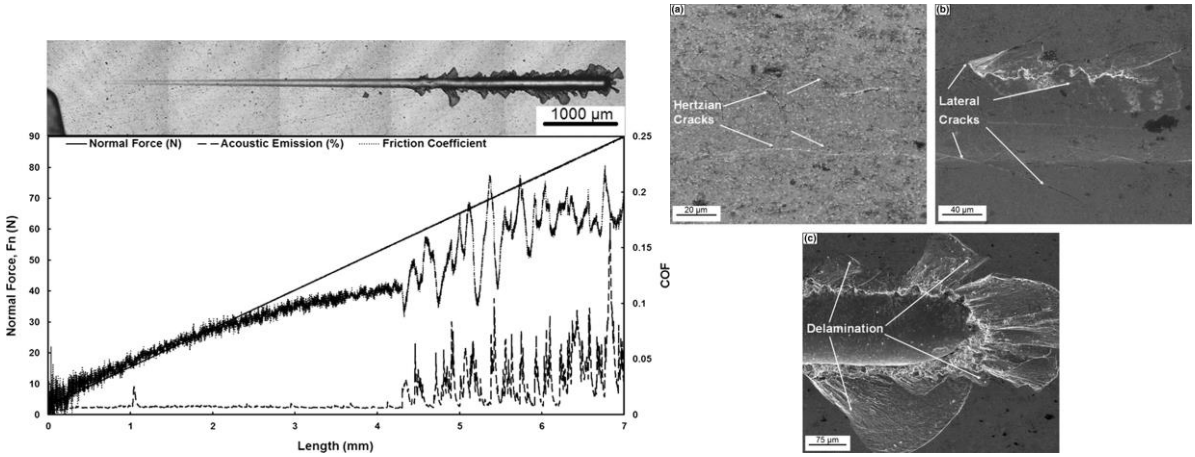

Figure.1.3.4 The failure mechanisms of AISI M2 borided steel observed in a scratch test conducted at a temperature of 1173 K for a period of six hours [55].

The research conducted by Meneses-Amador *et al.* showed that the critical load increased after 10 hours of exposure compared to 6 hours. This was due to the formation of two layers (FeB and Fe_2B) over the 10-hour period, leading to a decrease in impact strength. Once the yield strength is surpassed, fractures occur rapidly, with cracks in the FeB phase resulting from tensile stresses at the coating surface. The study also found that the thickness of the coating was the main factor affecting cohesive and adhesive strength. Additionally, the modulus of resilience and the distribution of residual stress in each of the boride phases were identified as significant factors influencing the overall mechanical properties.

- The findings of the empirical investigations conducted by *I. Campos-Silva et al. (2018)* indicate that the critical load required for scratch adhesion is linearly dependent on both the substrate hardness and the thickness of the applied layer.

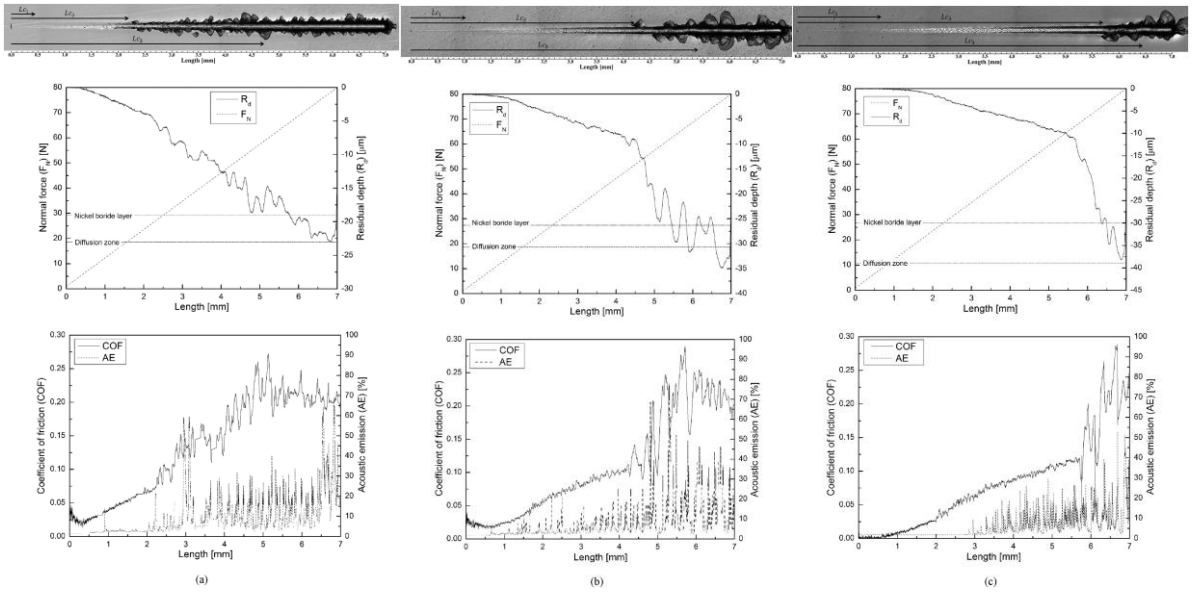

Figure.1.3.5 Borided Inconel 718 superalloy Scratch test failure mechanisms

This research investigates the behavior of four variables, namely FN, COF, Rd, and AE, as functions of the track length (L) in the context of scratching. (a) Borided Inconel 718 superalloy obtained after 2 hours of exposure, (b) after 4 hours, and (c) after 6 hours .

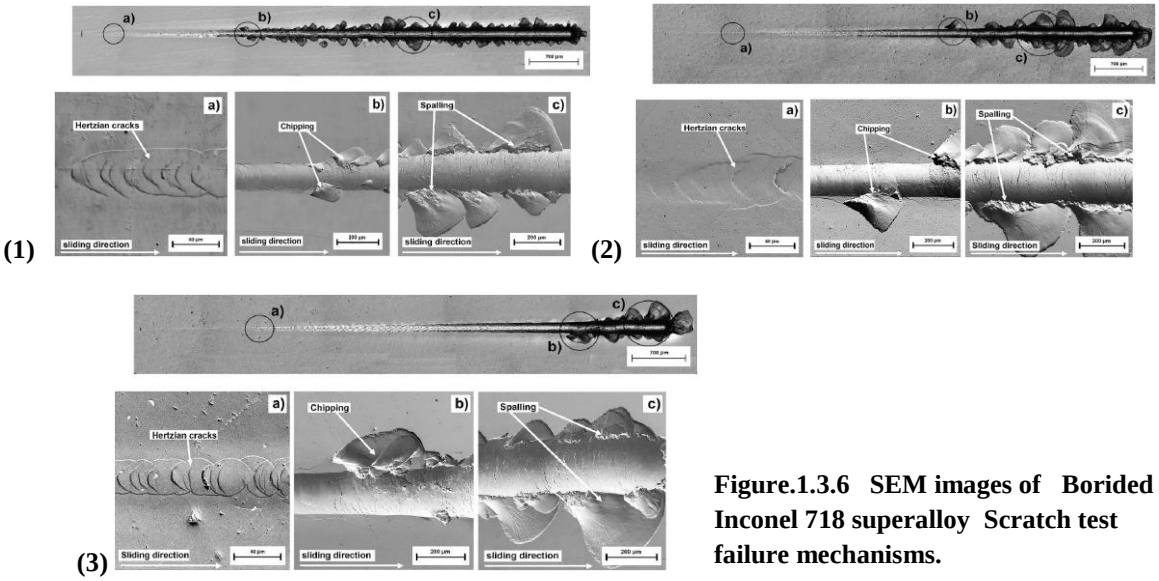

Figure.1.3.6 SEM images of Borided Inconel 718 superalloy Scratch test failure mechanisms.

The failure mechanisms observed on the surface of the scratch track were obtained through a series of experiments conducted at 1223 K with varying durations of exposure, specifically: (1) 2 h, (2) 4 h, and (3) 6 h.

1.3.2 Tribology : Tribological Properties

Tribology is the science and engineering of interacting surfaces in relative motion, including the study of friction, wear, and lubrication [62]. It involves understanding how surfaces interact with each other and their environments during motion and how these interactions can be manipulated to control friction, reduce wear, and improve the efficiency and reliability of mechanical systems [63]. Tribology plays a crucial role in various industries, including automotive, aerospace, manufacturing, and energy, where minimizing friction and wear is essential for optimal performance and longevity of machinery and equipment.

1.3.2.1 Friction

Friction is a force that opposes the relative motion or tendency of such motion of two surfaces in contact. It occurs due to irregularities in the surfaces, which interlock and resist sliding past each other. Friction can be categorized into static friction, which prevents an object from moving when a force is applied, and kinetic friction, which acts between moving surfaces. The coefficient of friction is a measure of the amount of friction between two surfaces. It depends on factors such as the nature of the surfaces and the presence of lubricants. Understanding and controlling friction is essential in various applications, from engineering to everyday activities, as it affects the efficiency, wear, and performance of mechanical systems.

1.3.2.2 Wear

Wear is the gradual removal or deformation of material at solid surfaces in contact, leading to changes in shape and surface properties. It can be caused by various mechanisms, including abrasion, adhesion, and fatigue. Wear can significantly affect the lifespan and performance of mechanical components, making it a critical factor in materials selection and design.

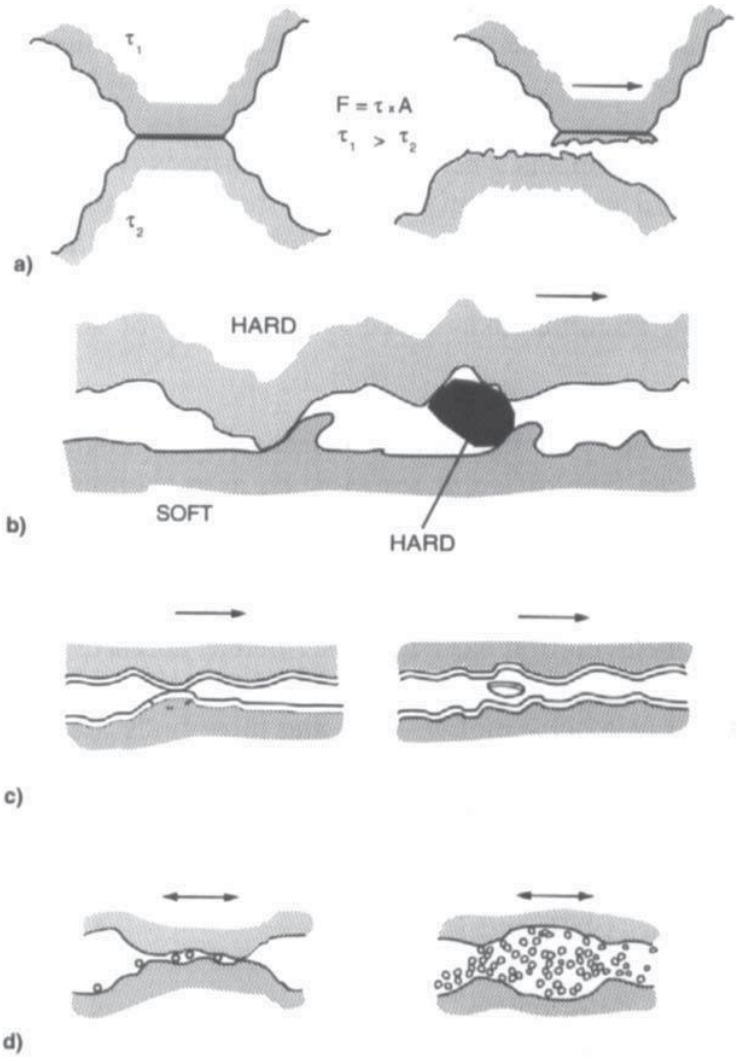

Figure 1.3.7 Schematic representation of the basic mechanisms of wear: a)adhesive, b) abrasive, c) fatigue, and d) chemical [62].

a. Adhesive wear, also known as galling or scuffing, is a form of wear that occurs when two surfaces slide against each other under load and adhere together, causing material transfer between the surfaces. This type of wear is common in metal-to-metal contact and can lead to surface damage and loss of material. Adhesive wear is influenced by factors such as surface roughness, contact pressure, sliding speed, emperatures, and the properties of the materials involved.

b. Abrasive wear is a type of wear caused by the mechanical action of abrasive particles or hard surfaces sliding or rolling against a softer material. This abrasive

action leads to the removal of material from the softer surface, resulting in wear. Abrasive wear is common in industrial applications where materials are exposed to abrasive contaminants or environments. It can lead to the degradation of surfaces and components, reducing their functional lifespan.

c. **Fatigue wear** is a type of wear that occurs over time due to repeated loading and unloading cycles, leading to material damage and failure. It typically occurs in materials subjected to cyclic stress, such as mechanical components like gears, bearings, and springs. The repeated stress cycles cause microscopic cracks to form and propagate, eventually leading to material failure. Fatigue wear is influenced by factors such as the magnitude and frequency of the applied stress, the material's fatigue strength, and the presence of defects or surface irregularities.

d. **Chemical wear**, also known as chemical erosion, is a form of wear caused by chemical reactions between a material and its environment. This type of wear occurs when a material is exposed to corrosive substances, such as acids, alkalis, or salts, which can degrade the material's surface over time. Chemical wear can lead to material loss, surface roughening, and structural damage, impacting the performance and integrity of the affected components.

Boriding treatment is a thermochemical surface modification process that has been extensively studied due to its profound effects on the tribological properties of materials. The process involves the diffusion of boron atoms into the material's surface, forming hard boride layers. These layers significantly reduce the coefficient of friction, improving the material's wear resistance and enhancing its tribological performance. Moreover, the enhanced surface hardness achieved through boriding enhances the material's resistance to wear during sliding contact conditions. Additionally, borided surfaces demonstrate improved lubrication properties, which decrease the likelihood of seizure and increase the efficacy of lubricants in reducing friction and wear. Overall, boriding treatment is a promising approach for enhancing the tribological properties of materials, making them more suitable for demanding applications where friction, wear, and lubrication are critical factors.

Several studies have investigated the tribological behavior of borided surfaces in different materials. According to Dearnley (1985) and Gutierrez-Noda (2019), boriding has the potential to improve wear and corrosion resistance[64] [65]. They also reported a substantial

increase in microhardness and a reduction in friction coefficient and wear response in AISI M2 steel. Kim (2014) supports enhancing the thermal and mechanical properties of a boron nitride-polyurethane composite[66]. Arteaga-Hernandez (2021) demonstrates that boriding treatment can improve the tribological performance and corrosion resistance of AISI 316L stainless steel, making it a promising approach for various applications in the biomedical field[67]. Cuao-Moreu (2019) discovered that boriding treatment considerably enhanced the wear resistance of CoCrMo cast alloy[68]. The best results were obtained after 6 hours at 1223 K. Similarly, Arteaga-Hernandez (2021) observed a reduction in wear rate in AISI 316L stainless steel after boriding treatment, although the specific parameters were not specified[67]. Carrera-Espinoza (2016) found that the coefficients of friction on boride layers of AISI 1018 steel were independent of boriding potential[69]. The wear scar diameter was characterized by SEM. Greco (2011) suggested a combination of boriding treatment and nano-colloidal lubricant additives for wind turbine gearbox applications, resulting in improved wear resistance[70]. These studies collectively demonstrate the potential of boriding treatment in enhancing the tribological behavior of various materials.

Boriding is a thermochemical treatment that has been proven to significantly enhance the tribological properties of cast iron. According to Şen (2004), boronizing at higher temperatures and for longer durations increased the hardness of the boride layer on ductile cast irons[17]. Additionally, Medvedovski (2016) demonstrated that iron boride-based coatings on cast iron exhibited superior wear resistance due to their high hardness and self-lubricating properties[20]. Meriç (2006) reported improved abrasive wear behavior in boronized cast irons[21]. The boride layer showed increased thickness and microhardness. Gutierrez-Noda (2019) found that a boride diffusion layer on AISI M2 steel led to a significant increase in microhardness and a reduction in friction coefficient, indicating improved tribological properties[65]. These studies collectively support the effectiveness of boriding in enhancing the tribological properties of cast iron.

1.3.3 Electrochimical properties

Electrochemistry is a field of chemistry that studies the chemical processes that involve the movement of electrons. This movement is achieved through the transfer of ions between two electrodes and is facilitated by an electrolyte solution. Electrochemistry is essential in various applications, such as batteries, corrosion prevention, electroplating, and sensors. Understanding redox reactions is fundamental as they involve the transfer of electrons between chemical species.

Boriding treatment is a surface modification technique that involves the diffusion of boron into the material substrate. This technique significantly influences the electrochemical behavior of materials, particularly in the context of corrosion prevention. The formation of a boride layer on the material surface alters its electrochemical properties, leading to enhanced corrosion resistance. The layer of boride acts as a barrier, limiting the diffusion of corrosive substances and reducing the material's susceptibility to corrosion. Additionally, the boride layer can alter the surface chemistry, resulting in a more stable oxide layer that provides further protection against corrosion. Studies have shown that surfaces treated with boriding exhibit lower corrosion rates and improved corrosion resistance compared to untreated surfaces. This highlights the effectiveness of boriding in enhancing the electrochemical performance of materials for corrosion prevention applications.

Boriding has been shown in various studies to significantly improve the electrochemical performance of materials. Sabuz (2023) found that borided low-alloy steel exhibited improved corrosion and wear resistance due to the hard FeB/Fe_2B layers and reduced adsorbed sulfur[71]. Tavakoli (2010) also reported improved corrosion resistance in borided steels[72]. Wu (2020) demonstrated that boric acid, a key component in the boriding process, can increase the overpotential of lead grids in lead-acid batteries, reducing water loss and extending battery life[73]. Similarly, Ye (2002) found that the addition of boron to hydrogen storage alloys improved their electrochemical kinetics[74]. Taken together, these studies highlight the effectiveness of boriding in improving the electrochemical performance of materials.

The corrosion resistance of iron boride coatings has been extensively studied through various processes. Campos (2006) found that a boron paste thickness of 4mm and a treatment time of 4 hours maximized corrosion resistance in AISI 304 steel[75]. Similarly, Tavakoli

(2010) reported improved corrosion resistance in special steels treated at 1220K for 6 hours[72]. Panda (2021) observed that carbon steel with iron boride coatings exhibited enhanced wear resistance, which was attributed to the coatings' hardness and chemical inertness[76]. Alavi (2011) further demonstrated increased corrosion resistance in AISI H13 steel with boride coatings synthesized using pulsed plasma electrolytic boronising[77]. These studies collectively highlight the potential of iron boride coatings in enhancing corrosion resistance in various steel types.

Conclusion

In conclusion, this comprehensive research on cast irons has yielded valuable insights into their composition, thermochemical treatments, and surface properties. The research has demonstrated the significance of comprehending the impact of composition on microstructures and properties, as well as the function of heat treatments in optimizing mechanical performance. Thermochemical treatments, particularly boriding, have demonstrated considerable potential for improving surface properties. The findings underscore the enhanced mechanical, tribological, and electrochemical characteristics of borided layers on cast irons. In conclusion, this research contributes to the advancement and optimization of cast irons for various industrial applications, ensuring enhanced performance, durability, and reliability.

REFERENCES

[1] R. Elliott, "An introduction to cast irons," 1988.

[2] M. Ngqase and X. J. J. o. P. C. S. Pan, "An Overview on Types of White Cast Irons and High Chromium White Cast Irons," vol. 1495, 2020.

[3] I. Chakrabarty, "2.10 Heat Treatment of Cast Irons," 2017.

[4] J. M. Radzikowska, "Metallography and Microstructures of Cast Iron," 2004.

[5] K. N. Vdovin, D. A. Gorlenko, and A. N. J. S. i. T. Zavalishchin, "Influence of industrial tempering on the composition of complex cast iron," vol. 43, pp. 288-290, 2013.

[6] O. Tokova, Y. A. J. I. t. I. C. o. C. S. Savchenko, and I. Technologies, "Modelling of Dependence of Mechanical Properties of Cast Iron on Chemical Composition of Raw Materials," vol. 1, pp. 179-182, 2019.

[7] K. V. Mikhailovich and P. E. Vasilyevna, "Structure features and properties of high-alloy white irons," 2013.

[8] G. I. Silman and K. V. Makarenko, "CAST IRON," 2014.

[9] J. M. J. M. T. Radzikowska, "A New Look at Cast Iron Microstructure," vol. 11, pp. 42 - 45, 2003.

[10] D. Lubyanoi, E. Pudov, E. Kuzin, O. Semenova, and R. Rybár, "Application of Alloyed Cast Iron to Increase the Durability of Products of the Mining and Metallurgical Industry," in *E3S Web of Conferences*, 2020, vol. 174, p. 03022: EDP Sciences.

[11] Р. Фарисов, М. Иоффе, and В. J. И. С. н. ц. Р. а. н. Козловский, "ВАЖНЫЕ АСПЕКТЫ УПРАВЛЕНИЯ КАЧЕСТВОМ ЧУГУННОГО ЛИТЬЯ," vol. 24, no. 3 (107), pp. 69-75, 2022.

[12] J. A. G. de Sousa, W. F. Sales, and A. R. J. T. I. J. o. A. M. T. Machado, "A review on the machining of cast irons," vol. 94, pp. 4073-4092, 2018.

[13] F. R. Rasulov, "Improvement of the properties of the surface layer of cast iron castings," 2020.

[14] N. Vodolazskaya and O. J. S. S. P. Sharaya, "Modifying of the Surface of Products from Cast Iron as the Element of Production Modernization," vol. 299, pp. 588 - 593, 2020.

[15] T. P. Govorun, E. A. Belous, A. I. J. M. S. Lyubich, and H. Treatment, "Improvement of Properties of High-Strength Cast Irons by Surfacing a Metal with Globular Graphite," vol. 59, pp. 675-681, 2018.

[16] K. S. Raghul Anandh, K. Thilipkumar, R. J. I. C. S. M. S. Saravanan, and Engineering, "Surface modification of Ni-hard 4 cast iron with titanium using GTA heat source," vol. 577, 2019.

[17] U. Şen, Ş. Şen, and F. J. K. E. M. Yılmaz, "Improving the Surface Properties of Ductile Irons by Boronizing," vol. 264-268, pp. 541 - 544, 2004.

[18] F. E. Mariani, G. B. d. Assis, L. C. Casteletti, A. L. Neto, G. E. J. M. P. Totten, and Characterization, "Austempering and Boro-Austempering Treatments in Gray Cast Iron," vol. 6, pp. 262-271, 2017.

[19] A. D. Boccardo, N. Catalán, D. J. Celentano, E. J. M. Ramos-Moore, and M. T. B, "A Thermo-metallurgical Model for Laser Surface Engineering Treatment of Nodular Cast Iron," vol. 52, pp. 854 - 870, 2021.

[20] E. Medvedovski, J. R. Jiang, and M. J. A. i. A. C. Robertson, "Boride-based coatings for protection of cast iron against wear," vol. 115, pp. 483 - 494, 2016.

[21] C. Meric, S. Sahin, B. Backir, N. J. M. Koksal, and Design, "Investigation of the boronizing effect on the abrasive wear behavior in cast irons," vol. 27, no. 9, pp. 751-757, 2006.
[22] A. P. Krelling, J. C. G. Milan, and C. E. d. J. S. E. Costa, "Tribological behaviour of borided H13 steel with different boriding agents," vol. 31, pp. 581 - 587, 2015.
[23] E. Medvedovski, J. Jiang, and M. J. C. I. Robertson, "Iron boride-based thermal diffusion coatings for tribo-corrosion oil production applications," vol. 42, no. 2, pp. 3190-3211, 2016.
[24] H. Kazdal Zeytin *et al.*, "Effect of Boron and Heat Treatment on Mechanical Properties of White Cast Iron for Mining Application," vol. 18, pp. 31-39, 2011.
[25] J. J. Zhang, Y. Gao, J.-d. Xing, S. Ma, Y. Li, and L. J. K. E. M. Liu, "Effects of Forging and Heat Treatment on Microstructure and Properties of High Boron White Cast Iron," vol. 457, pp. 225 - 230, 2010.
[26] A. Bedolla-Jacuinde, F. V. Guerra, A. J. Guerrero-Pastran, M. A. Sierra-Cetina, and S. J. W. Valdez-Medina, "Microstructural effect and wear performance of high chromium white cast iron modified with high boron contents," 2021.
[27] H. J. I. L. Mindivan and Tribology, "Investigation of thermochemical boriding effect on wear behavior of a GGG 50 quality as-cast ductile iron," vol. 68, pp. 476-481, 2016.
[28] J. Zhang *et al.*, "Effects of Plastic Deformation and Heat Treatment on Microstructure and Properties of High Boron Cast Steel," vol. 20, pp. 1658-1664, 2011.
[29] Y. Kayalı, Y. J. M. Yalçın, and Design, "The effects of boro-tempering heat treatment on microstructural properties of ductile iron," vol. 32, pp. 1414-1419, 2011.
[30] R. A. García-León, J. F. Martínez-Trinidad, and I. J. T. o. t. I. I. o. M. Campos-Silva, "Historical Review on the Boriding Process using Bibliometric Analysis," vol. 74, pp. 541 - 557, 2021.
[31] J. T. Cataldo, F. Galligani, D. J. A. M. Harraden, and Processes, "Boride surface treatments," vol. 157, 2000.
[32] I. Campos-Silva and G. A. Rodriguez-Castro, "Boriding to improve the mechanical properties and corrosion resistance of steels," 2015.
[33] M. Krukovich, B. A. Prusakov, and I. G. Sizov, "The Use of Boriding Processes in the Industrial Treatment of Details and Tools," 2016.
[34] M. J. C. T. i. B. Kulka, "Trends in Thermochemical Techniques of Boriding," 2018.
[35] H. Kunst, O. J. H. J. o. H. T. Schaaber, and Materials, "Borieren von Eisenwerkstoffen und Titan," vol. 26, no. 1, pp. 18-20, 1971.
[36] M. J. Lee, K. Y. Lee, J. H. Lee, and Y. H. Kim, "BORIDING OF STEEL WITH PECVD METHOD," 1999.
[37] R. Kouba, M. Keddam, and M. J. S. E. Kulka, "Modelling of paste boriding process," vol. 31, pp. 563 - 569, 2015.
[38] I. Gunes, S. Ulker, S. J. M. Taktak, and Design, "Plasma paste boronizing of AISI 8620, 52100 and 440C steels," vol. 32, pp. 2380-2386, 2011.
[39] I. Campos, G. Ramírez, U. Figueroa, and C. V. J. S. E. Velázquez, "Paste boriding process: evaluation of boron mobility on borided steels," vol. 23, pp. 216 - 222, 2007.
[40] K. Anthymidis, G. Stergioudis, D. Roussos, P. Zinoviadis, and D. N. J. S. E. Tsipas, "Boriding of Ferrous and Non-Ferrous Metals and Alloys in Fluidised Bed Reactor," vol. 18, pp. 255 - 259, 2002.
[41] K. Anthymidis, N. E. Maragoudakis, G. Stergioudis, O. Haidar, and D. N. J. M. L. Tsipas, "A comparative study of boride coatings obtained by pack cementation method and by fluidized bed technology," vol. 57, pp. 2399-2403, 2003.

[42] E. A. Smol'nikov, L. J. M. S. Sarmanova, and H. Treatment, "Study of the possibility of liquid boriding of high-speed steels," vol. 24, pp. 785-788, 1982.
[43] L. P. Skugorova, A. I. J. M. S. Nechaev, and H. Treatment, "Investigation of the gas boriding process," vol. 15, pp. 989-990, 1973.
[44] M. Kulka, N. Makuch, A. Pertek, and A. J. M. C. Piasecki, "An alternative method of gas boriding applied to the formation of borocarburized layer," vol. 72, pp. 59-67, 2012.
[45] L. Qin, K. Yang, C.-s. Liu, and B. J. M. L. Tang, "Enhanced plasma boriding with molybdenum using double glow plasma surface alloying technique," vol. 82, pp. 127-129, 2012.
[46] B. Yavas, G. J. I. J. o. R. M. Goller, and H. Materials, "A novel approach to boriding of TZM by spark plasma sintering method," 2019.
[47] X. He, H. Xiao, M. Fevzi Ozaydin, K. Balzuweit, H. J. S. Liang, and C. Technology, "Low-temperature boriding of high-carbon steel," vol. 263, pp. 21-26, 2015.
[48] N. Ueda *et al.*, "Boriding of nickel by the powder-pack method," vol. 126, pp. 25-30, 2000.
[49] A. Kaouka, K. J. J. o. M. R. Benarous, and Technology, "Electrochemical boriding of titanium alloy Ti-6Al-4V," vol. 8, no. 6, pp. 6407-6412, 2019.
[50] M. Kulka, M. Kulka, and Castro, *Current trends in boriding*. Springer, 2019.
[51] A. J. M. Minkevich, Moscow, "Khimiko-termicheskaya obrabotka metallov i splavov," 1965.
[52] K. M. Döleker, Y. Özgürlük, O. Gokcekaya, A. Günen, A. J. S. Erdoğan, and C. Technology, "High-temperature corrosion and oxidation properties of borided CoCrFeNiAl0. 5Nb0. 5 HEA," vol. 470, p. 129856, 2023.
[53] İ. Türkmen, E. J. J. o. A. Yalamaç, and Compounds, "Growth of the Fe2B layer on SAE 1020 steel employed a boron source of H3BO3 during the powder-pack boriding method," vol. 744, pp. 658-666, 2018.
[54] I. Campos-Silva *et al.*, "Effects of scratch tests on the adhesive and cohesive properties of borided Inconel 718 superalloy," vol. 349, pp. 917-927, 2018.
[55] A. Meneses-Amador *et al.*, "Adhesive and cohesive strength in FeB/Fe 2 B systems," vol. 27, pp. 2089-2098, 2018.
[56] I. Morgado-González, M. Ortiz-Dominguez, and M. J. M. T. Keddam, "Characterization of Fe2B layers on ASTM A1011 steel and modeling of boron diffusion," vol. 64, no. 1, pp. 55-66, 2022.
[57] N. Vidakis, A. Antoniadis, and N. J. J. o. m. p. t. Bilalis, "The VDI 3198 indentation test evaluation of a reliable qualitative control for layered compounds," vol. 143, pp. 481-485, 2003.
[58] M. Keddam *et al.*, "Kinetics of Formation, Metallurgical and Tribological Properties of Iron Boride Surface Layer on Steel ASTM A572," vol. 65, no. 1, pp. 74-81, 2023.
[59] I. Campos-Silva *et al.*, "Improving the adhesion resistance of the boride coatings to AISI 316L steel substrate by diffusion annealing," vol. 25, pp. 3852-3862, 2016.
[60] T. Eckardt *et al.*, "Improving tribological properties of sputtered boron carbide coatings by process modifications," vol. 126, pp. 69-75, 2000.
[61] C. I. Chiang, O. Meyer, R. J. N. I. Silva, M. i. P. R. S. B.-b. I. W. Materials, and Atoms, "The modification of mechanical properties and adhesion of boron carbide sputtered films by ion implantation," vol. 117, pp. 408-414, 1996.
[62] K. Holmberg and A. Matthews, *Coatings tribology: properties, mechanisms, techniques and applications in surface engineering*. Elsevier, 2009.
[63] B. J. N. Y. Bhushan, "Introduction to Tribology, john Wiley& sons," 2002.

[64] P. A. Dearnley and T. J. S. E. Bell, "Engineering the Surface with Boron Based Materials," vol. 1, pp. 203-217, 1985.
[65] L. Gutierrez-Noda, C. A. Cuao-Moreu, O. Perez-Acosta, E. Lorenzo-Bonet, P. D. C. Zambrano-Robledo, and M. A. L. J. W. Hernandez-Rodriguez, "The effect of a boride diffusion layer on the tribological properties of AISI M2 steel," 2019.
[66] K. Kim, M. Kim, and J. J. P. f. A. T. Kim, "Enhancement of the thermal and mechanical properties of a surface-modified boron nitride–polyurethane composite," vol. 25, pp. 791-798, 2014.
[67] L. A. Arteaga-Hernandez, C. A. Cuao-Moreu, C. González-Rivera, M. Alvarez-Vera, J. A. Ortega-Saenz, and M. A. L. J. W. Hernandez-Rodriguez, "Study of boriding surface treatment in the tribological behavior of an AISI 316L stainless steel," 2021.
[68] C. A. Cuao-Moreu, E. Hernandez-Sanchez, M. Alvarez-Vera, E. Garcia-Sanchez, A. J. Perez-Unzueta, and M. A. L. J. W. Hernandez-Rodriguez, "Tribological behavior of borided surface on CoCrMo cast alloy," 2019.
[69] R. Carrera-Espinoza, U. Figueroa-López, J. F. Martínez-Trinidad, I. Campos-Silva, E. Hernandez-Sanchez, and A. J. W. Motallebzadeh, "Tribological behavior of borided AISI 1018 steel under linear reciprocating sliding conditions," vol. 362, pp. 1-7, 2016.
[70] A. C. Greco, K. Mistry, V. Sista, O. L. Eryilmaz, and A. J. W. Erdemir, "Friction and wear behaviour of boron based surface treatment and nano-particle lubricant additives for wind turbine gearbox applications," vol. 271, pp. 1754-1760, 2011.
[71] E. H. Sabuz, M. Noor-A-Alam, W. M. Haider, I. J. C. Shabib, and M. Degradation, "Improving the Mechanical and Electrochemical Performance of Additively Manufactured 8620 Low Alloy Steel via Boriding," 2023.
[72] H. Tavakoli, S. M. M. J. M. C. Khoie, and Physics, "An electrochemical study of the corrosion resistance of boride coating obtained by thermo-reactive diffusion," vol. 124, pp. 1134-1138, 2010.
[73] Z. Wu, Y. Liu, C. Deng, H. Zhao, R. Zhao, and H. J. J. o. e. s. Chen, "The critical role of boric acid as electrolyte additive on the electrochemical performance of lead-acid battery," vol. 27, p. 101076, 2020.
[74] H. Q. Ye, Y. Huang, T. S. Huang, H. F. J. J. o. A. Zhang, and Compounds, "Influence of the boron additive on the electrochemical properties of the MmNi3.55Co0.75Mn0.4Al0.3 hydrogen storage alloy," vol. 330, pp. 866-870, 2002.
[75] I. Campos, M. Palomar, A. S. Amador, R. Ganem, J. H. J. S. Martínez, and C. Technology, "Evaluation of the corrosion resistance of iron boride coatings obtained by paste boriding process," vol. 201, pp. 2438-2442, 2006.
[76] J. N. Panda, B. C. Wong, E. Medvedovski, and P. J. T. I. Egberts, "Enhancement of tribo-corrosion performance of carbon steel through boronizing and BN-based coatings," vol. 153, p. 106666, 2021.
[77] S. H. Alavi, C. Dehghanian, and P. J. S. E. Taheri, "Investigation of corrosion behaviour of carbon steel coated by pulsed plasma electrolytic boronising technique in 3·5 wt-%NaCl aqueous solution," vol. 27, pp. 509 - 514, 2011.

CHAPTER 2:

MATERIALS

AND EXPERIMENTAL

TECHNIQUES

Introduction:

Ductile cast iron, unlike gray cast iron, has a unique microstructure featuring spheroidal graphite nodules that enhance its mechanical properties, including improved ductility, toughness, and impact resistance. This nodularity counters the flake-like graphite formation in gray cast iron, which results in its relatively brittle nature. The nodular structure found in ductile cast iron contributes to greater tensile strength and elongation, making it a suitable choice for applications that require greater load-bearing capacity. Furthermore, ductile cast iron exhibits improved machinability due to its reduced abrasiveness on cutting tools. While gray cast iron offers good vibration damping and excellent thermal conductivity, ductile cast iron's superior mechanical characteristics make it a preferred choice in scenarios that require both strength and malleability.

In this study, we analyze the mechanical, tribological, and electrochemical properties, as well as the structure, adhesion, hardness, and scratch resistance of borided gray and ductile cast iron. We will explore the effects of boriding on these properties in order to better understand the potential industrial applications of these materials.

2.1. Materials Studied

The study samples were obtained from thick, flat plates of cast iron grades FT-25 and GS38-15 in the SNVI-Ruiba industry. Their chemical composition in weight percentage is displayed in Table 2.1. It is worth noting that both grades studied exhibit high tensile limits, good creep, fatigue, and wear resistance.

Table 2.1: Chemical Composition of Study Materials.

Element %	C	Si	Mn	P	S	Mg	Cr	Cu	Al	Sn
Ductile cast iron GS38-15	**3.30**	**2.769**	**0.070**	**0.0143**	**0.008**	**0.050**	**0.021**	**0.0855**	**0.004**	**0.001**
Gray cast iron FT-25	**3.25**	**1.65**	**0.80**	**0.017**	**0.013**	**/**	**/**	**0.049**	**0.020**	**/**

2.2. Thermochemical Treatments:

In order to carry out the boriding process using the powder method (fig 2.1), the surfaces of the samples were polished and cleaned with ultrasonic waves. Next, the samples were placed in a stainless steel container with a mixture of 85% B_4C and 15% Na_2CO_3 fresh-powders, which were lightly compressed to ensure they were in direct contact with the samples. The boriding process was then carried out in an electric furnace at a temperature of approximately 950°C, with hold times of either 1 or 4 hours. The container containing the samples and powders was sealed with glass to prevent the return of any escaping gases "this method recommended by Pr. Boudebane.S". After treatment, the container was removed from the furnace and allowed to cool gradually at room temperature. The coated alloy was then removed from the container and washed in an ultrasonic cleaning machine to remove any remaining powders from its surface. Finally, the coated alloy was washed again in an ultrasonic cleaning machine to ensure that no residual powders remained on the surface of the specimen.

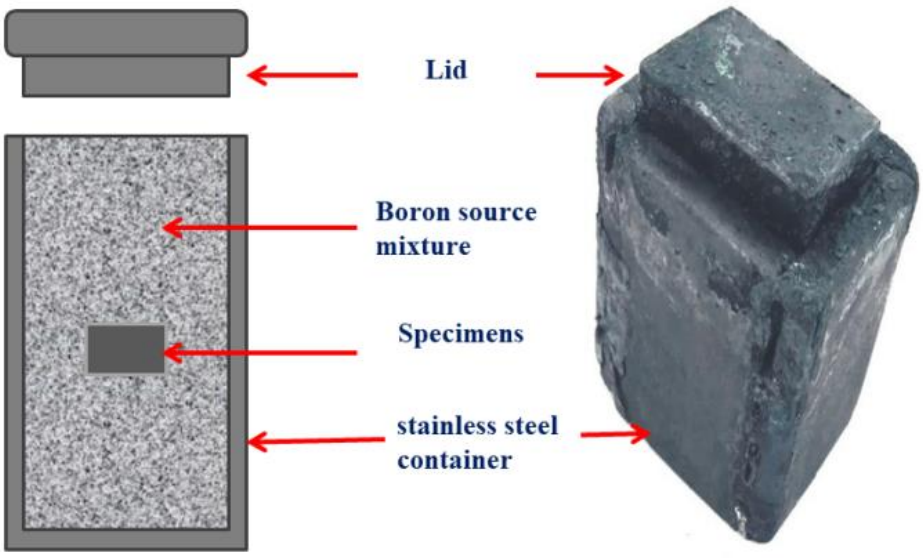

Figure 2.1 the powder-pack boriding process.

2.3. Experimental Techniques Used

2.3.1 X-ray diffraction (XRD) analysis

Samples GS1, GS4, GL1, and GL4 were analyzed using the X-ray diffraction technique after boriding treatment. Phase analysis was conducted with an Ultima IV diffractometer (fig 2.2), scanning at angles ranging from 10° to 90° using copper radiation (CuKα) and continuous scanning at a rate of 2° per minute. The operational parameters included an acceleration voltage of 40 kV, a current of 40 mA, and a scanning duration of 40 minutes. The XPert HighScore Plus was utilized to confidently identify the different phases.

Figure 2.2 Ultima IV diffractometer

2.3.2 Optical Microscopy

To analyze the microstructures of the boride samples, we used a ZEIZZ optical microscope (fig 2.3), using different magnifications. The samples underwent a series of preparation steps, including cutting, hot coating, and polishing with graded abrasive papers (from 320 to 4000), finishing with an alumina finish (01µm). The samples were then etched with a solution of 2% Nital (2 ml nitric acid in 98 ml ethyl alcohol).

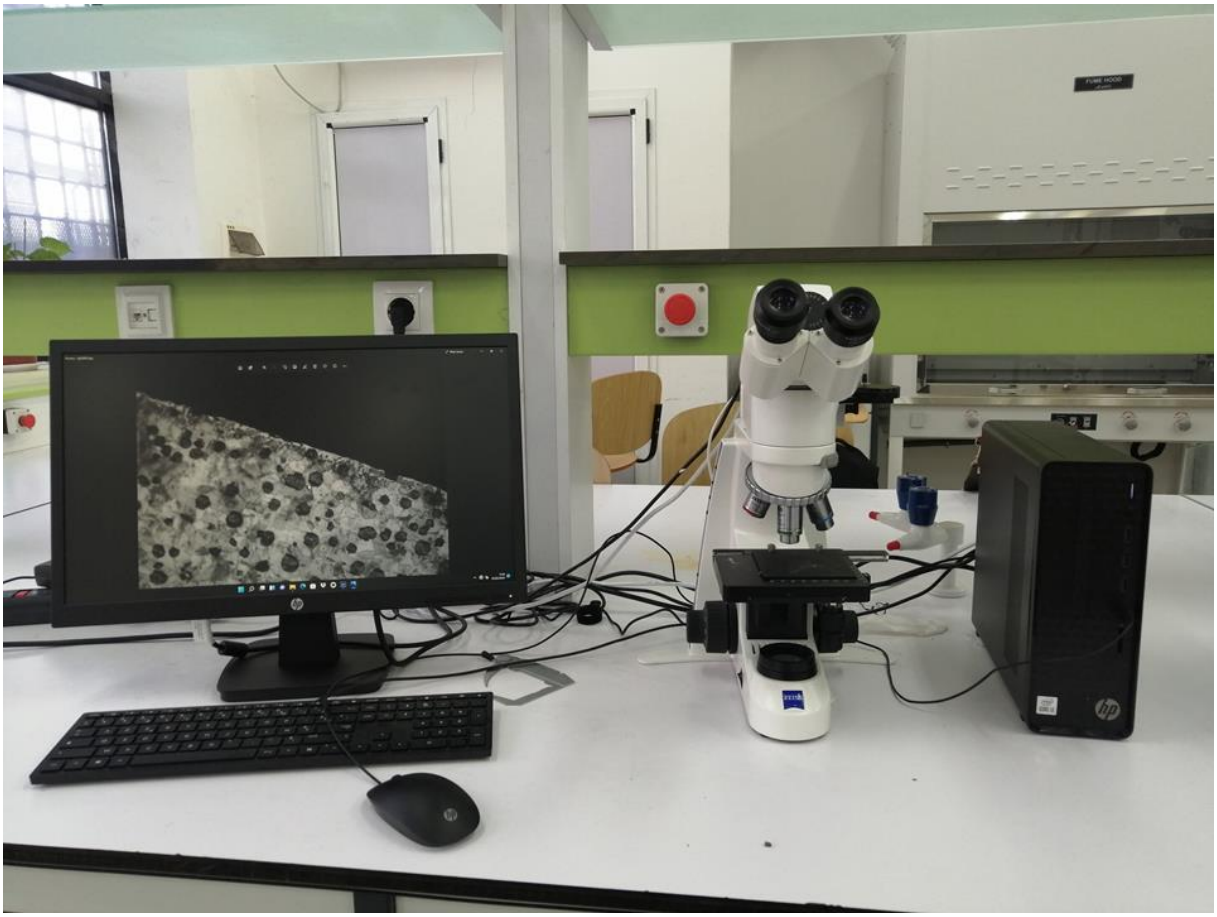

Figure 2.3 ZEIZZ Opticl microscope

2.3.3 Scanning Electron Microscopy and Elemental Microanalysis

Scanning Electron Microscopy (SEM) coupled with Energy Dispersive Spectroscopy (EDS) is a powerful tool for precise surface analysis. This study utilized Quanta 250/FEI SEM (fig 2.4) to analyze different surface layers formed after boriding treatments, as well as to examine surfaces damaged by abrasion and electrochemical tests, performing corresponding elemental analysis.

Figure 2.3 Scanning Electron Microscope (SEM) Quanta 250/FEI.

2.3.4 Vickers Micro-hardness Test:

The INNOVATEST microhardness tester (fig 2.5) was utilized to obtain Micro-Vickers hardness profiles for samples GS1, GS4, GL1 and GL4. The measurements were taken by applying a 50 gf load, which allowed for accurate and precise results. The thickness of the relevant layers can be found in (table .3.1), which provides important information for further analysis and interpretation.

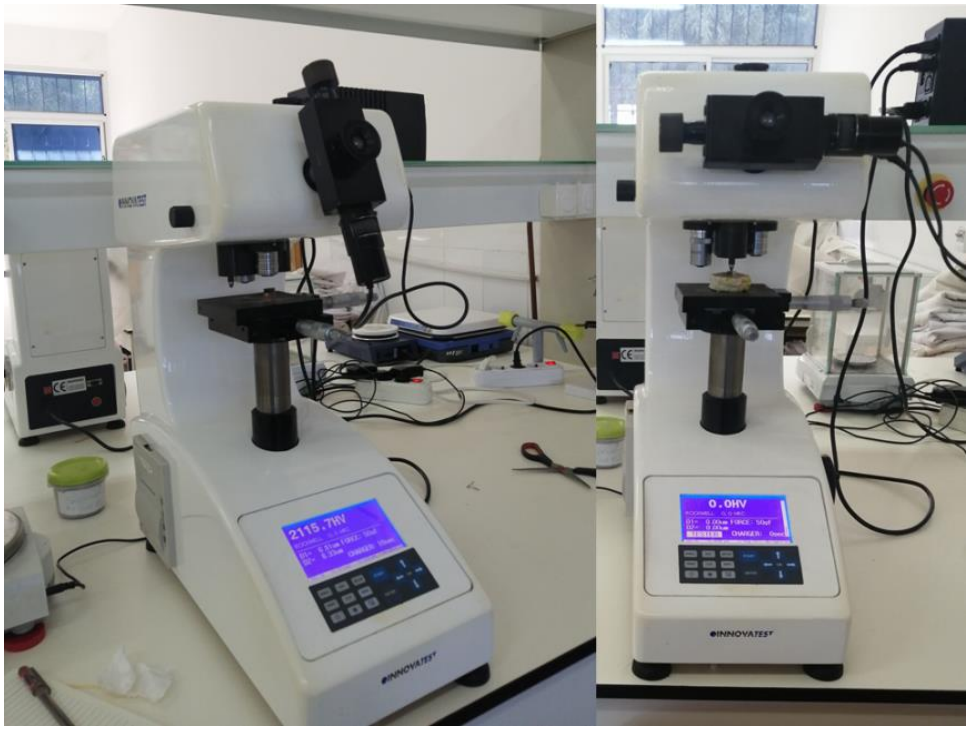

Figure 2.4 INNOVATEST Microhardness Tester

2.3.5 Adhesion Tests (Interfacial Indentation and Daimler Benz Rockwell)

The Daimler-Benz Rockwell-C adhesion test was used to determine the boride layers' adhesion strength quality for samples GS1, GS4, GL1 and GL4. The VDI 3198 standard requires the Rockwell-C adhesion test (fig 2.6). A load of 1471N was applied to cause boride layer damage. The test was evaluated using Quanta 250/FEI SEM (fig 2.3). The adhesion strength quality maps in the norm were compared to the layer damage.

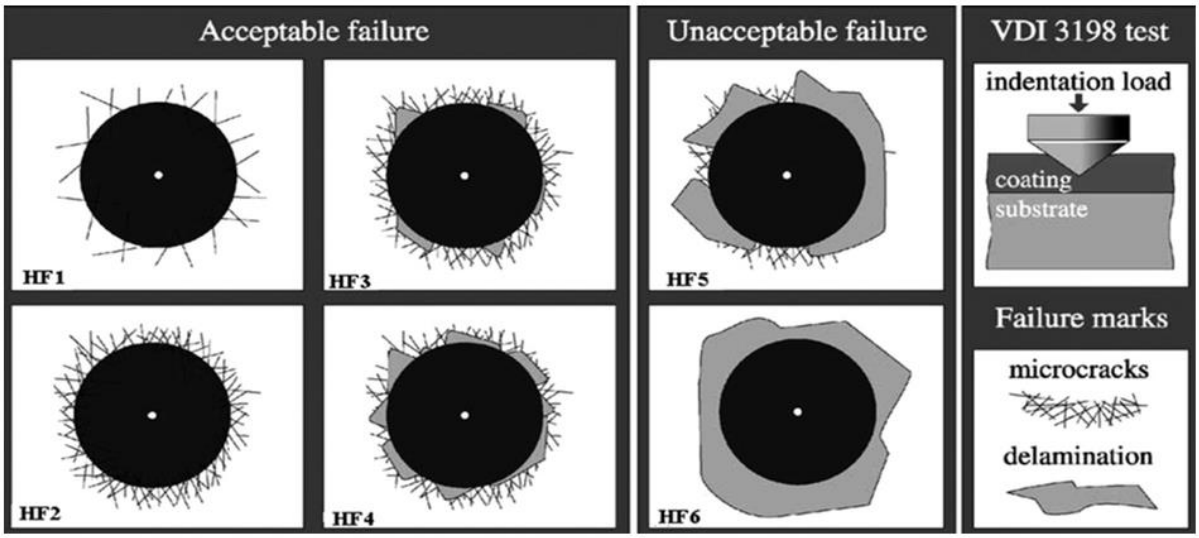

Figure 2.5 The standard card according to VDI 3198.

2.3.6 Surface profile analysis.

The study used a three-dimensional surface profiler with a Cyber Technology CT100 laser source (fig 2.7) to reliably analyze the surface profiles of specimens after scratch, indentation and tribological tests.

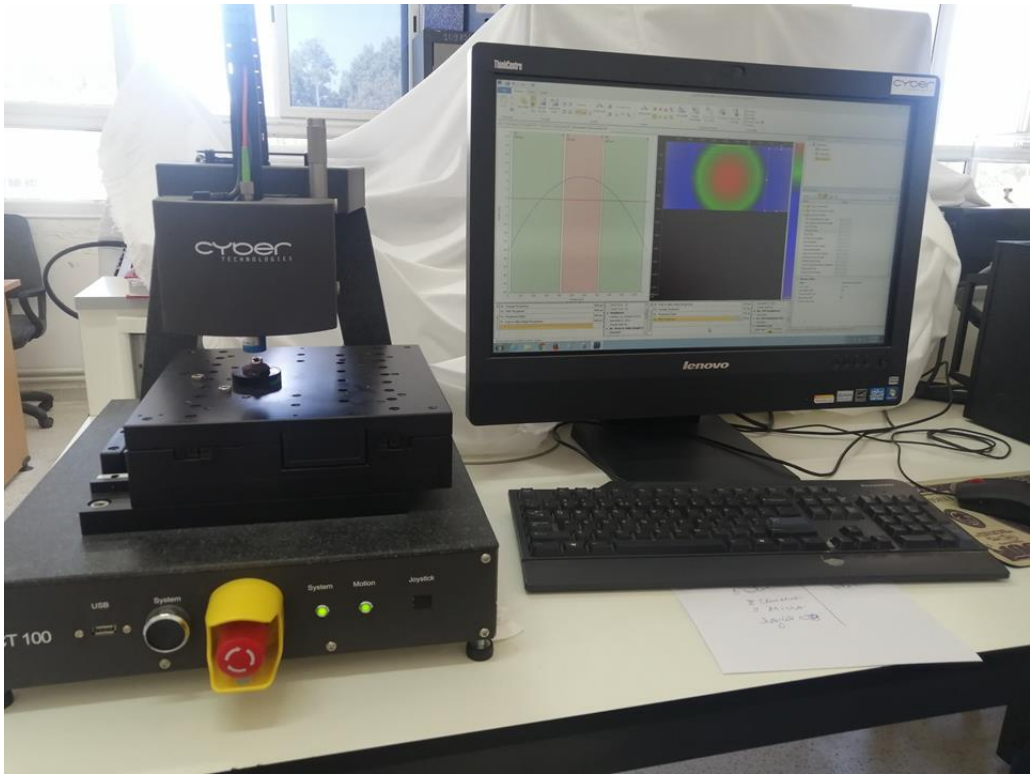

Figure 2.6 Three-dimensional surface profiler with a laser-source type Cyber-Technologies CT100.

2.3.7 Scratch test

In the scratching assessment, we employed a REVETEST scratch tester (fig 2.8) with an incorporated acoustic emission detector. The boride layer-substrate interactions were subjected to scratching using a Rockwell I-216 diamond tip featuring a 200 µm radius. The scratching apparatus maintained a consistent velocity of 2 mm/min, with a load velocity of 79.6 N/min. Incremental normal loads ranging from 1 to 200 N were applied over a 5 mm distance. To determine critical loads (Lc) on the scratched test tracks, a variety of methodologies, including electron microscopy, acoustic emission (AE), penetration (Pd), and residue depths (Rd) analysis, were employed. Transition points were pinpointed through abrupt alterations in depth measurements. Detailed insights into plastic and elastic deformations were obtained through depth data acquired prior to, during, and following the scratch test.

Figure 2.7 REVETEST scratch tester.

2.3.8 Tribology Testing

2.3.8.a Wear Test Conducted Under Dry Conditions

All tests are conducted without lubrication under ambient temperature and pressure conditions. The tribometer is enclosed hermetically and maintains a relative atmospheric humidity of around 25%. Before and following each friction test, the sample and ball are cleaned and degreased in an ultrasonic bath with ethanol for 2 minutes. Table 2.2 summarizes test parameters. The Tribometer module utilized in this study is "csm Instruments TRIOMOMETRE Version 4.5.Q" (fig 2.9) We confidently observed the wear marks on the test samples using SEM and plotted the friction coefficient curves using Origin Lab2018 software.

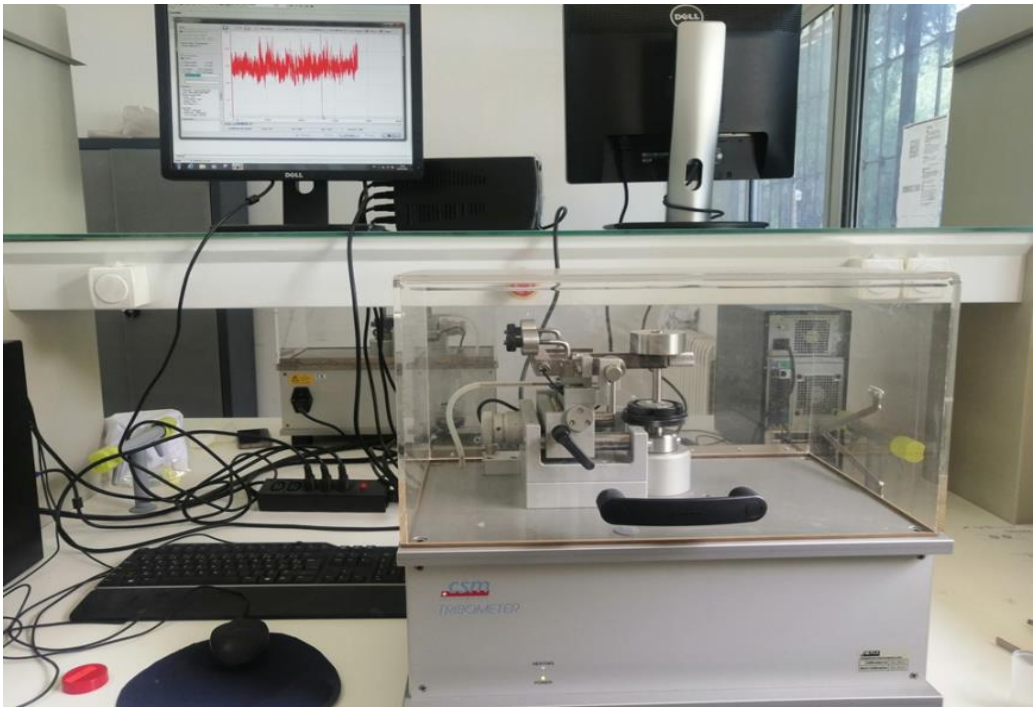

Figure 2.8 csm Instruments TRIOMOMETRE Version 4.5.Q

Table.2.2: Tribological-Test Parameters.

Pin	Alumina ball (Al2O3).
Applied Loads (N)	2 ; 6 ;10
Sliding Speed(mm/s)	4
Sliding Distance (m)	100
Track Radius (mm)	2
Test Temperature (°C)	25°C
Atmosphere	Air atmosphérique

2.3.8.b Wear Test Conducted Under Lubricated Conditions

The friction and wear resistance of GL0, GL1, and GL4 were thoroughly evaluated using a tribo-reciprocating test rig (fig 2.10) in the Department of Mechanical Engineering Automotive Division at Yildiz Technical University. These results provide a clear and reliable understanding of the performance of these lubricants under these specific conditions. The test was conducted with an 8mm 100Cr6 ball moving under boundary-lubricated conditions, using Shell Helix Oil Ultra 5W-40, at a load of 60N, sliding speed of 8mm/s, frequency of 2 Hz, stroke of 10mm, and temperature of 100°C. The sliding trajectory lasted for 1200 seconds. The procedure was repeated three times to ensure consistency, with each test using fresh 100Cr6 steel balls.

Figure 2.9 Reciprocating-test-rig.

2.3.9 Electrochemical (Corrosion) Test

The experimental results of the corrosion resistance of the materials were recorded in the GAMRY FRAMEWORK measurement software with a computer-controlled Gamry 600+ interface potentiostat/galvanostat (fig 2.11) for samples (GS0, GS1, GS4, GL0, GL1, and GL4) with confidence. All electrochemical tests utilized a conventional three-electrode cell with a platinum wire auxiliary electrode, a saturated calomel reference electrode (ECS), and working electrodes including GS0, GS1, GS4, GL0, GL1, and GL4. The evaluation was carried out using a customized corrosion cell filled with a solution of 100 ml of distilled water and 3.5% NaCl. After passivating the samples for one hour, the potentiodynamic test was initiated. The test applied a voltage range of -1 to 1 V with a sweep rate of 1 mV/s. Each surface underwent two tests. The electrochemical test data was confidently analyzed using EC-Lab FRAMEWORK software. Additionally, SEM/EDS were employed to investigate the corrosion surfaces.

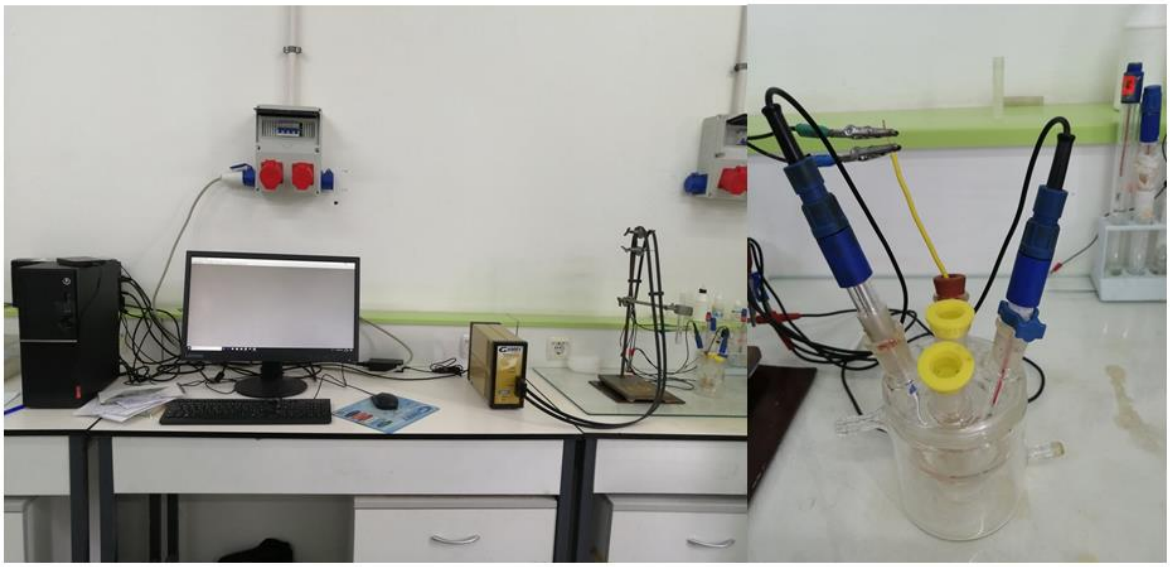

Figure 2.10 GAMRY 600+ potentiostat

Conclusion:

In conclusion, this chapter outlines the materials and experimental techniques used in the study, emphasizing their crucial roles in ensuring the reliability and validity of our findings. We have established a strong foundation for subsequent analyses and interpretations, enhancing the credibility of our study and paving the way for future research in the field.

CHAPTER 3

RESULTS AND DISCUSSIONS

3.1. Microstructures Properties

3.1.1. Examination of Formed Microstructure

Figures 3.1, and 3.2 show optical and SEM micrographs of borided cross sections of gray and ductile cast iron grades FT-25 and GS38-15. The samples underwent boriding at 950°C for 1 and 4 hours, resulting in a microstructure consisting of sawtooth boride layers and a smooth interface (boride/matrix layer) [1-3]. Additionally, the samples exhibited single-phase Fe_2B layer, which is typical of boronized gray cast iron [2-4]. The matrix's microstructure contained ferrite with visible graphite nodules, and a soft region rich in ferrite and some zones of perlite were located in the transition zone of GS1/GS4 (fig 3.1.A). The microstructure of the matrix contained ferrite with visible graphite nodules, and a soft region rich in ferrite and some zones of perlite were located in the transition zone of GS1/GS4. The GL1/GL4 gray cast iron also exhibits a transition zone, which contains a soft region rich in perlite and visible graphite flakes.

The stability and development of the Fe_2B phase are influenced by the carbon content and the absence of alloying elements, resulting in the formation of a single-phase Fe_2B layer over the FeB layer. Boride layers dissolve alloying elements, which act as diffusion barriers for boron atoms and induce the formation of the FeB phase in ferrous alloys. Goeuriot, et al. [5], Petrova, et al. [6], and other researchers support this finding [2, 7-11].

Gray and ductile cast iron have lower alloying elements and higher carbon content than steel, resulting in the formation of Fe_2B mono-phase (Fig 3.2)[3]. Boronizing is a process of thermochemical diffusion that gradually forms a boride layer over time [3]. As shown in Figure 3.1, this layer thickens as the process continues. Table 3.1 demonstrates that a longer boronizing time results in a thicker boride layer due to increased diffusion.

Table 3.1: Fe_2B layer thickness of Gray (GL) and Ductile (GS) cast iron.

Specimens	**Unboride**		**Borided for 950°C/1h**		**Borided for 950°C/4h**	
Cast iron type	**Ductile**	**Gray**	**Ductile**	**Gray**	**Ductile**	**Gray**
Code	**GS0**	**GL0**	**GS1**	**GL1**	**GS4**	**GL4**
Fe_2B thickness (µm)	/	/	**41±2**	**27 ± 5**	**96±5**	**83 ± 3**

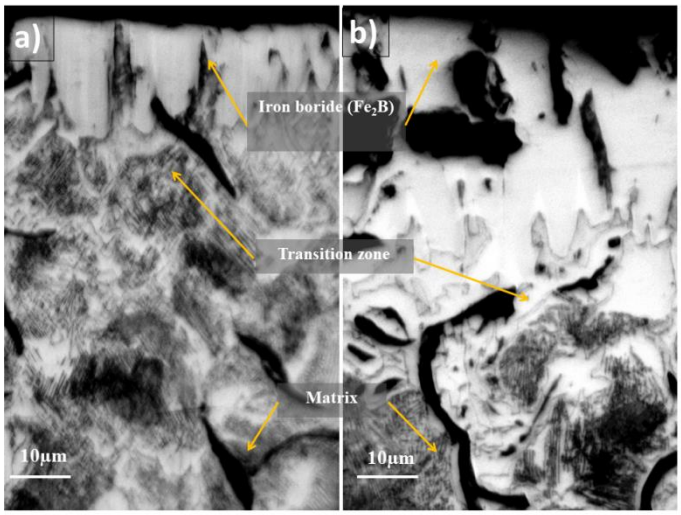

Figure 3.1.A. Optical micrographs of the cross-sections of the boride layers formed on FT-25 cast iron during a) 1h (GL1) and ; b) 4 h (GL4) heat treatments at 950° C.

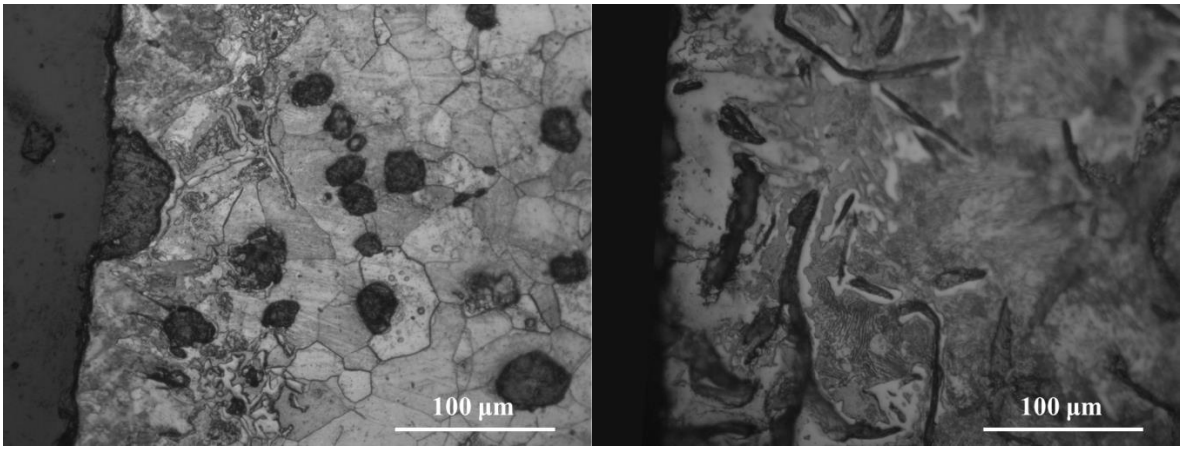

Figure 3.1B. Optical micrographs of the cross-sections of the boride layers formed on GS4 and GL4 during 4 h heat treatments at 950° C.

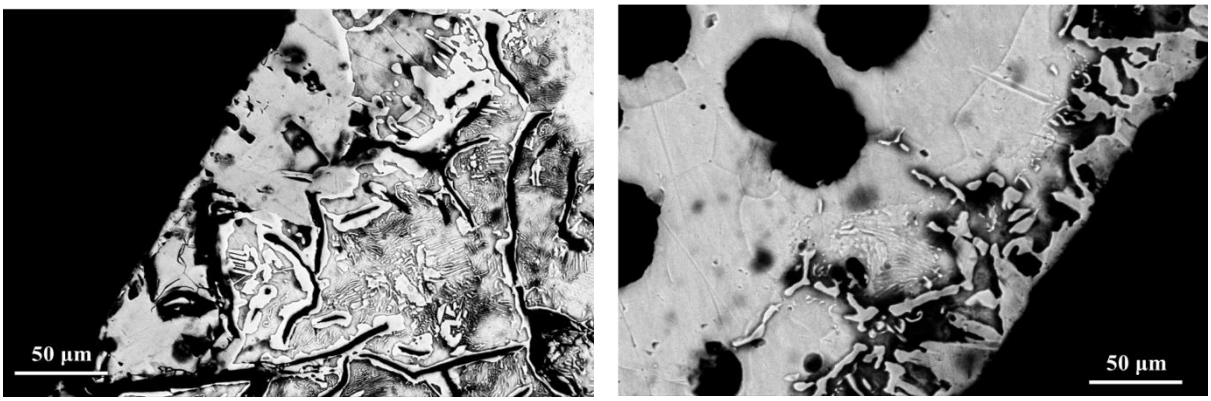

Fig 3.1.C. Cross-section view of boride layer formed on a) GL4; b) GS1 shows the formation of the Perlite phases on the transition zone .

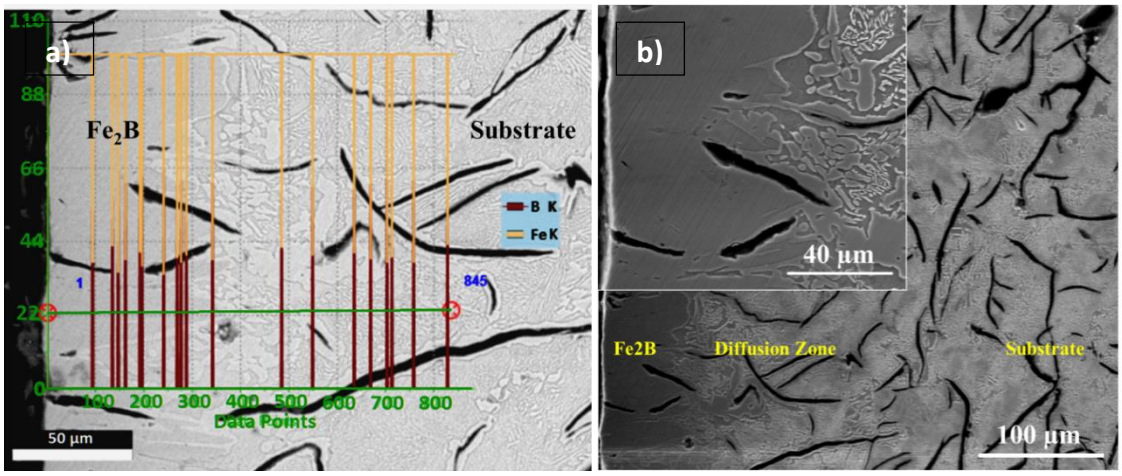

Figure 3.2. a) EDS analysis profile ; b) Cross-section view of boride layer formed on GL4 during 4h heat treatment at 950°C

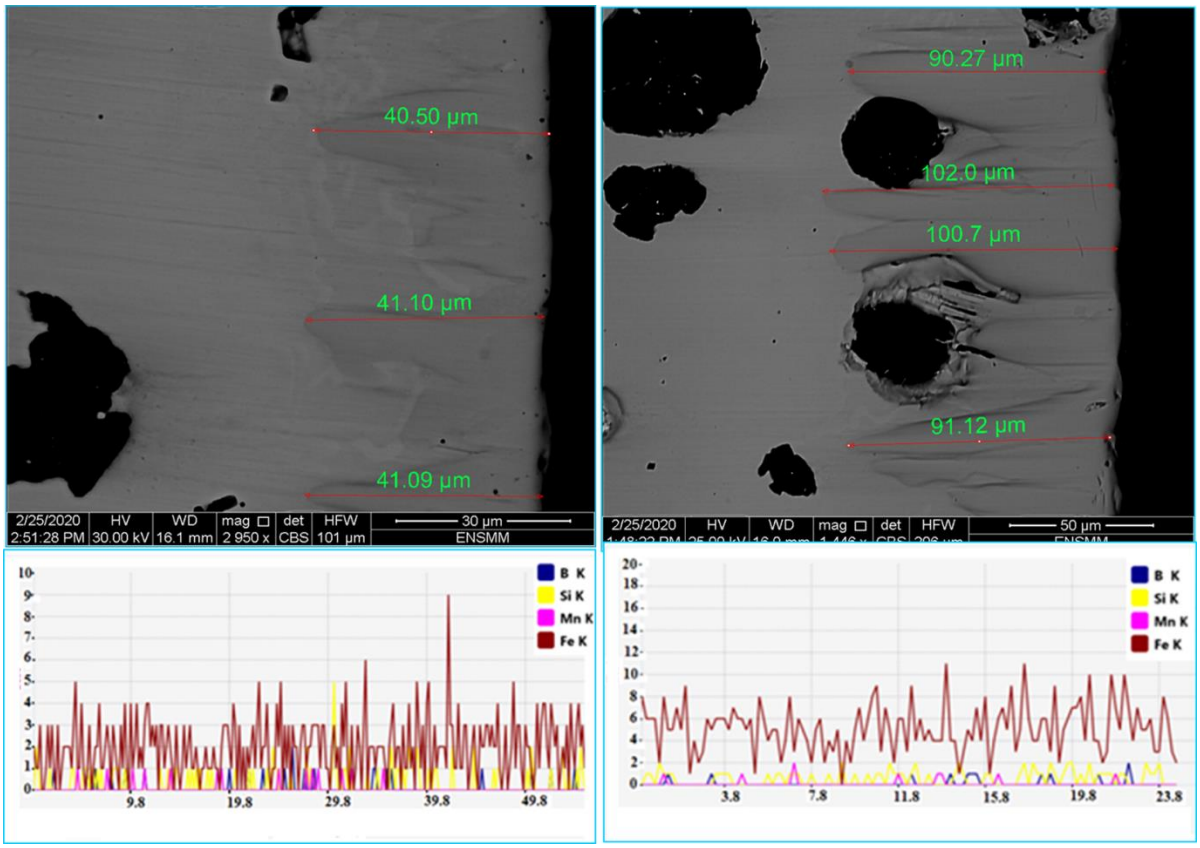

Figure 3.3 Cross-section view and elements concentration profile of boride layer formed on a) GS1 and; b) GS4 heat treated at 950°C.

3.1.2. XRD Analyses

The figure 3.4 presents the X-ray diffraction (XRD) diffractograms of borided samples after 1 and 4 hours. The analysis of these patterns shows that the observed peaks correspond to the emergence of the Fe_2B phase in all samples. Identical boride phases are formed regardless of the boriding conditions. However, the intensity of the diffracted phase peaks varies depending on the duration of the boriding process. These findings are consistent with the observations made through scanning electron microscopy (SEM) and the results obtained from energy-dispersive spectroscopy (EDS) analysis.

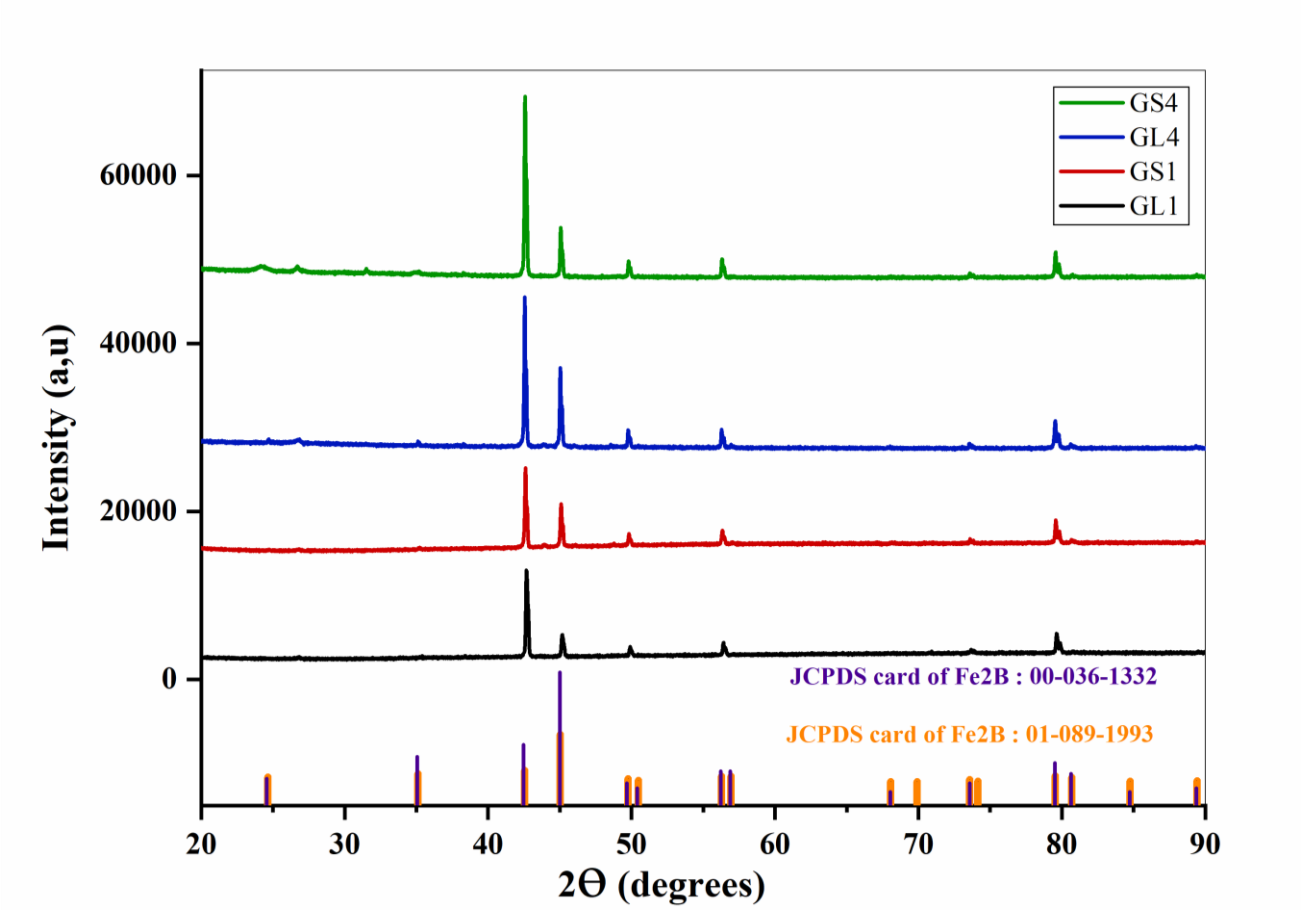

Figure 3.4. XRD patterns of the specimens borided at 950°C for 1h and 4h.

3.2. Mechanical Behaviour

3.2.1. Adhesion Tests (Interfacial Indentation and Daimler Benz Rockwell)

The (SEM) micrograph, as depicted in Figure 3.5, shows the effects of indentation on borided cast iron (GL1, GL4, GS1 and GS4).The indentation impact conforms to the VDI3198 standard [12], revealing radial cracks encircling the perimeter of the indentation craters. The complete absence of delamination is solid proof of the strong adhesion between the surfaces. Therefore, it is conclusive that GL1 and GL4 qualify as HF1, while GS1 and GS4 are undoubtedly qualified as HF1 and HF2 respectively. The robust bonding of these surfaces demonstrates their excellent resistance to any form of separation under stress. Moreover, it is worth noting that despite the thicker and harder coating of GS4 and GL4, which suggests a greater strength, they notably exhibited a smaller indentation radius and depth than GS1 and GL1. This observation implies that the latter surfaces might have a more flexible and compliant coating, leading to a larger deformation under the indentation load.

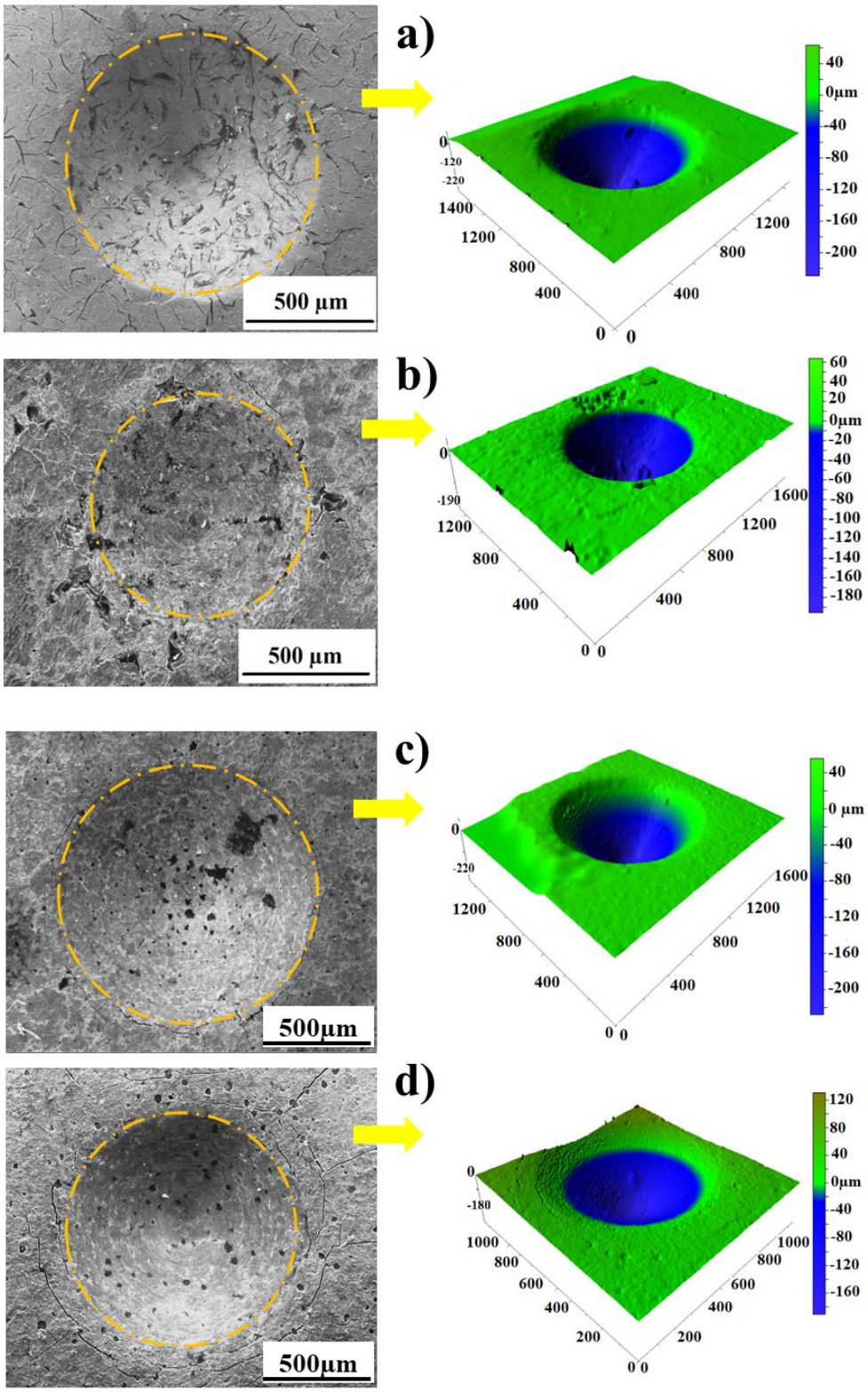

Figure 3.5. The cast iron layers' adhesion strength quality SEM and profilometer for borided at 950°C for : a) GL1, b) GL4, c) GS1, d) GS4.

3.2.2. Hardness Profile

Figure 3.6 shows the micro-hardness profile on the cross-sections of GL, GL4, GS1 and GS4. The hardness near the surface is 1780± 8 HV0.05 and 1985± 5 HV0.05 for GL1 and GS1 respectively, whereas it's 2100±5 HV0.05 and 2008± 3 HV0.05 for GL4 and GS4 respectively and increases with boronizing time. This increase is due to the thickening of the boronized layer as shown in Fig 3.1. In all samples, the hardness decreases until it equals that of the substrate FT-25 and GS38-15. This is conformable with the Fe_2B tetragonal body-centred structure.

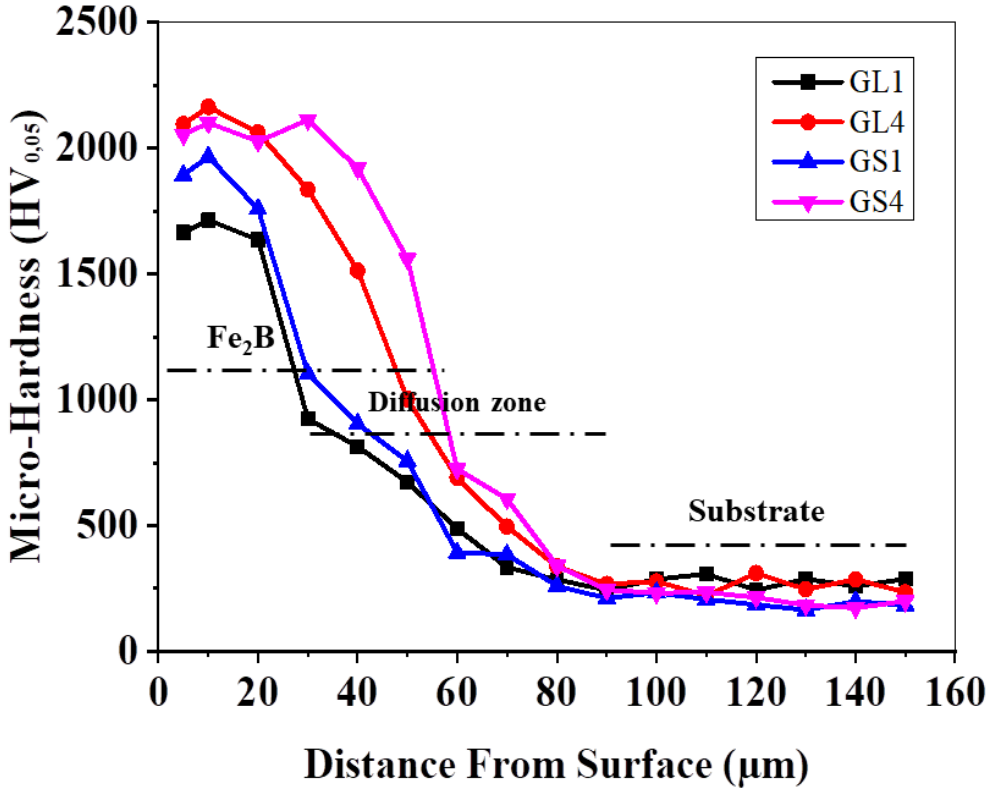

Fig 3.6. The variation in hardness from the surface to the interior of borided cast irons .

3.2.3. Scratch Test

Figures 3.7 and 3.8 illustrate the SEM of borided specimens after being fully scratched. The scratch test revealed that GS1, GS4, GL1 and GL4 responded differently due to variations in their material properties, specifically their graphite morphology, thickness and hardness.

The SEM images depicted in Figure 3.7 showcases the borided specimens after being subjected to a thorough scratch test. Upon analysis, it was discovered that the specimens GS1 and GS4 exhibited varying responses, which can be attributed to the differences in their material properties. Specifically, the morphology, thickness, and hardness of their graphite content played a crucial role in the observed variations.

3.2.3.a. Gray Cast Iron Scratches Behavior

GL1 demonstrated different types of failures at critical loads of varying magnitude. At a load of 21.25 N, the material showed cracking, indicating limited resistance to crack initiation. At 46.57 N, there was a transition to chipping, and at 170.06 N, the material underwent peeling, suggesting substantial load-bearing capacity, as shown in Figure 3.8.a.

At a load of 74.23 N, GL4 exhibited primarily chipping behavior, demonstrating superior resistance compared to GL1. This was followed by a transition to peeling behavior at 90.89 N, indicating sustained integrity, as shown in Figure 3.8.b.

We observed different behaviors in two specimens with varying thickness of borided layer (Table 3.1). GL1, which had a thinner Fe_2B layer, showed an initial form of plastic deformation in the shape of cracking at 21.25 N. On the other hand, GL4 had a thicker Fe_2B layer and higher hardness (Fig3.6), and initially experienced plastic deformation through chipping at 74.23N, which then transitioned to peeling at 90.89N. The thickness and hardness of the coating influenced the material's ability to resist plastic deformation. GL4 demonstrated more resilience and was able to withstand cracking even at lower loads. The change from chipping to peeling in GL4 might have occurred due to plastic deformation [3, 13-15].

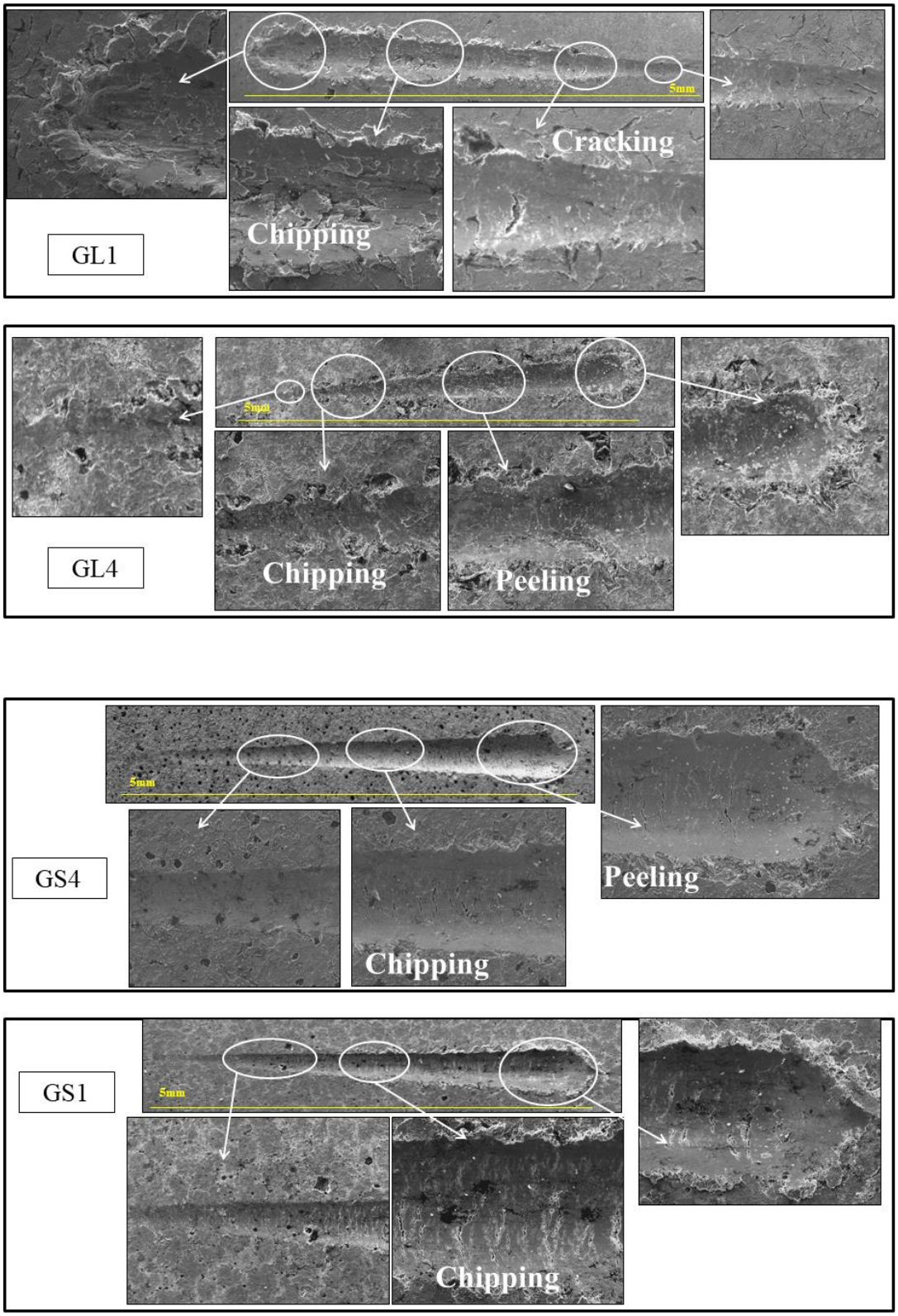

Figure 3.7. SEM micrographs of full scratches and cracking types produced by scratch test.

3.2.3.b. Ductile Cast Iron Scratches Behavior

During the scratch test, GS1 with a boriding layer thickness of ±44 µm exhibited chipping at 89.5 N and subsequent peeling at 116.7 N, indicating its response to increasing applied loads. Chipping involves localized detachment or fragmentation, while peeling indicates a more advanced stage of material failure involving the separation of material layers. The specimen's critical load of 116.7 N marks the point at which peeling began, indicating the material's threshold under the applied stress. The thinner boriding layer may have impacted the specimen's performance, affecting its resistance to advanced stages of damage.

In GS4, chipping occurred at 113.32 N, followed by peeling at 137.4 N and eventual failure at 186.49 N, with a boriding layer thickness of 100 micrometers. This sequence indicates a progression from initial localized detachment to a more severe form of material failure as the load increased. The critical loads at 137.4 N and 186.49 N denote the points where peeling and subsequent failure occurred, indicating the specimen's resilience and structural integrity up to these loads. The thicker boriding layer in GS4 may have contributed to its ability to withstand higher loads before experiencing severe material failure.

When comparing GS1 and GS4, it was found that SG4 had a higher critical load for both peeling and failure. This suggests that SG4 has a greater resistance to advanced stages of scratch-induced damage compared to GS1. The influence of the thickness of the boriding layer is apparent, as the thicker layer in Specimen 2 may have contributed to its enhanced mechanical performance. The observed critical loads highlight differences in the mechanical behavior of the two specimens under the applied stress. The scratch test results of the specimens were likely influenced by the interplay between the thickness of the boriding layer, its hardness, and the extent of elastic and plastic deformation.

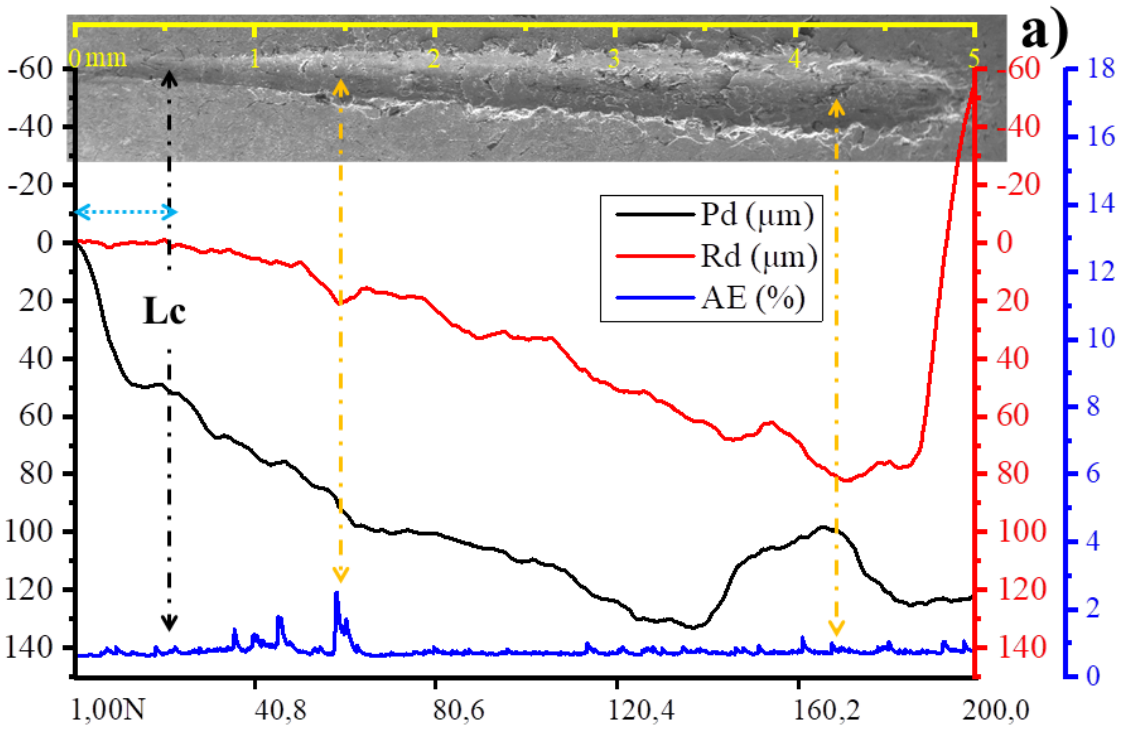
a)
0 mm
1
2
3
4
5
Lc
Pd (µm)
Rd (µm)
AE (%)
-60
-40
-20
0
20
40
60
80
100
120
140
18
16
14
12
10
8
6
4
2
0
1,00N
40,8
80,6
120,4
160,2
200,0

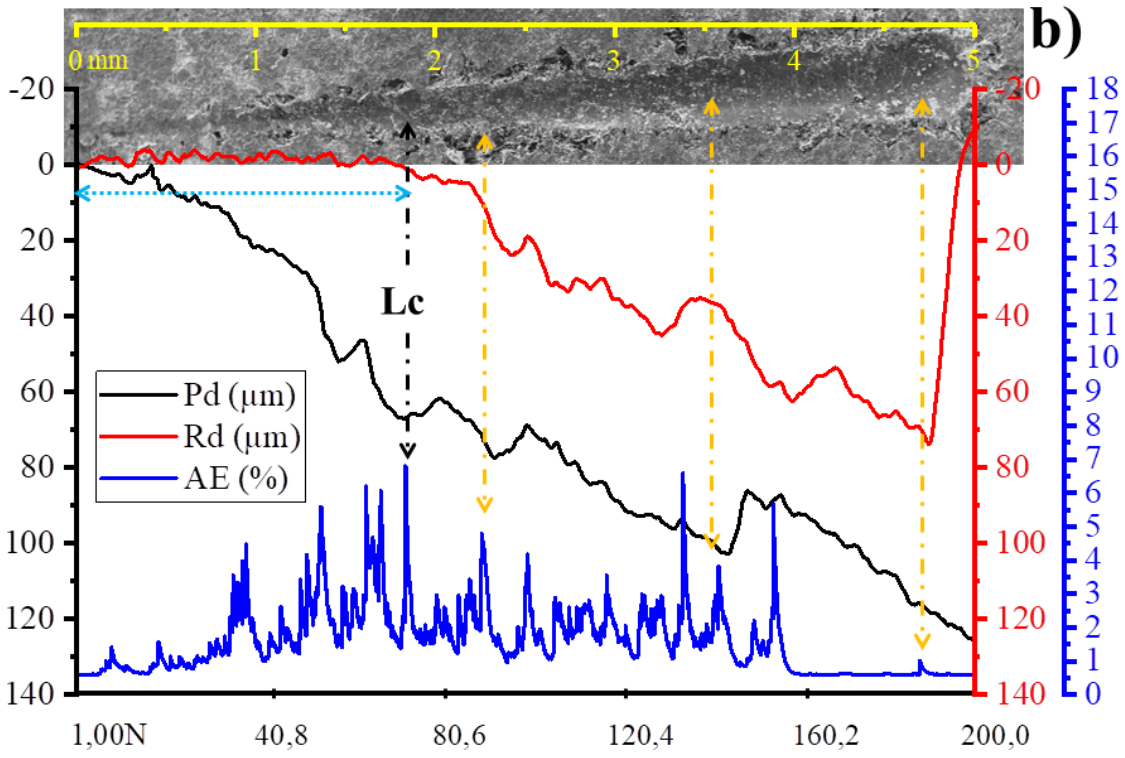
b)
0 mm
1
2
3
4
5
Lc
Pd (µm)
Rd (µm)
AE (%)
-20
0
20
40
60
80
100
120
140
18
17
16
15
14
13
12
11
10
9
8
7
6
5
4
3
2
1
0
1,00N
40,8
80,6
120,4
160,2
200,0

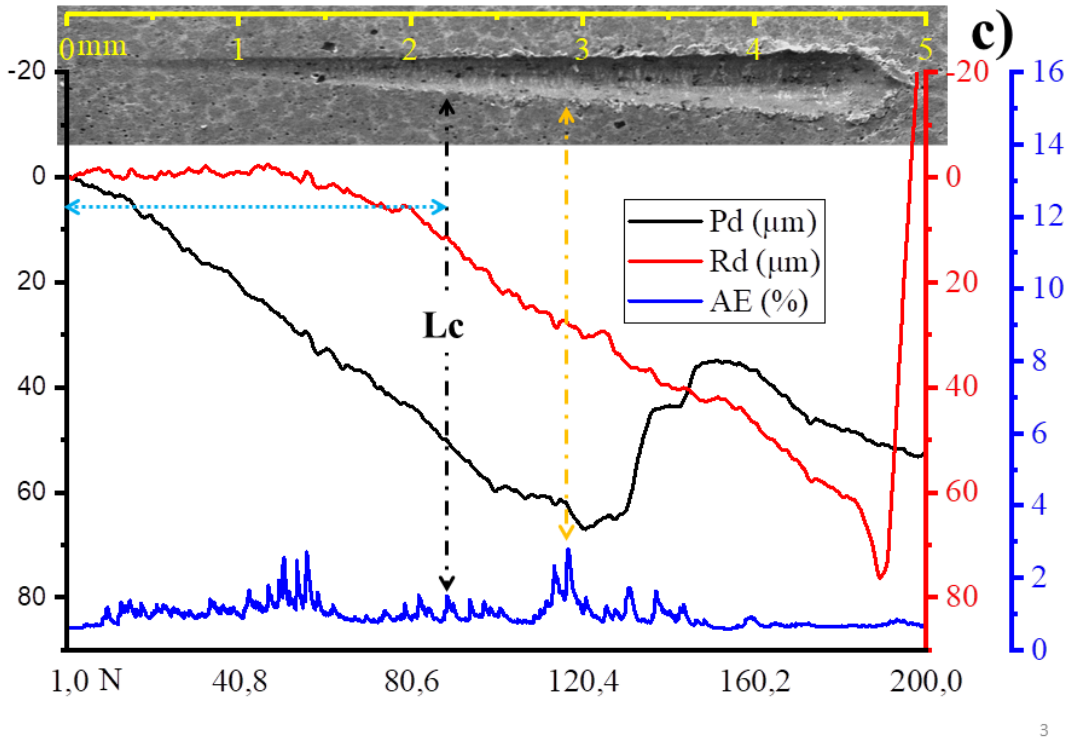

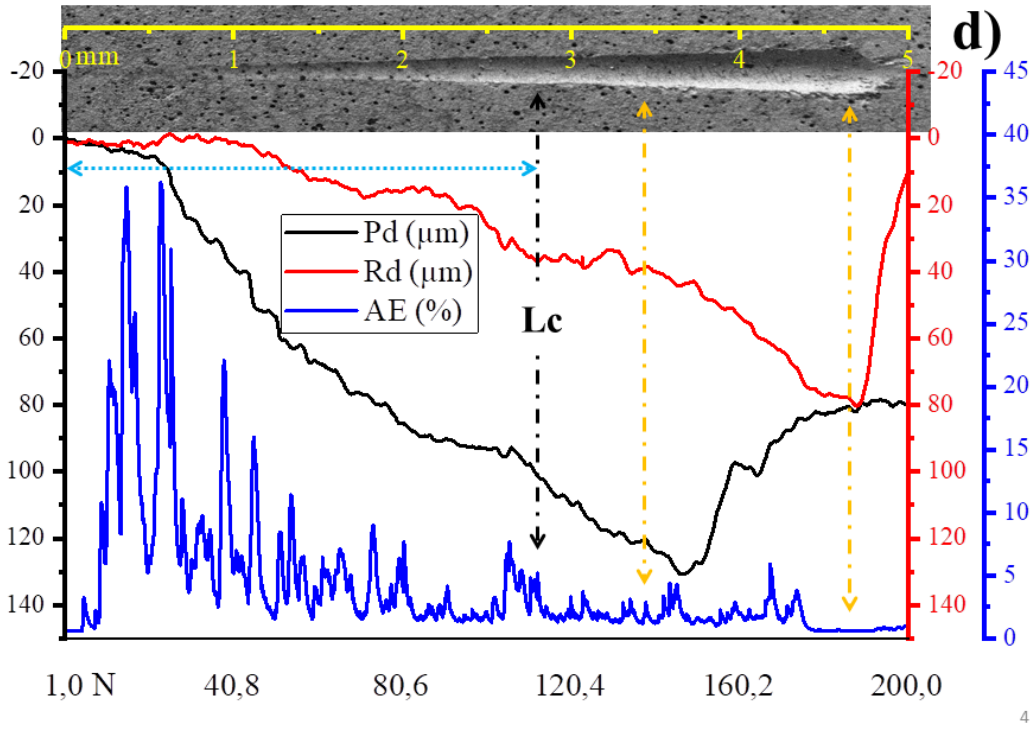

Figure 3.8. Penetration, residual depths, acoustic emission as function of normal force and SEM of full scratch: a) GL1, b) GL4, c) GS1, d) GS4.

3.2.3.c. Compare GS with GL (treated for 4h)

When comparing the scratch behavior of GL4 with lamellar graphite and Specimen GS4 with spheroidal graphite, both featuring a boriding layer thickness of approximately 100 µm, it becomes clear that the morphology of the graphite has a significant impact on scratch resistance. GL4 exhibited a lower critical load for chipping initiation at 74.23 N compared to GS4, which initiated chipping at 113.32 N. This observation suggests that lamellar graphite in GL4 provides enhanced resistance to the initial chipping phase. Additionally, GL4 transitioned at a lower critical load of 90.89 N during the subsequent peeling phase compared to GS4's 137.4 N, indicating a more robust mechanical performance in terms of peeling initiation.

Although both specimens had the same boriding layer thickness, the scratch behavior was influenced by the inverse graphite forms. The lamellar graphite flakes in GL4 distributed stress differently than the spheroidal graphite nodules in GS4. These findings highlight the subtle mechanical responses associated with different graphite morphologies.

This comparative analysis provides valuable insights into the intricacies of scratch resistance, emphasizing the significance of graphite morphology when tailoring materials for applications where scratch resistance is a critical performance factor. The results demonstrate the importance of optimizing materials based on specific graphite forms. This comparative analysis provides valuable insights into the intricacies of scratch resistance, emphasizing the significance of graphite morphology when tailoring materials for applications where scratch resistance is a critical performance factor.

These results emphasize the significance of Fe_2B layer characteristics and the interaction between elastic and plastic deformation in response to external stress and wear, guiding material selection and coating enhancement. Numerous studies have indicated that boride coatings with increased thickness and hardness exhibit greater resistance to scratches. For instance, Dearnley et al. **[**16**]** observed that WB (AMOR) coated WC-Co displayed high resistance to both adhesive and cohesive failure. Campos-Silva et al. **[**17**]** illustrated that the Fe_2B/substrate system achieved via diffusion annealing primarily exhibited cohesive failure, indicating improved adhesion resistance. Park et al. **[**18**]** demonstrated that multilayer c-BN coatings with a thickness exceeding 5 µm exhibited exceptional adhesion even under high residual stress conditions. Tharajak et al. **[**19**]** noted that an increase in h-BN content in

PEEK coating resulted in increased hardness, indicating enhanced scratch resistance. Consequently, these investigations imply that thicker and harder borided coatings generally possess superior scratch resistance while maintaining high levels of adhesion quality. Our tribological analysis comprised scratch and adhesion tests on two cast iron grades specimens with varying Fe_2B layer thicknesses. Thicker and harder coatings exhibited superior resistance to stress, while both specimens achieved HF1 quality adhesion. To summarize, Fe_2B layer properties significantly influence material behavior and adhesion.

3.3. Tribological Behavior

3.3.1. COF Evolution (Dry Test)

The figures 3.9 illustrate the evolution of the coefficient of friction (COF) in relation to sliding distance for the following pairs: (GS0/Al_2O_3, GS1/Al_2O_3, GS4/Al_2O_3) and (GL0/Al_2O_3, GL1/ Al_2O_3, GL4/ Al_2O_3) under loads of 2N, 6N, and 10N, respectively. Upon analysis of these curves, a similar pattern is observed, allowing for the distinction of two successive periods of friction. The first period is known as the running-in or transition period, during which the coefficient increases rapidly until it reaches a maximum value. This period is characterized by wear and plastic deformation of surface asperities. The friction process can be divided into two distinct periods. The second period corresponds to the stabilization of the friction coefficient, and its value remains constant irrespective of the sliding distance. This stage corresponds to the formation of solid wear debris (third body) during the sliding process. It is noteworthy that all samples have a shorter running-in period. Additionally, the average values for the friction coefficient can be found in Table 3.2.

Table 3.2: Average COF values for ductile and gray cast iron

Samples	COF (2N)	COF (6N)	COF (10N)
GL0	0,512	0,200	0,172
GL1	0,346	0,229	0,292
GL4	0,348	0.313	0,212
GS0	0,383	0,176	0,105
GS1	0,323	0,245	0,240
GS4	0,425	0,354	0,340

The samples GL1 and GS1 under the three loads exhibit an average COF that is nearly identical, ranging from 0,346 to 0,229. While the sample GS0 displayed the lowest average COF of 0.105 under a 10N load, When specimen GS4 showed the highest average COF of about 0,340 under the same load.

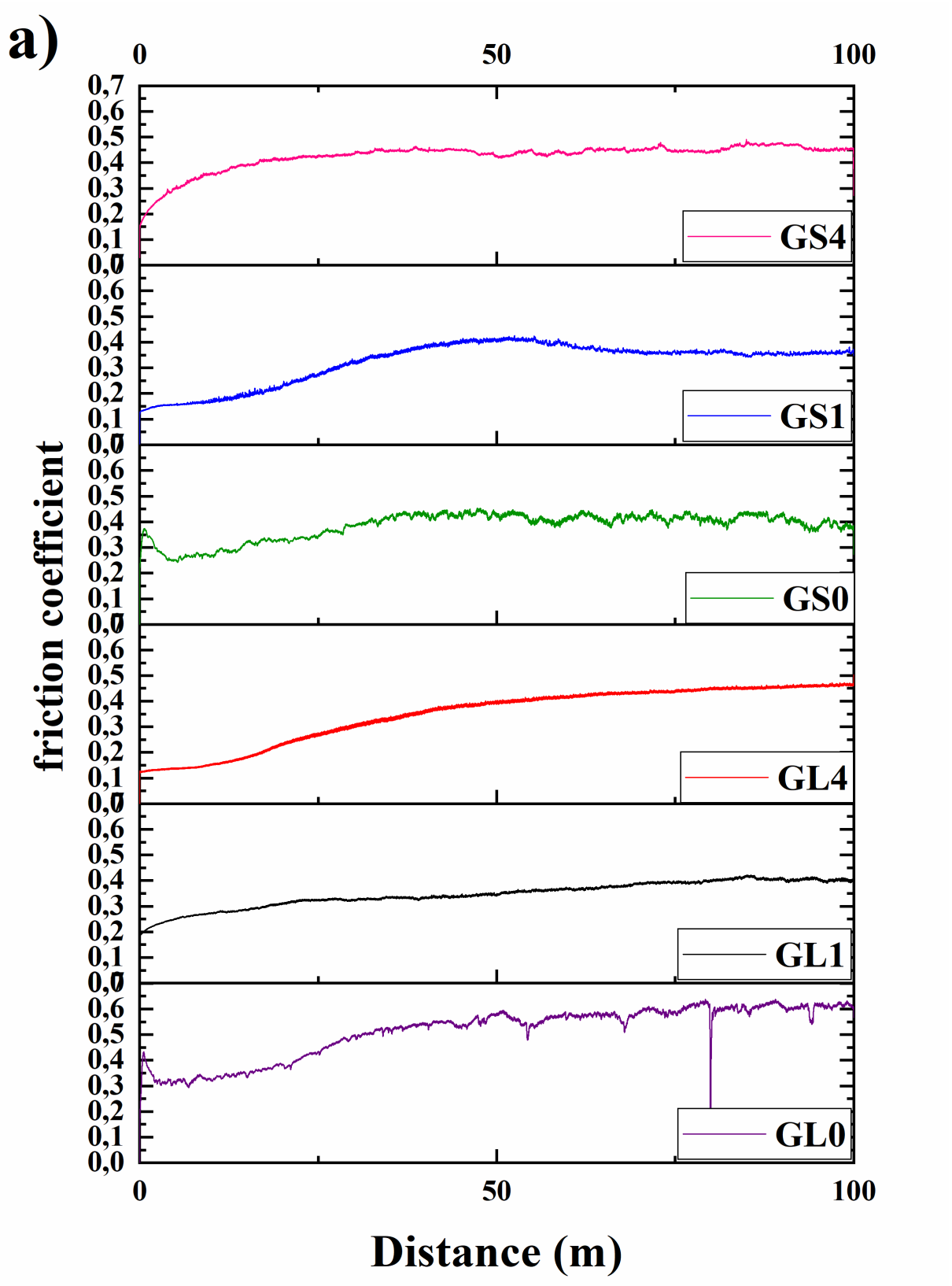
a)
friction coefficient
Distance (m)
GS4
GS1
GS0
GL4
GL1
GL0

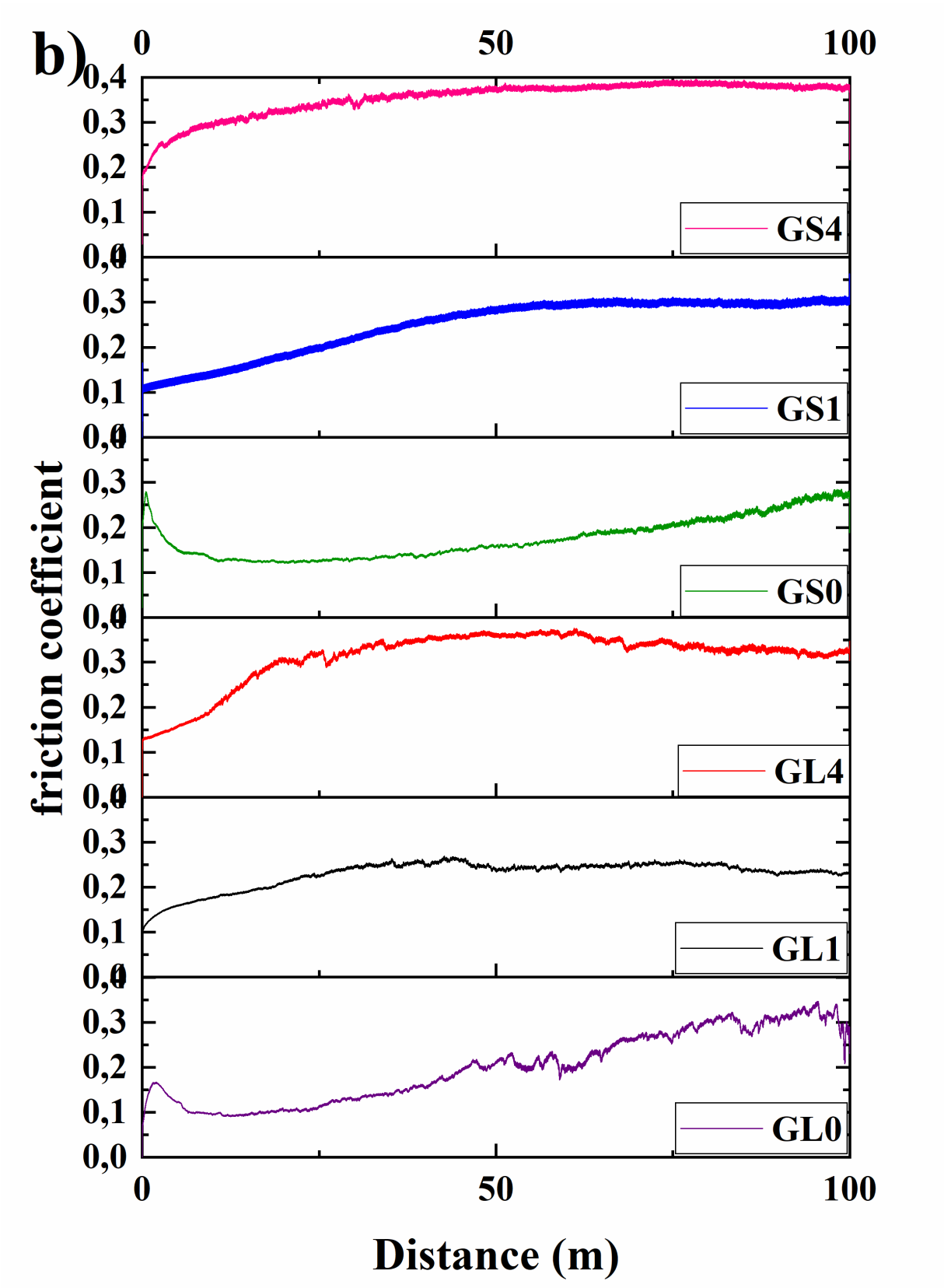
b)
0
50
100
0,4
0,3
0,2
0,1
0,0
GS4
GS1
GS0
GL4
GL1
GL0
friction coefficient
Distance (m)

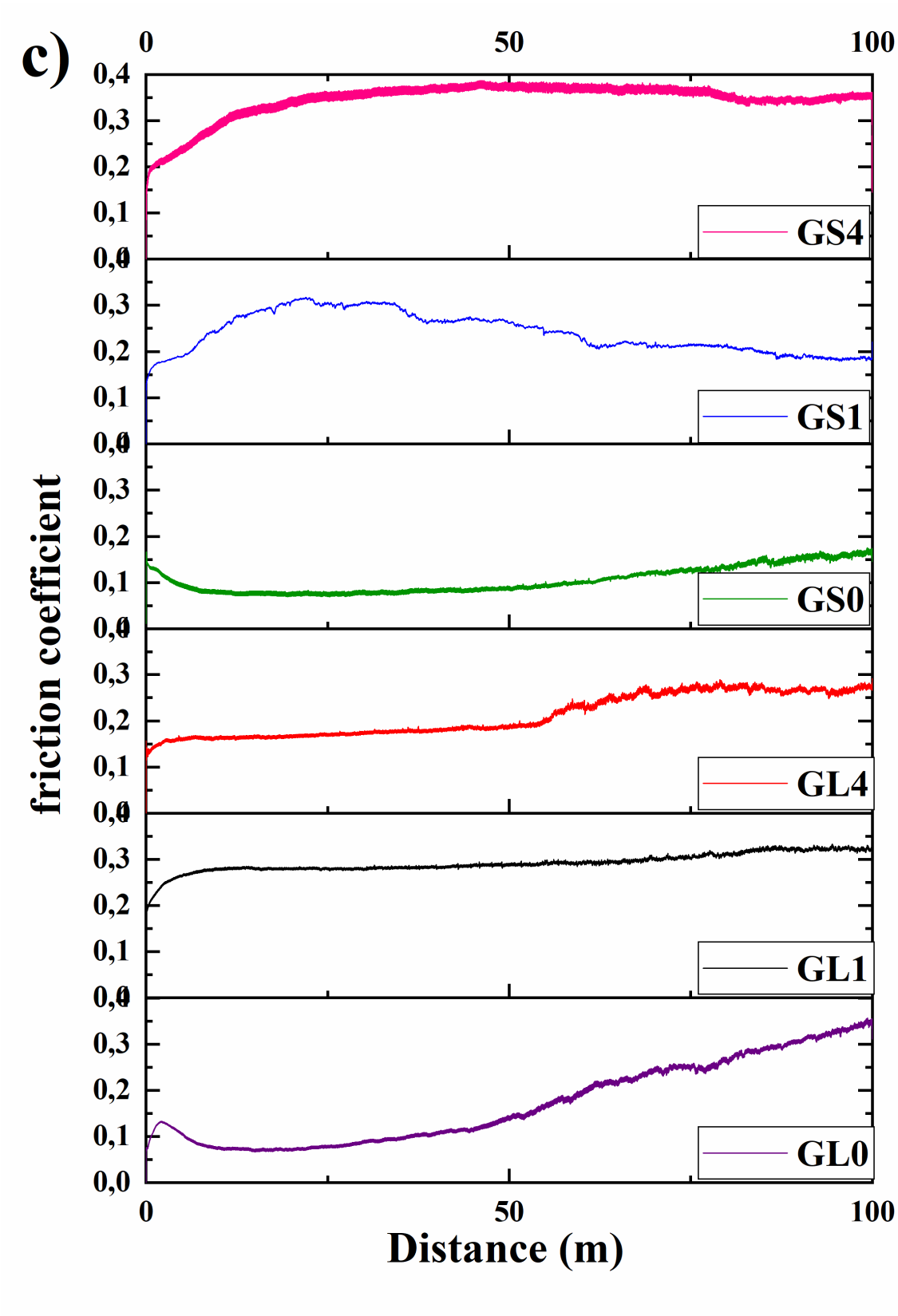

Figure 3.9. Evolution of the friction coefficient of samples under different applied loads: a) 2N, b) 6N, and c) 10N.

3.3.2. Wear Track Morphology (Dry Test)

Figures 3.10 and 3.11 present the three-dimensional map and SEM images of the worn surfaces morphology of six specimens (GL0, GL1, GL4, GS0, GS1, and GS4) under different loads (2N, 6N, and 10N). The data analysis indicates that:

GL0 (± 225 HV):

The presence of graphite in GL0 may provide some level of lubrication, but its lower hardness still leads to significant adhesive wear and material transfer to the Al_2O_3 ball. Additionally, the GL0 softer matrix experienced abrasive wear from the harder Al_2O_3 ball, resulting in grooves or scratches on the wear track. Due to the repeated contact with the Al_2O_3 ball, GL0 is susceptible to surface fatigue wear, which can result in the formation of cracks and the removal of material. This phenomenon is illustrated in Fig. 3.11.

GL1 (±1600 HV):

GL1 may exhibit reduced adhesive wear and possibly lower abrasive wear compared to GL0 due to its higher hardness and the presence of graphite. The lubricating effect of graphite could help mitigate wear to some extent. Surface fatigue wear could occur, but it is likely to be less severe due to the hardness match.

GL4 (±2010 HV):

The combination of higher hardness and graphite in GL4 may result in minimal adhesive wear and lower abrasive wear. The lubricating effect of graphite may further contribute to reduced wear rates. It is less prone to surface fatigue wear compared to GL0 and GL1 due to its higher hardness.

GS0 (±144 HV):

The presence of graphite in GS0 may provide some lubrication, but it is unlikely to be sufficient to prevent significant adhesive wear and abrasive wear. Furthermore, surface fatigue wear may be pronounced due to the lower hardness and repeated contact with the Al_2O_3 ball.

GS1 (±1900 HV):

The higher hardness of GS1 and the presence of graphite may result in reduced adhesive wear and possibly lower abrasive wear compared to GS0. However, the lubricating effect of graphite may be limited compared to gray cast iron.

GS4 (±2000 HV):

As with GL4, GS4's higher hardness and the presence of graphite may result in minimal adhesive wear and lower abrasive wear. The lubricating effect of graphite may contribute to its superior wear resistance among the specimens.

In conclusion, the wear morphology of each specimen is contingent upon its hardness relative to the Al_2O_3 ball. Specimens with lower hardness values (GL0, GS0) are anticipated to exhibit more pronounced adhesive wear, abrasive wear, and surface fatigue wear compared to specimens with higher hardness values (GL4, GS4), which are likely to demonstrate less severe wear characteristics.

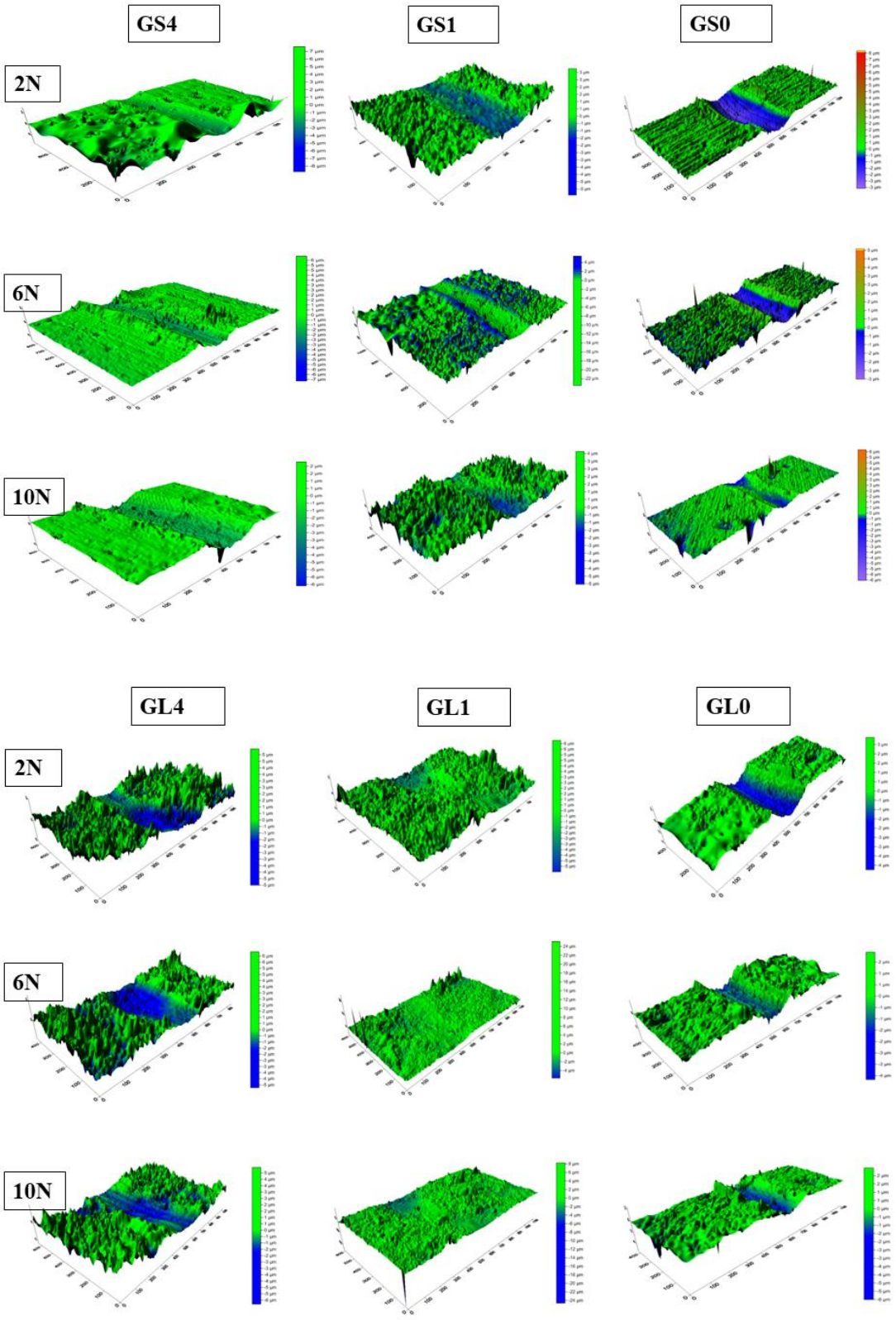

Figure 3.10. 3D map of the worn surfaces of cast iron under different applied loads .

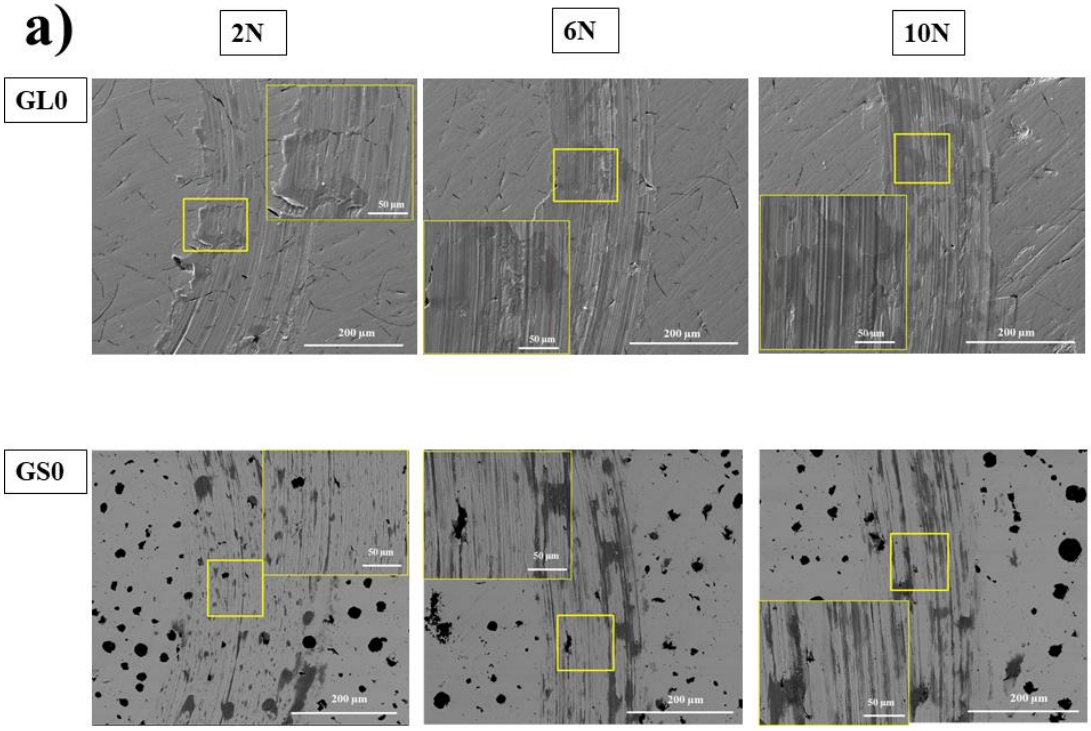
a)
2N
6N
10N
GL0
GS0
50 µm
200 µm

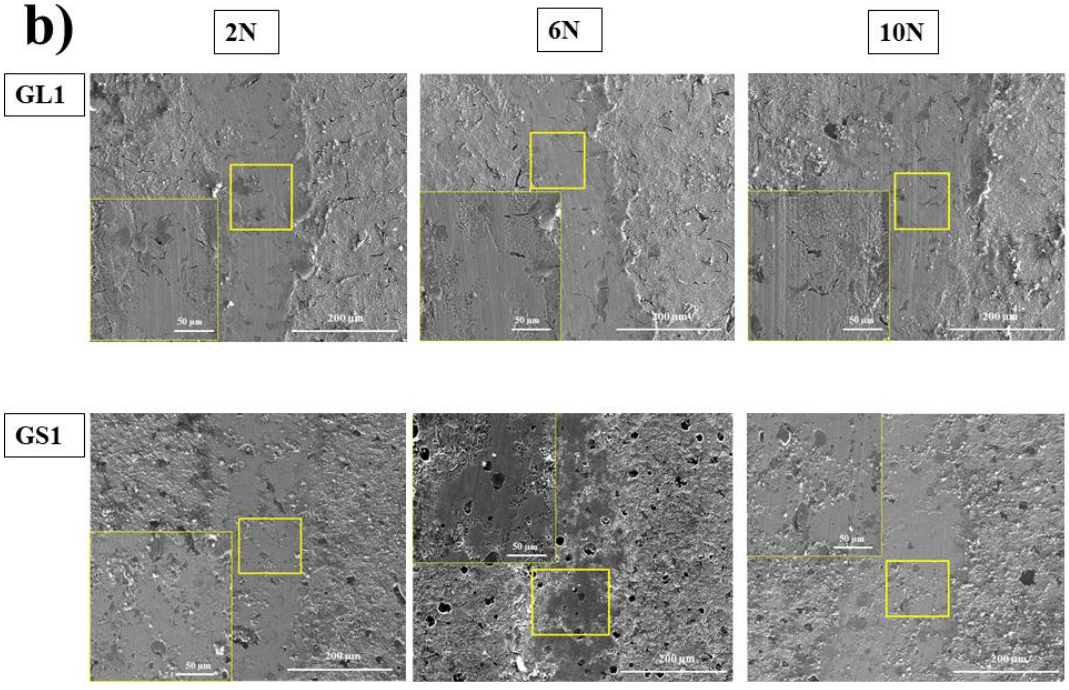
b)
2N
6N
10N
GL1
GS1
50 µm
200 µm

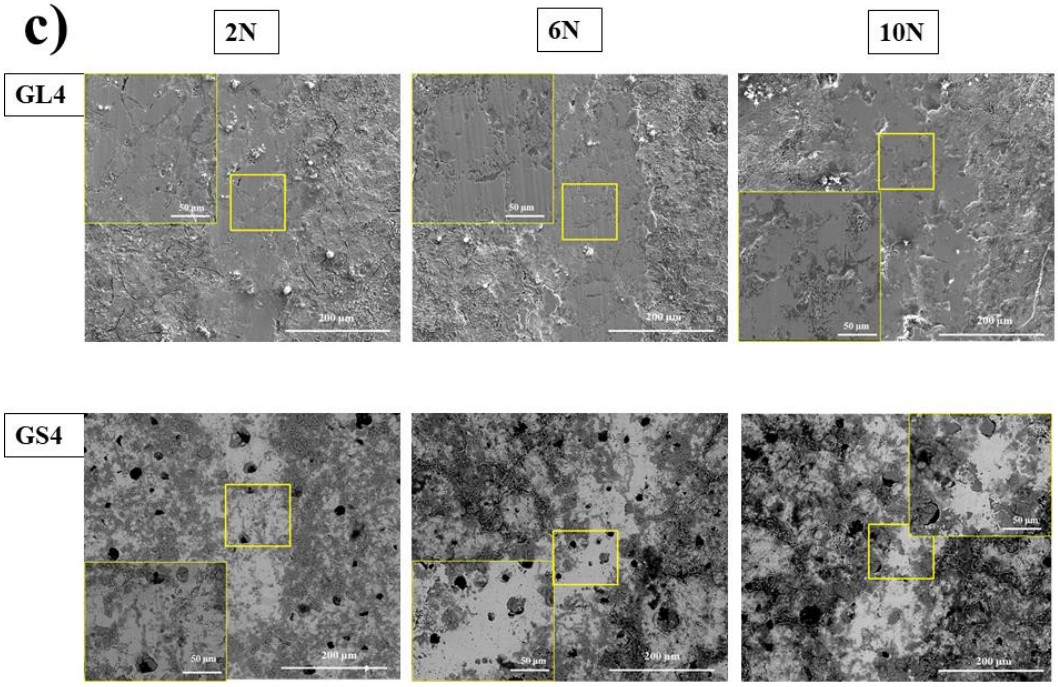

Figure 3.11. Worn surfaces morphology of: a) unboried; b) borided for 1h; c) borided for 4h under different applied loads (2, 6 and 10N).

3.3.3. Wear Rate Evolution (Dry Test)

Figure 3.12 illustrates the wear rate evolution as a function of the applied forces. The wear rates (in $mm^3/N \cdot m$) of six specimens (GL0, GL1, GL4, GS0, GS1, and GS4) were measured under different loads (2N, 6N, 10N).

The data analysis reveals that for a load of 2N, the wear rates from highest to lowest are: GL0 (22.46) > GL1 (21.11) > GS0 (13.28) > GL4 (13.02) > GS1 (9.403) > GS4 (2.793).

For a load of 6N, the wear rates from highest to lowest are: GL0 (9.515) > GS1 (9.319) > GL1 (9.285) > GL4 (5.892) > GS0 (3.172) > GS4 (1.59).

For a load of 10N, the wear rates from highest to lowest are: GL0 (7.721) > GL1 (6.68) > GS1 (2.525) > GS0 (2.289) > GS4 (1.882) > GL4 (1.656).

The data indicates that, for most materials, the wear rate tends to decrease as the load increases.

Specimen GS4 consistently exhibits the lowest wear rate, indicating the best performance among the specimens.

Conversely, specimen GL0 generally exhibits the highest wear rate, indicating the poorest performance among the specimens.

Overall, specimen GS4 performs the best under all loads, while specimen GL0 performs the worst. The other specimens (GL1, GL4, GS0, GS1) fall in between these two extremes.

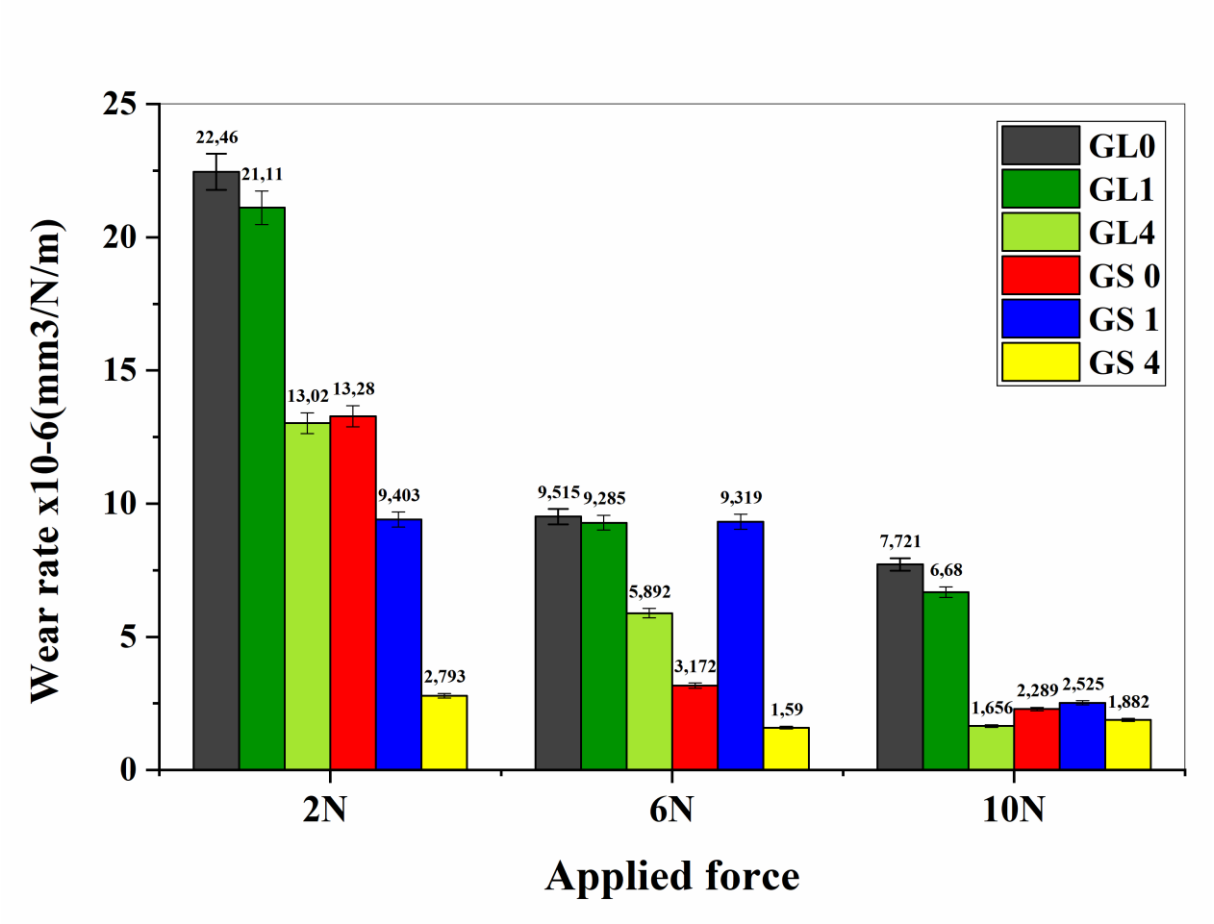

Figure 3.12. Evolution of wear rate of cast iron under different applied loads.

The study shows that surface boriding treatments have a significant impact on the wear rates of both gray cast iron (GL) and ductile cast iron (GS) under different loads.

For gray cast iron (GL), wear rates decrease with increasing boriding treatment duration (from 0 to 1 to 4 hours) under all loads. This indicates that boriding treatment enhances the wear resistance of gray cast iron, with longer treatment durations resulting in lower wear

rates. However, even with boring treatment, gray cast iron, especially GL0, still exhibits higher wear rates compared to ductile cast iron, GS.

The wear rates of ductile cast iron, GS, are generally lower than those of gray cast iron under all loads. Furthermore, the wear rates of ductile cast iron remain relatively consistent regardless of the duration of boriding treatment (0, 1, and 4 hours). This suggests that the effect of boriding treatment on wear resistance is less significant in ductile cast iron when compared to gray cast iron.

Overall, the results indicate that surface boriding treatment enhances the wear resistance of both gray and ductile cast iron. Ductile cast iron exhibits superior wear resistance compared to gray cast iron, particularly when subjected to longer boriding treatment durations.

3.3.4. COF Evolution (Lubricant Test)

Figure 3.8 illustrates the evolution of the friction coefficient for both unborided and borided specimens sliding against a 100Cr6 ball in 5W-40 oil under a load of 60N at 100°C. During the boundary lubricant test, notable observations were made:

The gray cast iron sample (GL0) exhibited a gradual increase in the coefficient of friction (COF) throughout the running-in period, indicating progressive wear and surface degradation.

In contrast, the GL4 specimen showed a different trend due to the protective boriding surface (±83µm). The boundary lubrication test revealed a significant decrease in COF during the running-in period, indicating improved friction performance and better surface behavior attributed to the effectiveness of the protective treatment.

The GL1 specimen demonstrated a significant initial increase before stabilizing at a constant value of ±0.14 without fluctuations. The friction curve of GL1 displayed two stages: an initial running-in phase with a rapid COF increase, followed by a stabilization phase where the COF remained constant regardless of the sliding distance. This behavior is attributed to the surface protection provided by the Fe_2B layer of GL1 and the presence of chromium oxide (Cr_2O_3) acting as a solid lubricant on the surface of the 100Cr6 ball [20-22].

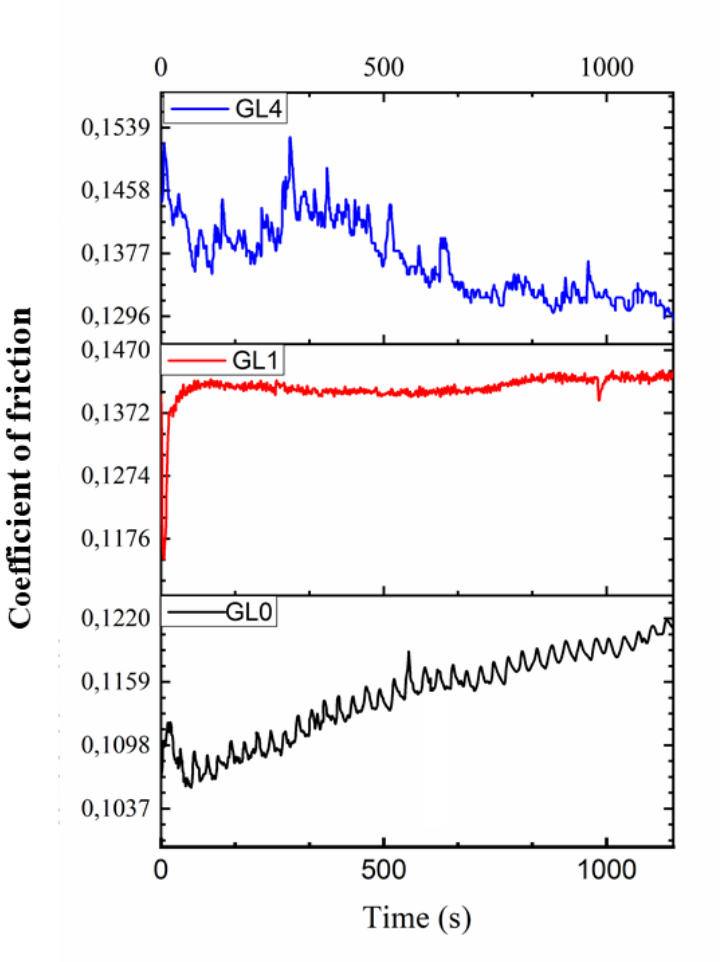

Figure 3.13 Friction coefficient evolutions of samples, which named GL0, GL1 and GL4 tested at 100°C.

The co-presence of chromium oxide (Cr_2O_3) and an Fe_2B layer provides protection against friction and wear in a tribological system. At 100°C, iron oxide (Fe_3O_4, Fe_2O_3), boron oxide (B_2O_3) and various mixed oxide phases contribute to enhanced surface protection.[20, 23-25] In contrast, untreated gray cast iron exhibits different interactions with oxide films, which influence the coefficient of friction (COF) during running-in. The formation of oxides affects wear mechanisms and tribological behavior, underscoring the importance of surface treatments in enhancing COF and wear performance under specific test conditions. The low friction coefficient of approximately 0.11 observed in untreated specimens is attributed to the presence of the graphite phase, which serves as a fundamental friction material that also acts as an oil sump [22].

3.3.5. Wear Rate Evolution (Lubricant Test)

In contrast, the boronized specimens exhibited friction coefficients comparable to those of the uncoated specimens. However, the unboronized GL0 specimen displayed a significantly higher wear rate of 9.828x10-4(mm3/N/m) compared to other boronized specimens (up to 0.03468x10-4(mm3/N/m) for specimen GL4) as shown in Fig 4.9. It was attributed to the formation of low-friction H_3BO_3 on the worn surfaces of the boronized specimens. This is because the worn surfaces of metal and alloy substrates are typically covered with thin oxide films during oil lubrication [22, 26, 27]. Additionally, it is known that H_3BO_3 forms on the surfaces of B_2O_3 substrates by reacting with water molecules in the air [20, 23, 25, 28-30] and this H_3BO_3 exhibits low friction due to its layered crystal structures [28, 30].

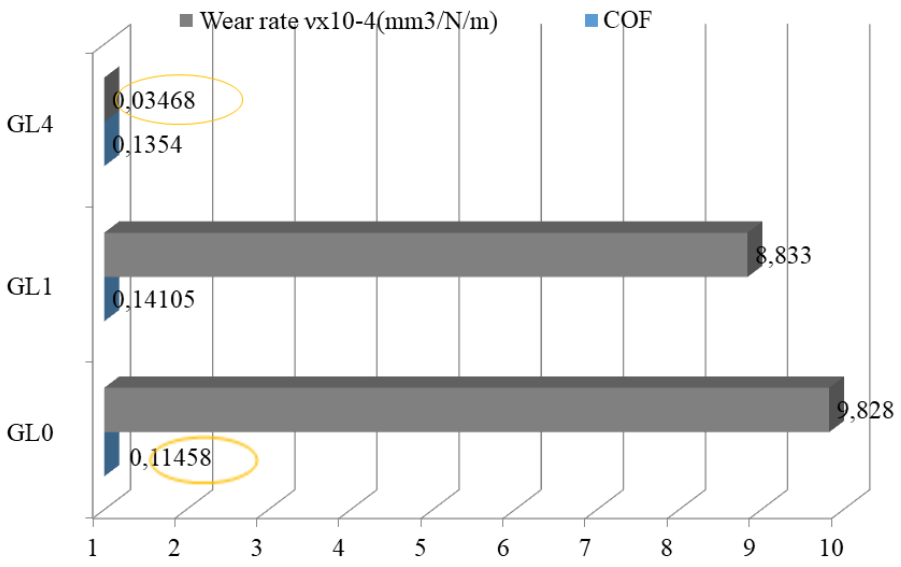

Figure 3.14 Variation of COF and wear rates.

3.3.6. Wear Track Morphology (Lubricant Test)

The fine grooves aligned with the sliding direction on the worn surfaces, as seen in the wear trace of the unborided specimen (Fig. 3.10a), indicate the abrasive nature of the third body of wear debris, providing evidence of severe wear (Fig. 3.10a'). In contrast, although the SEM images of the GL1 specimen (Fig. 3.10b) show no surface deformation or wear lines, slight wear is evident when abrasive debris enters the lubricating oil. The rate of metal removal is slow due to the fine nature of the abrasive (Fig. 3.10b'), and wear becomes visible

over time. Regarding the GL4 sample, adhesive wear on the surface is apparent (Fig. 3.10c), with a notable accumulation of debris in the wear tracks of the borided sample, despite recording the lowest wear loss volume (Fig. 3.10c").

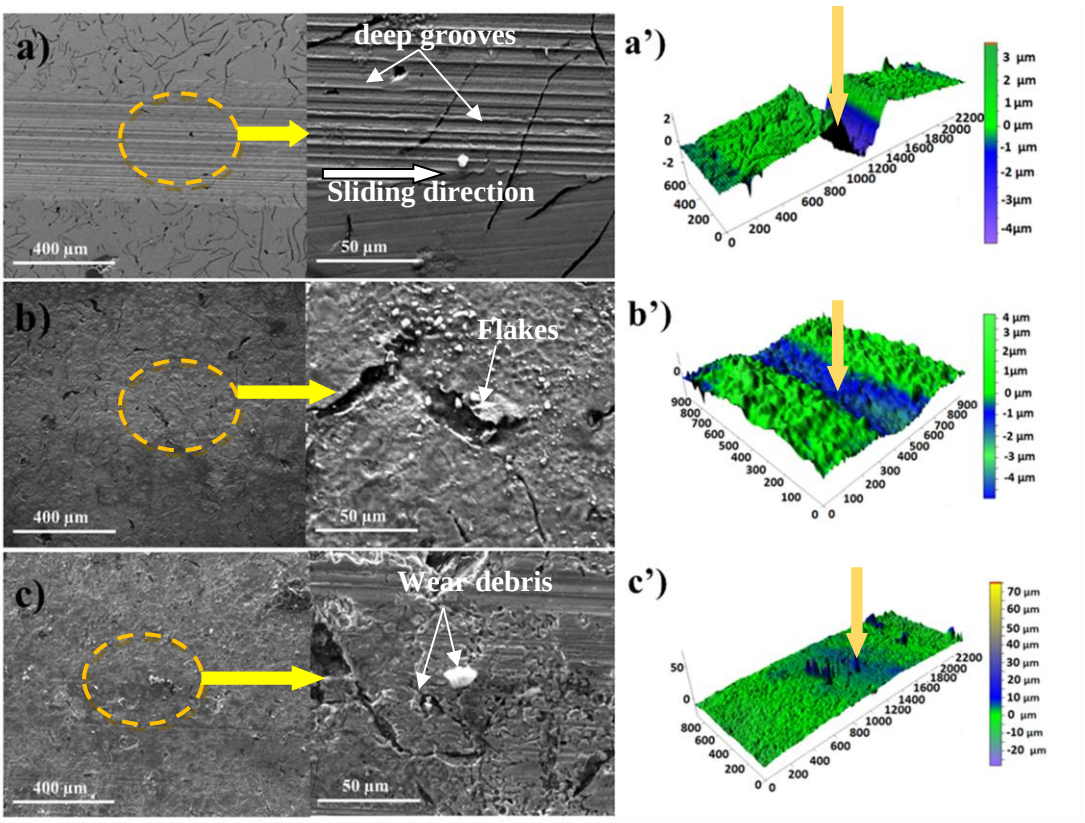

Figure 3.15 SEM micrographs of the worn surfaces: a) GL0 un-borided specimens, b) GL1 borided for 1h at 950°C and c) GL4 borided for 4h at 950°C.

3.3.7. Tribological Parameters Evolution (Lubricant Test)

The volume parameters "Vmp" (peak material volume), "Vmc" (core material volume), and "Vvv" (void volume of the valleys) represent the progression of the functional parameters Rk, Rpk, Rvk (profile), and Sk, Spk, and Svk (surface). They are derived from the Abbott curve[31]. These parameters play a crucial role in tribology as they enable the assessment of functional surface quality and their performance during operation concerning lubrication and wear [32].

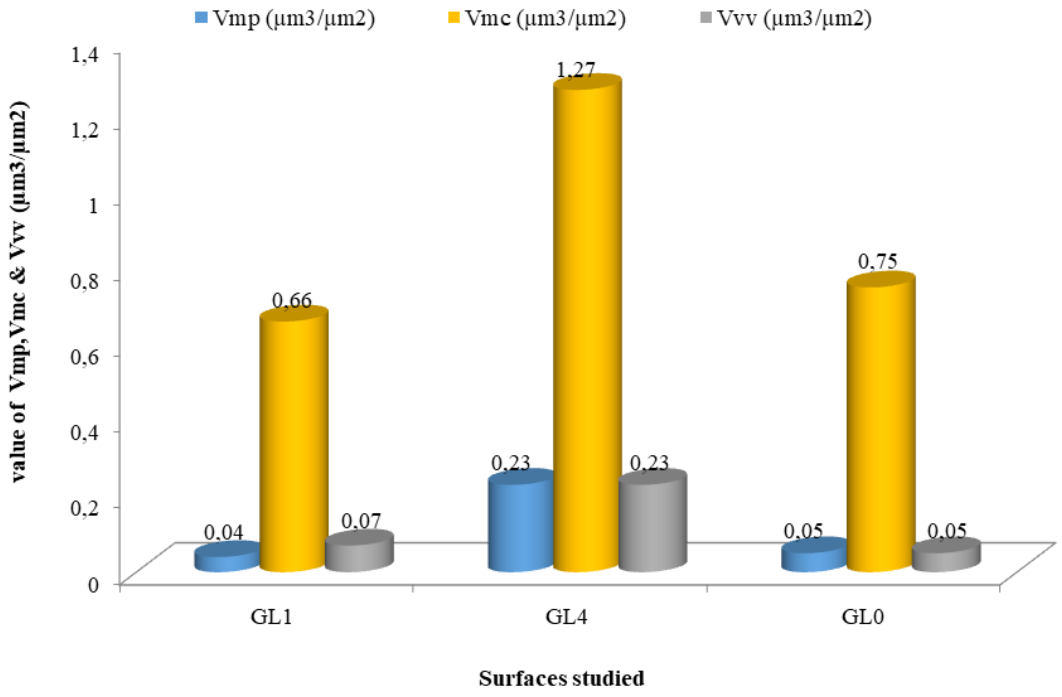

Figure 3.16. Progression of volume parameters across various surfaces

Following the formation of a boriding layer on the prepared surfaces, the graph in Fig 3.11 shows that for the coated surface GL4, the parameter Vmp converges to a value of 0.23(µm3/µm2), indicating a higher peak volume compared to surfaces GL1 and GL0, where Vmp reaches values of 0.04(µm3/µm2) and 0.05(µm3/µm2), respectively. This implies that the running-in phase for the latter two surfaces is reduced compared to surface GL4. A decrease in Vmp leads to an increase in the bearing rate, which is beneficial during the running-in phase **[**33**]**. Additionally, the parameter Vmc is significant in the operating phase as it represents the volume of material that will wear **[**34**]**. A higher Vmc indicates better surface fatigue resistance, thus improving service life. Therefore, the GL4 surface has a Vmc value of 1.27(µm3/µm2), higher than the values obtained for the GL1 and GL0 surfaces (0.66(µm3/µm2) and 0.75(µm3/µm2), respectively). This can be attributed to the boron diffusion layer adhering well to the GL4 surface compared to GL1.

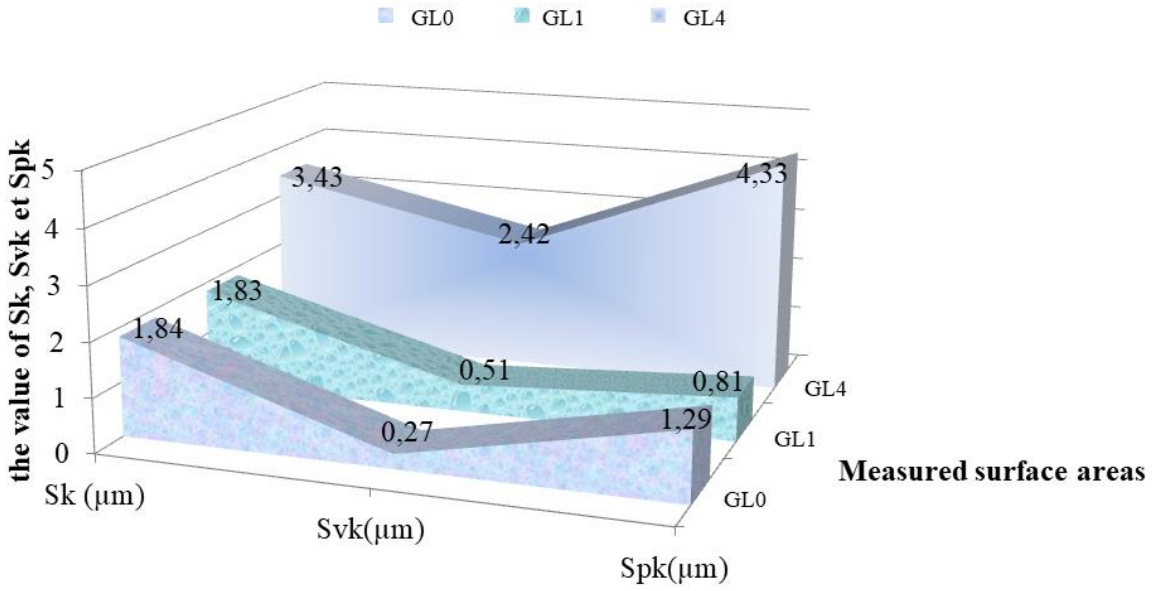

Figure 3.17. Development of functional parameters across varied surfaces

Similarly, the valley volume parameter (Vvv) was measured at 0.23(µm3/µm2) for the GL4 surface, whereas it only reached values of 0.07 and 0.05(µm3/µm2) for the GL1 and GL0 surfaces, respectively. The void volume of the valleys "Vvv" provides an estimate of lubricant reserves; an increase in Vvv is beneficial for the surface because it enhances lubricant retention [32], which can reduce friction and preserve the surface condition. The values obtained for the surface parameters (Spk, Sk, Svk) in Fig. 3.17 support those obtained for the volume parameters (Vmp, Vmc, Vvv). Thus, the GL4 surface represents a balance between the functional parameters, with adequate values of Vmc, Vmp, and Vvv, as well as improved wear behavior. For this surface, the wear rate is Ws = 0.03468 10-4 (mm3/N/m), whereas for the GL1 surface, Ws = 8.833 10-4 (mm3/N/m), and for the GL0 surface, Ws = 9.828 10-4 (mm3/N/m).

3.4. Electrochemical Behavior

3.4.1. Electrochemical Impedance Spectroscopy (EIS)

The figure 3.18 shows electrochemical impedance spectroscopy results for unborided and borided cast iron samples in a 3.5% NaCl solution. Nyquist is used to analyze the electrochemical performance of samples. The electrochemical parameters values obtained by EIS for the corrosion of these specimens are presented in the table below.

Table 4.3: The electrochemical impedance spectroscopy data for the various samples

Substrate	R_e ($\Omega.cm^2$)	CPE_{layer} ($\mu F/cm^2$) .10-3	a_1	R_{pore} ($\Omega.cm^2$)	CPE_{dl} ($\mu F/cm^2$) .10-3	a_2	R_{ct} ($\Omega.cm^2$)
GS0	6.598	0.188 5	0.741 3	656.5	5.077	0.871	**209.5**
GS1	10.22	0.577 4	0.759 8	4.275	6.552	0.789 1	**10 493**
GS4	7.972	**6.703**	0.712 9	5.732	12.42	0.776 9	6 838
GL0	7.023	0.486 5	0.709 9	1.665	0.419 7	0.441 5	1 874
GL1	13.67	1.668	0.529	30.18	2.003	0.720 3	**5 116**
GL4	7.8	**2.332**	0.545 5	82.92	1.886	0.682 8	4 716

The Nyquist plot for the GS0 specimens indicates a semi-circular arc with different radii of curvature, with GS1 having a larger radius of curvature, indicating greater resistance to the charge transfer process. The Nyquist plots show two capacitive loops at high and low frequencies. Sample GS1 shows high charge transfer resistance (R= 10,493.10^3 $\Omega.cm^2$) compared to GS0 (0,2095.10^3 $\Omega.cm^2$) and GS4 (6,838.10^3 $\Omega.cm^2$).

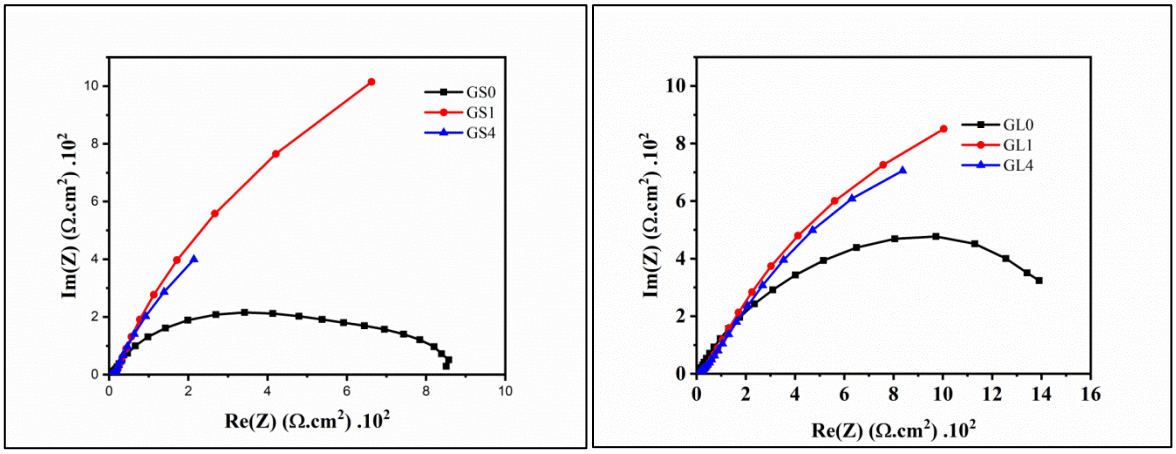

Figure 3.18 Electrochemical impedance spectroscopy (EIS)

Analysis of these results, shows by the Nyquist plot for the GL specimens, shows a semicircular arc with different radii of curvature. The larger radius of curvature of the sample GL1 suggests that it offers greater resistance to the charge transfer process. The presence of two-time constants, one of which is a low-frequency capacitive loop, reflects the double layer at the metal/electrolyte interface and the presence of a corrosion product layer for all three samples tested "raw and treated", i.e. the shape of the curve remains the same with only a change in the radius of curvature. In addition, the Nyquist plots show two capacitive loops at high and low frequencies. Sample GL1 shows high charge transfer resistance (R= $5.116.10^3 \Omega.cm^2$) compared to GL0 ($1.874.\ 10^3\ \Omega.cm^2$) and GL4 ($4.761.10^3\ \Omega.cm^2$).

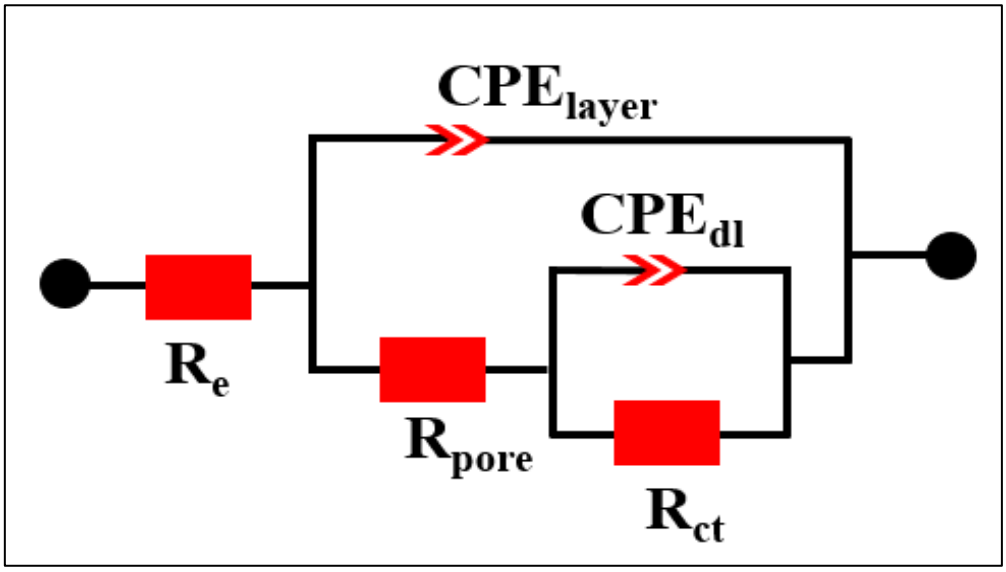

Figure 3.19 Equivalent electrical circuit.

Results were interpreted with an equivalent electrical circuit consisting of **Re** (electrolyte resistance), **CPElayer** (boride layer capacitance), **CPEdl** (double-layer capacitance in parallel with Rct), and **Rpore** (resistance of pores and surface defects).

3.4.2. Potentiodynamic Polarization Test (Tafel's)

Tafel's representation of the non-stationary characteristic involves plotting the decimal logarithm of current density against voltage. Polarization curves are obtained in potentiodynamic mode after immersing the electrode in the electrolyte for one hour to reach equilibrium shown in Fig 3.20 . The anodic and cathodic regions of all curves exhibit identical characteristics. The data obtained from the Tafel analysis of corrosion is presented in the table 3.4.

The study found that the presence of a boride layer on the surface of the ductile iron sample GS1 reduced the anodic and cathodic current densities compared to the untreated GS0 sample. This suggests that the deposited layer can be considered a corrosion protection layer for the ductile cast iron.

Additionally, the boriding layer was observed to lower the anodic and cathodic current density in samples GS1 and GS4, indicating that it affects the corrosion resistance of the raw GS0 sample. In the anodic branch, all samples formed a self-passivating domain that created a self-passivating film. The size of the domain corresponded to the polarization resistance of the material, with and without the boriding layer. Breaking the passive film is trans-passivation, causing a sudden increase in current density as the material corrodes.

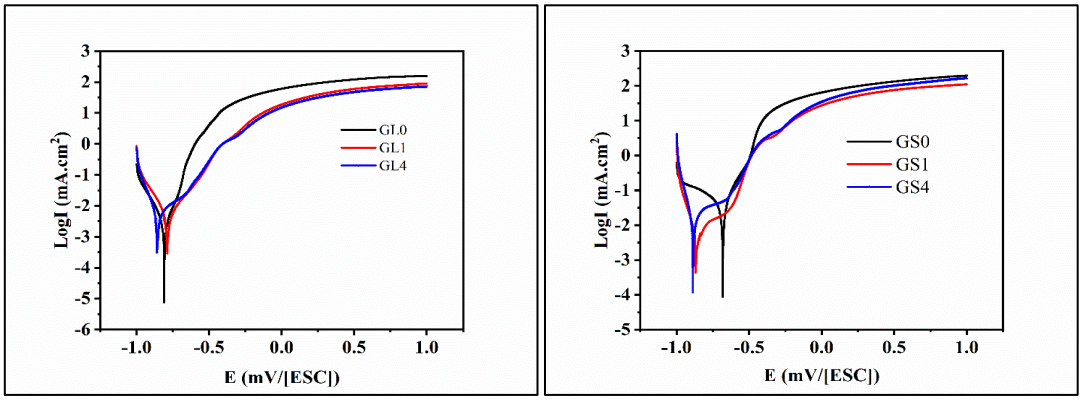

Figure 3.20. Potentiodynamic polarization curves

Table 3.4: The Potentiodynamic polarisation data for the various samples.

Substrate	E (mV)	I ($\mu A.cm^{-2}$)	βa ($mV.dec^{-1}$)	βc ($mV.dec^{-1}$)	Corrosion rate (mmpy)*	Rp ($\Omega.cm^2$)
GL0	-812.412	3.337	85.4	125.0	0.088 035 4	6.59936
GL1	-791.332	1.614	76.2	42.8	0.062 450 5	**7.37029**
GL4	-857.557	2.367	101.2	49.5	0.092 408 3	**6.21932**
GS0	-679.915	6.659	31.2	41.8	0.171 771	1.16448
GS1	-867.342	3.734	173.2	61.5	0.135 45	**5.27560**
GS4	-888.877	6.112	80.9	32.6	0.136 438	1.65014

*****(*mm per year)

$$\mathbf{Rp}=\frac{\boldsymbol{\beta a.\beta c}}{\mathbf{2{,}3039(\boldsymbol{\beta a}+\boldsymbol{\beta c})}}\times\frac{\mathbf{1}}{\boldsymbol{Icorr}}$$

These curves provide the slope values for anodic and cathodic corrosion parameters. Lower corrosion density and higher potential indicate better resistance. The table presents the potentiodynamic polarization parameters of various borided samples in 3.5% NaCl.

It is evident that the boride layer on the surface of the gray cast iron sample GL1 reduced the anodic and cathodic current densities compared to the raw (untreated) GL0 sample, which lacks a boride layer on the surface. This suggests that the tested deposited layer can serve as a corrosion protection layer for the gray cast iron.

The boriding layer reduced the anodic and cathodic current density for samples GL1 and GL4, indicating that this deposit affects the corrosion resistance of the raw GL0 sample. In the anodic branch, it is observed that all samples form a self-passivating domain, which leads to the formation of a self-passivating film. The size of this domain corresponds to the polarization resistance of the material in the absence and presence of the boriding layer. The breaking of the passive film is known as trans-passivation, which causes a sudden increase in current density as the material begins to corrode.

The provided curves allow for the calculation of corrosion parameters for each sample, specifically the anodic and cathodic slope values. A lower corrosion current density and higher corrosion potential indicate better corrosion resistance.

The Table reports the values of corrosion current density (**Icorr**), corrosion potential (**Ecorr**), anodic and cathodic Tafel slopes (**βa** and **βc**) for the different alloys used.

3.4.3. Examination of Formed Oxides

Figure 3.21 illustrates the surface morphology and oxides formed on the surfaces of unborided and borided cast iron samples following an electrochemical test in a 3.5% NaCl solution. The images were obtained using SEM and EDS.

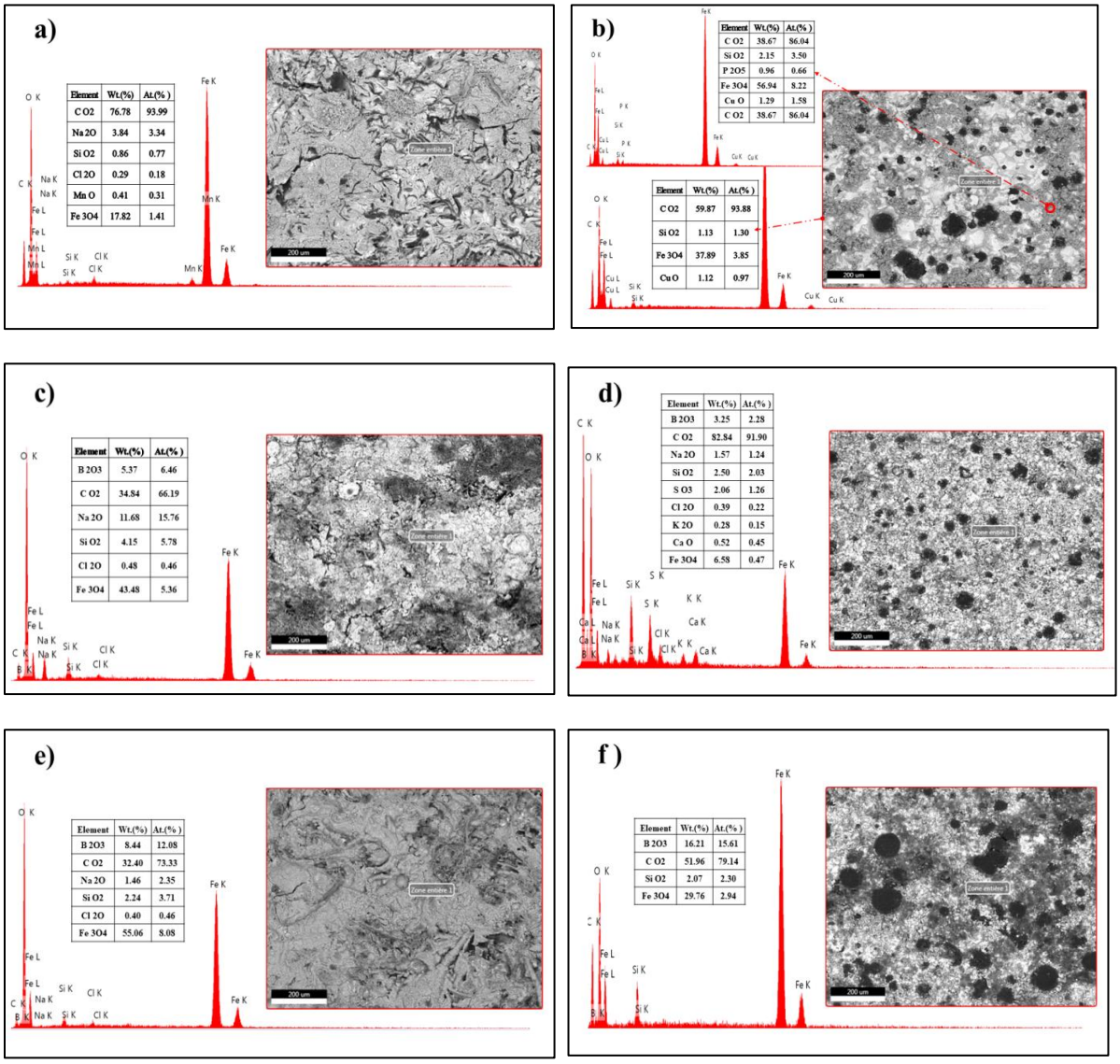

Figure 3.21 EDS and SEM images of the surface morphology and oxides formed on the surfaces (a) GL0; (b) GS0; (c) GL1; (d) GS1; (e) GL4; and (f) GS4, after electrochemical testing in a 3.5% NaCl solution.

The electrochemical behavior of borided gray and ductile cast iron in a 3.5% NaCl solution can be elucidated by examining the oxides formed on the surface of the specimens. The EDS and SEM images of the surface morphology and oxides formed on the surfaces (a) GL0; (b) GS0; (c) GL1; (d) GS; (e) GL4; and (f) GS4) after electrochemical testing in a 3.5% NaCl solution are presented in Fig. 4.21. Boriding is a surface treatment that involves diffusing boron atoms into the material at high temperatures, forming hard boride compounds that enhance corrosion resistance. In this study, GS1, GS4, GL1, and GL4 specimens underwent boriding surface treatment, leading to the formation of boride layers on their surfaces.

The presence of boron trioxide (B_2O_3) in the oxide formations of borided specimens (GL1, GL4, GS1, GS4) indicates the effectiveness of boriding treatment in improving corrosion resistance. Boride compounds, such as FeB and Fe_2B, act as physical barriers to corrosive species, reducing their diffusion into the material and slowing down the corrosion process. The increased hardness and wear resistance of the boride layer further contribute to the material's corrosion resistance by reducing the likelihood of surface damage that can initiate corrosion.

In contrast, non-borided specimens (GL0, GS0) exhibited the formation of oxides such as CO_2, Na_2O, SiO_2, Cl_2O, CuO, and P_2O_5, which are indicative of ongoing corrosion processes. The presence of these oxides suggests that the untreated surfaces are more susceptible to corrosion compared to borided surfaces. Additionally, the absence of boron oxide in the oxide formations of non-borided specimens further highlights the protective role of boriding treatment in enhancing the electrochemical behavior of gray and ductile cast iron in chloride-containing environments.

Overall, the study demonstrates that boriding surface treatment significantly improves the electrochemical behavior of gray and ductile cast iron by forming protective boride layers on the surfaces, which inhibit corrosion processes and enhance the materials' durability in harsh environments.

REFERENCES

[1] E. Medvedovski, J. R. Jiang, and M. J. A. i. A. C. Robertson, "Boride-based coatings for protection of cast iron against wear," vol. 115, pp. 483 - 494, 2016.

[2] C. Zouzou, M. Keddam, B. Bouarour, A. Piasecki, A. Miklaszewski, and M. Kulka, "Characterization and Boronizing Kinetics of EN-GJL-250 Lamellar Gray Cast Iron," in *Annales de Chimie-Science des Matériaux*, 2020, vol. 44, no. 1, pp. 23-28.

[3] D. Charmati, S. Tlili, M. Touhami, M. Bourebia, and E. H. J. T. I. J. o. A. M. T. Kaleli, "Investigation of the influence of Fe2B layer thickness on the enhancement of tribological behavior of borided EN-GJL-250 cast iron: a comprehensive investigation under optimized lubrication," vol. 129, no. 9, pp. 4605-4615, 2023.

[4] O. Azouani, M. Keddam, O. Allaoui, A. J. M. P. Sehisseh, and Characterization, "Kinetic Analysis of pack-borided gray cast iron," vol. 10, no. 1, pp. 226-236, 2021.

[5] P. Goeuriot, R. Fillit, F. Thevenot, J. Driver, H. J. M. S. Bruyas, and Engineering, "The influence of alloying element additions on the boriding of steels," vol. 55, no. 1, pp. 9-19, 1982.

[6] R. S. Petrova, N. Suwattananont, V. J. J. o. M. E. Samardzic, and Performance, "The effect of boronizing on metallic alloys for automotive applications," vol. 17, no. 3, pp. 340-345, 2008.

[7] O. Azouani, M. Keddam, O. Allaoui, A. J. M. P. Sehisseh, and Characterization, "Kinetics of the Formation of Boride Layers on EN-GJL-250 Gray Cast Iron," vol. 6, no. 4, pp. 510-522, 2017.

[8] R. Ipek, B. Selçuk, M. Karamiş, V. Kuzucu, and A. J. J. o. M. P. T. Yücel, "An evaluation of the possibilities of using borided GG25 cast iron instead of chilled GG25 cast iron (surface properties)," vol. 105, no. 1-2, pp. 73-79, 2000.

[9] C. Meriç, S. Sahin, M. J. S. Uzkut, t. o. welding, and joining, "Investigation of effect of boronising on welding zone," vol. 7, no. 2, pp. 107-110, 2002.

[10] C. Badini, C. Gianoglio, G. J. S. Pradelli, and C. Technology, "The effect of carbon, chromium and nickel on the hardness of borided layers," vol. 30, no. 2, pp. 157-170, 1987.

[11] M. İzciler and H. J. J. o. M. P. T. Celik, "Two-and three-body abrasive wear behaviour of different heat-treated boron alloyed high chromium cast iron grinding balls," vol. 105, no. 3, pp. 237-245, 2000.

[12] N. Vidakis, A. Antoniadis, and N. J. J. o. m. p. t. Bilalis, "The VDI 3198 indentation test evaluation of a reliable qualitative control for layered compounds," vol. 143, pp. 481-485, 2003.

[13] S. J. T. i. Bull, "Failure mode maps in the thin film scratch adhesion test," vol. 30, no. 7, pp. 491-498, 1997.

[14] T. Tamam, M. Touhami, M. Zahzouh, A. E. G. J. J. o. M. E. Mohamed, and Performance, "Microstructural, Mechanical and Corrosion Characterizations of Borided Cast Irons Formed by a Recycled Boriding Agent," pp. 1-19, 2023.

[15] G. A. Rodríguez-Castro *et al.*, "Damage mechanisms in AISI 304 borided steel: scratch and daimler-benz adhesion tests," vol. 18, pp. 1346-1353, 2015.

[16] P. A. Dearnley, M. Schellewald, and K. L. J. W. Dahm, "Characterisation and wear response of metal-boride coated WC–Co," vol. 259, no. 7-12, pp. 861-869, 2005.

[17] I. Campos-Silva *et al.*, "Improving the adhesion resistance of the boride coatings to AISI 316L steel substrate by diffusion annealing," vol. 25, pp. 3852-3862, 2016.

[18] S.-T. Park, J.-G. Han, M. Keunecke, K. J. I. J. o. R. M. Lee, and H. Materials, "Mechanical and structural properties of multilayer c-BN coatings on cemented carbide cutting tools," vol. 65, pp. 52-56, 2017.

[19] J. Tharajak, T. Palathai, and N. J. A. M. R. Sombatsompop, "Scratch resistance and adhesion properties of PEEK coating filled with h-BN nanoparticles," vol. 747, pp. 303-306, 2013.

[20] K. Li *et al.*, "The tribological properties of bulk Fe2B with pre-oxidation treatment at 750° C in air," 2019.

[21] J. Hou, M. Zhang, H. Yang, J. Qiao, and Y. J. M. L. Wu, "Surface strengthening in Al0. 25CoCrFeNi high-entropy alloy by boronizing," vol. 238, pp. 258-260, 2019.

[22] T. Murakami, K. Matsuzaki, Y. Gomi, S. Sasaki, and H. J. M. O. P. L. Inui, "Microstructure and tribological properties of gray cast iron specimens coated by aluminizing, boronizing, chromizing and siliconizing," vol. 1516, no. 1, pp. 115-120, 2013.

[23] S. A. da Costa Aichholz, M. S. Meruvia, P. C. S. Júnior, R. D. J. S. Torres, and C. Technology, "Tribocorrosion behavior of boronized AISI 4140 steel," vol. 352, pp. 265-272, 2018.

[24] K. Li, Z. Huang, Y. Jian, T. Min, X. Lou, and S. J. T. T. Wang, "Friction and wear behavior of single-phase Fe2B bulk under dry sliding condition," vol. 61, no. 3, pp. 513-521, 2018.

[25] A. Erdemir, C. J. S. Bindal, and C. Technology, "Formation and self-lubricating mechanisms of boric acid on borided steel surfaces," vol. 77, 1995.

[26] T. Murakami, H. Mano, Y. Hibi, and S. J. T. i. Sasaki, "Friction and wear properties of Fe7Mo6-based alloy in ethyl alcohol," vol. 43, no. 11, pp. 2183-2189, 2010.

[27] T. Murakami, K. Kaneda, M. Nakano, H. Mano, A. Korenaga, and S. J. I. Sasaki, "Friction and wear properties of Fe–Mo intermetallic compounds under oil lubrication," vol. 15, no. 12, pp. 1573-1581, 2007.

[28] X. Ma, W. Unertl, and A. J. J. o. m. r. Erdemir, "The boron oxide–boric acid system: Nanoscale mechanical and wear properties," vol. 14, no. 8, pp. 3455-3466, 1999.

[29] R. Schoen, C. E. J. A. M. J. o. E. Roberson, and P. Materials, "Structures of aluminum hydroxide and geochemical implications," vol. 55, no. 1-2, pp. 43-77, 1970.

[30] B. R. Burroughs, J.-H. Kim, and T. A. J. T. t. Blanchet, "Boric acid self-lubrication of B2O3-filled polymer composites," vol. 42, no. 3, pp. 592-600, 1999.

[31] Z. Khawaja, "Analyse des états de surface en science des matériaux: caractérisation multi-échelles par ondelette et détermination de l'anisotropie des surfaces," Université de Technologie de Compiègne, 2014.

[32] M. Bourebia, H. Bounezour, L. Laouar, and H. J. S. R. d. S. e. d. l. T. Hamadache, "Evaluation of surface quality by Fractal Dimension and Volume Parameters," vol. 33, pp. 117-127, 2016.

[33] N. I. 13565-2, "Characterization of heights by the load-bearing length rate curve (courbe d'Abbott).".

[34] F. Blateyron, "Digital Surf mesures 787 " no. www. mesures. com, pp. 44-47, septembre 2006 septembre 2006

GENERAL CONCLUSION AND PROSPECTS

The present study examines the influence of microstructure on the mechanical, tribological, and electrochemical behavior of borided gray and ductile cast iron. The boriding process was conducted using a powder technique, with a mixture of B_4C (85% wt) and Na_2CO_3 (15% wt) at 950°C for 1 and 4 hours. The aforementioned behaviors were determined through the use of optical microscopy (OM), scanning electron microscopy (SEM), energy-dispersive X-ray spectroscopy (EDS), X-ray diffraction (RDX), microhardness testing, adhesion tests, tribological tests, and electrochemical tests. The data obtained from these tests were subjected to rigorous analysis using X'Pert HighScore Plus, OriginLAB, and EC-Lab FRAMEWORK software.

After comparing non-borided and borided specimens, the following conclusions were drawn:

- The boride layers obtained on treated samples are monophasic, consisting of only Fe_2B in the layer produced.
- Longer boronizing time results in a thicker boride layer due to increased diffusion.
- A saw-toothed morphology was observed in the interface of the boride layers, comprising a monophase Fe_2B layer. The thickness of the monolayer was found to be 27, 41, 83, and 96 micrometres for GL1, GS1, GL4, and GS4, respectively.
- X-ray diffraction identified the presence of a single type of iron boride (Fe_2B).
- The complete absence of delamination is solid proof of the strong adhesion between the surfaces. Therefore, it is conclusive that GL1 and GL4 qualify as HF1, while GS1 and GS4 are undoubtedly qualified as HF1 and HF2 respectively.
- The thicker and harder coating of GS4 and GL4, which suggests a greater strength, they surprisingly exhibited a smaller indentation radius and depth than GS1 and GL1.
- The Vickers microhardness test provides a microhardness profile on the cross-sections. The hardness near the surface is 1780± 8 HV0.05 and 1985± 5 HV0.05 for GL1 and GS1, respectively. In contrast, it is 2100±5 HV0.05 and 2008± 3 HV0.05 for GL4 and GS4, respectively. The hardness increases with the boronizing time. In all samples, the hardness decreases until it reaches a value equal to that of the substrate, FT-25 and GS38-15.
- The scratch test results demonstrate the influence of Fe_2B thickness and hardness on the wear resistance of the material, as well as the interplay between elastic and plastic deformation.

- Consequently, these investigations imply that thicker and harder borided coatings generally possess superior scratch resistance while maintaining high levels of adhesion quality. Our tribological analysis comprised scratch and adhesion tests on two cast iron grades specimens with varying Fe_2B layer thicknesses.
- Thicker and harder coatings exhibited superior resistance to stress, while both specimens achieved HF1 quality adhesion. To summarize, Fe_2B layer properties significantly influence material behavior and adhesion.
- It can be observed that the diffusion rate is directly proportional to the boronizing time. Consequently, a thicker boride layer is achieved as the diffusion rate increases. Consequently, the wear resistance of the materials was markedly enhanced as the boronizing thickness increased.
- The samples GL1 and GS1 exhibited an average COF that was nearly identical under the three loads, ranging from 0.346 to 0.229. The lowest average COF was observed in sample GS0, which exhibited a value of 0.105 under a 10N load. The specimen GS4 exhibited the highest average COF of approximately 0.340 under the same load.
- The wear morphology of each specimen is contingent upon its hardness relative to the Al_2O_3 ball. It can be reasonably assumed that specimens with lower hardness values (GL0, GS0) will exhibit more pronounced adhesive wear, abrasive wear, and surface fatigue wear than those with higher hardness values (GL4, GS4). This is because specimens with lower hardness values are more susceptible to wear.
- The data indicates that specimen GS4 performs the best under all loads, while specimen GL0 performs the worst. The other specimens (GL1, GL4, GS0, GS1) fall in between these two extremes.
- Results indicate that surface boriding treatment enhances the wear resistance of both gray and ductile cast iron. In particular, ductile cast iron exhibits superior wear resistance compared to gray cast iron, particularly when subjected to longer boriding treatment durations.
- The coefficient of friction for GL0, GL1, and GL4 is 0.11458, 0.14105, and 0.13540, respectively. In contrast, the wear rates of boronized and non-boronized gray cast iron are recorded as 0.03468 10-4 (mm3/N/m), 8.833 10-4 (mm3/N/m), and 9.828 10-4 (mm3/N/m), respectively. Notably, the boronized sample treated for four hours at 950°C exhibits significantly greater wear resistance compared to the others, showing a

300-fold increase. This enhancement is attributed to its elevated surface hardness and thicker high-strength layer.

- As volume parameters increase, leading to a thicker Fe_2B layer, Vmc reaches its peak at 1.27 (μm3/μm2), resulting in superior material wear resistance. Conversely, the maximum value of Vvv is 0.23 (μm3/μm2), indicating optimal surface hardness and adhesion conducive to effective lubricant retention.
- The findings of this study underscore the effectiveness of a high-hardness boronized layer in enhancing substrate wear resistance, particularly in high-temperature environments.
- The Nyquist plots for GS0 and GL0 specimens reveal semi-circular arcs with different radii. GS1 and GL1 display larger radii, indicating increased resistance to charge transfer. Furthermore, the high charge transfer resistances observed in GS1 (10,493.103 Ω.cm²) and GL1 (5.116.103 Ω.cm²) are in contrast to the untreated samples GS0 (0.2095.103 Ω.cm²) and GL0 (1.874.103 Ω.cm²), respectively.
- The boride layer reduces current densities on GS1/ GS4 and GL1/GL4 surfaces compared to untreated samples (GS0 and GL0), acting as an effective corrosion protection barrier.
- Boriding enhances corrosion resistance in raw samples, with self-passivating films forming on all surfaces.
- The study demonstrates that boriding surface treatment significantly improves the electrochemical behavior of gray and ductile cast iron. This is achieved by forming protective boride layers on the surfaces, which inhibit corrosion processes and enhance the materials' durability in harsh environments.
- The findings demonstrated a direct correlation between the thickness of the single-phase Fe_2B layer and its effect on the mechanical, tribological, and electrochemical properties of ductile and gray cast iron.

The findings of this study indicate the following medium-term prospects:

- Investigate the tribological behavior of borided ductile cast iron under optimized lubrication conditions.
- Investigate the electrochemical behavior of borided cast iron in different environments.
- Examine the deposition of sequential layers of boron compounds on cast iron surfaces with the aim of achieving superior mechanical and tribological performance.